A STUDY ON LIQUEFACTION CHARACTERISTICS OF A TYPICAL SAND COLLECTED FROM RIVER CHANNEL DEPOSIT IN AND AROUND KOLKATA

THESIS SUBMITTED IN PARTIAL FULFILMENT OF THE REQUIREMENT FOR THE AWARD OF THE DEGREE
OF

MASTER OF CIVIL ENGINEERING
IN
SOIL MECHANICS AND FOUNDATION ENGINEERING

By

ABHISHEK MONDAL

EXAMINATION ROLL NO. M4CIV1617
REGISTRATION NO. 92756 of 2005-06

Under the guidance of

Dr. R.B. SAHU

Department of Civil Engineering
Faculty of Engineering and Technology
Jadavpur University
Kolkata- 700032

May 2016

DECLARATION OF ORIGINALITY AND COMPLIANCE OF ACADEMIC ETHICS

I hereby declare that this thesis contains literature survey and original research work by the undersigned candidate, as part of his ***Master of Civil Engineering in Soil Mechanics & Foundation Engineering*** *studies.*

All information in this document have been obtained and presented in accordance with academic rules and ethical conduct.

I also declare that, as required by these rules and conduct, I have fully cited and referenced all material and results that are not original to this work.

Name : ABHISHEK MONDAL

Exam Roll No. : M4CIV1617

THESIS TITLE : A STUDY ON LIQUEFACTION CHARACTERISTICS OF A TYPICAL SAND COLLECTED FROM RIVER CHANNEL DEPOSIT IN AND AROUND KOLKATA

.....
(Signature with Date)

JADAVPUR UNIVERSITY

FACULTY OF ENGINEERING AND TECHNOLOGY

DEPARTMENT OF CIVIL ENGINEERING

CERTIFICATE OF RECOMMENDATION

It do hereby recommend that the thesis prepared under my supervision by **Abhishek Mondal** entitled "***A Study on Liquefaction Characteristics of a Typical Sand Collected from River Channel Deposit in and around Kolkata***" be accepted in partial fulfilment of the requirements for the Degree of ***Master of Civil Engineering*** with specialization in ***Soil Mechanics & Foundation Engineering*** from Jadavpur University.

In-Charge of Thesis : .....

(Prof. R. B. Sahu)
Civil Engineering Department
Jadavpur University

Countersigned by:

Head of the Department : .....

(Civil Engineering Department)

Dean : .....

(Faculty of Engineering & Technology)

JADAVPUR UNIVERSITY

FACULTY OF ENGINEERING AND TECHNOLOGY

DEPARTMENT OF CIVIL ENGINEERING

CERTIFICATE OF APPROVAL*

The foregoing thesis entitled, "***A Study on Liquefaction Characteristics of a Typical Sand Collected from River Channel Deposit in and around Kolkata***", is hereby approved as a creditable study of an engineering subject carried out and presented in a manner satisfactory to warrant its acceptance as a pre- requisite to the degree for which it has been submitted. It is implied that by this approval the undersigned do not necessarily endorse or approve any statement made, opinion expressed or conclusion drawn therein, but approved the thesis only for the purpose for which it is submitted.

FINAL EVALUATION FOR
EXAMINATION OF THESIS

1. _____

2. _____

(Signature of Examiners)

* Only in case the thesis is approved

ACKNOWLEDGEMENT

I am extremely thankful and indebted to Dr. R. B. Sahu, Professor of Civil Engineering Department, Jadavpur University, for his valuable guidance, constant support and encouragement throughout my thesis work. This thesis would never been completed without his blessings, guidance, constant vigil, careful supervision and inspiration at all stages of the work.

I am sincerely thankful and obliged to other professors of Soil Mechanics Division, Prof. S. Chakraborty, Prof. S. P. Mukherjee, Prof. S. Ghosh, Prof. P. Aitch, Prof. G. Bhandari, Prof. S. K. Biswas, Prof. N. Roy for their constant encouragement and continuous valuable suggestions throughout my thesis work.

I would like to mention the contribution of various Research Scholars of Soil Mechanics Specialization in successful completion of this experimental thesis and specially Shri Atriya Chowdhury for his kind help during conduction of experiments.

I sincerely acknowledge the help of Mr. Rabin Pal, Mr. Apurba Banerjee and Mr. Ranjit Kushari, Technical staffs of Soil Mechanics Laboratory and specially Shri Brindaban Naskar, Project Attendant, for assisting in preparation of soil samples and helping in testing. Thanks to all other professors and staff of Civil Engineering Department for their kind co-operation.

Last but not the least, I express my sincere gratitude to all of my colleagues of Soil Mechanics and Foundation Engineering section, Civil Engineering Department, for being with me.

This acknowledgement will never be complete unless I give a special mention to contribution of Shri Saurav Pal, one of my colleagues of Soil Mechanics and Foundation Engineering towards the completion of the thesis. He stood by me during all my tough times and also his kind support in various aspects for completing this thesis is beyond mention.

Place: Kolkata

Dated:

ABHISHEK MONDAL

EXAMINATION ROLL NO: M4CIV1617

REGD. NUMBER: 92756 of 2005-06

DEPARTMENT OF CIVIL ENGINEERING

FACULTY OF ENGINEERING & TECHNOLOGY.

JADAVPUR UNIVERSITY, KOLKATA-700032

ABSTRACT

Liquefaction denotes a condition where a soil will undergo continued deformation at a constant low residual stress or with no residual resistance, due to build-up and maintenance of high pore water pressure which reduces the effective confining pressure to a very low value. Two very well-known phenomena of liquefaction has been observed, viz, Flow Liquefaction and Cyclic Mobility. Liquefaction is generally observed in saturated, loose sand as because this type of soil generally compresses when load is applied. As the pore water pressure is increased, the effective stress reduces resulting in loss of strength. Transfer of inter-granular stress takes place from soil grains to pore water. When the transfer is complete, there is a complete loss of strength and the phenomena is called a complete liquefaction and the soil will flow like a liquid.

With the expansion of urban habitation, it is now extremely important to study the liquefaction characteristics of a soil prior to any construction over it. Subsoil in and around Kolkata, situated in Gangetic West Bengal, consists of typical Normal Kolkata Deposit consisting of a thick soft clay deposit at top followed by a stiff / very stiff/ hard silty clay and dense / very dense silty sand and River channel deposit consisting of loose / medium / dense silty sand down to considerable depth mainly along Adi Ganga channel / Tolly's nullah, a distributary of river Ganga. In this paper an attempt has been made to throw some light on the liquefaction characteristics of the river channel deposits in Kolkata.

Soil used in the present work was collected from the compound of Industrial Training Institute, Tollygunge, Kolkata. To investigate the Liquefaction phenomenon, a series of isotrpically consolidated undrained cyclic triaxial tests have been performed to determine the effect of relative density, initial effective confining pressure and cyclic shear strain on the liquefaction potential. Total twenty numbers of cyclic triaxial tests have been performed with relative densities of 25%, 50% and 75%; initial effective confining pressures of 50 kPa, 100 kPa and 150 kPa; cyclic shear strains of 0.5%, 0.67% and 0.83%. All the tests have been performed under a frequency of 1 Hz.

The soil sample has been prepared with moist tamping method by regulating the number of blows to achieve different relative densities. Also adequate time has been provided to ensure proper saturation of the sample.

Axial displacement, axial load and excess pore water pressure was recorded continuously during the test. The recorded data were processed and finally the liquefaction potential was provided in terms of number of cycles to failure and the variation was studied with three different parameters viz, relative density, cyclic shear strain and initial effective confining pressure.

Finally a semi-empirical hyperbolic model has been proposed for prediction of pore pressure generation with respect to number of elapsed cycle.

Table of Contents:

List of Figures

List of Tables

SYMBOLS USED

τ_{ave} = cyclic shear stress

σ_{vo}' = effective vertical overburden stresses

σ_{vo} = total vertical overburden stresses

a_{max} = peak horizontal ground acceleration

g = acceleration due to gravity

r_d = stress reduction factor

z = depth from ground level

$(N1)_{60}$ = the SPT blow count normalized to an overburden pressure of approximately 100 kPa and a hammer energy ratio or hammer efficiency of 60%

Nm = measured SPT value from field

C_N = factor to normalize Nm to a common reference effective overburden stress

$= (Pa/\sigma_{vo}')^{0.5} \leq 1.$

C_E = Correction for hammer energy ratio

C_B = Correction for Borehole dia.

C_R = Correction for rod length

C_S = Correction for samplers with/ without liners

$(N1)_{60CS}$ = an equivalent clean sand value $(N1)_{60}$

α and β = coefficients for fine content

FC = Fine Content

K_s = the bulk modulus of the solid skeleton

K_w = the bulk modulus of the water

n = porosity of soil

s = degree of saturation

u = pore water pressure

R_d = Relative Density

σ_{3c}' = effective confining pressure

K_σ = Stress Correction Factor

K_α = initial shear effect correction factor

MSF = Magnitude Scaling Factors

G_s = Specific gravity of soil solid

D_{50} = Mean grain size

D_{10} = Diameter corresponding to 10% finer

D_{60} = Diameter corresponding to 60% finer

GSD = Grain Size Distribution

C_u = Coefficient of uniformity

C_c = Coefficient of curvature

e_{max} = Maximum void ratio

e_{min} = Minimum void ratio

γ_{dmax} = Maximum dry density

γ_{dmin} = Minimum dry density

γ = Achieved density of the sample after saturation

γ_d = dry density of the soil

W = Weight of the sample at a particular moisture content

V = Volume of the sample

Ds = diameter of specimen

Hs = height of specimen

w = Water content (%)

σ_d = deviator stress

σ_1 = the major principal stress

σ_3 = the minor principal stress

σ_1' = the major effective principal stress

σ_3' = the minor effective principal stress

ε = Axial Strain

f = frequency

e = Void ratio of the sample

γ_w = density of water

N= Number of cycles

N_f = Number of cycles required to failure

Δu= change in pore pressure

CHAPTER 1

INTRODUCTION

1.1 Background

Liquefaction is one of the most important, interesting, complex and controversial topics in Geotechnical Earthquake Engineering. Its devastating effects got the attention of Geotechnical Engineers in a 3 months period in 1964 when the Good Friday Earthquake (M_W = 9.2) in Alaska was followed by the Niigata Earthquake (M_S = 7.5) in Japan. Both of these earthquakes caused spectacular examples of liquefaction-induced damage, including slope failures, bridge and building foundation failure and floatation of buried structures. Since then liquefaction has been studied extensively by hundreds of researchers around the world.

Liquefaction denotes a condition when a soil will undergo continued deformation at a constant low residual stress or with no residual resistance, due to the build-up and maintenance of high pore water pressure which reduces the effective confining pressure to a very low value.

Due to the increase of pore water pressure, effective stress decreases. When the excess pore water pressure equals the effective overburden pressure, the resulting effective stress becomes zero and the soil flows like a liquid which is termed as **complete liquefaction**. If there is some amount of resultant effective stress, it is called **partial liquefaction**.

1.2 Mechanism of Liquefaction

The strength of sand is primarily due to internal friction. In saturated state it may be expressed as (Fig 1.1)

$$S = \overline{\sigma_n} \tan \Phi \qquad (1.1)$$

Where, S = Shear strength of sand

$\overline{\sigma_n}$ = Effective normal pressure on any plane x-x at depth Z

$= \gamma h_w + \gamma_{sub} (Z-h_w)$

Φ = Angle of internal friction

γ = Unit weight of soil above water

γ_{sub}= Submerged unit weight of soil.

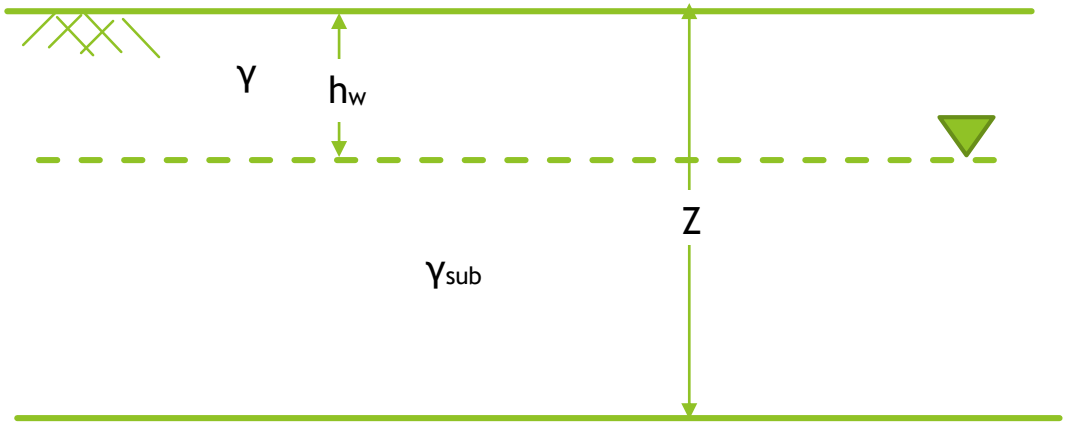

Fig 1.1 : Section of ground showing the position of water table

If a saturated sand is vibrated, it tends to compact and decrease in volume. If drainage is restrained the tendency to decrease in volume results in an increase in pore pressure. The strength may now be expressed as,

$$S_{dyn} = (\overline{\sigma_n} - u_{dyn}) \tan \Phi_{dyn} \qquad (1.2)$$

Where,

S_{dyn} = Shear strength of soil under vibration

u_{dyn} = Excess pore water pressure due to ground vibration

Φ_{dyn} = Angle of internal friction under dynamic condition

It is seen that with development of additional positive pore pressure, the strength of sand is reduced. In sands, Φ_{dyn} is almost equal to Φ, i.e. angle of internal friction in static conditions.

For complete loss of strength i.e. S_{dyn} is zero.

Thus, $\overline{\sigma_n} - u_{dyn} = 0$

Or, $\overline{\sigma_n} = u_{dyn}$

Or, $\frac{u_{dyn}}{\overline{\sigma_n}} = 1 \qquad (1.3)$

Expressing u_{dyn} in terms of rise in water head, h_w

i.e. $u_{dyn} = \gamma_w \times h_w$

and $\overline{\sigma_n} = \left(\frac{G-1}{1+e}\gamma_w\right) Z$

Putting in equation (1.3), $\frac{h_w}{Z} = \frac{G-1}{1+e} = i_{cr} \qquad (1.4)$

Where,

G = Specific gravity of soil particles

e = Void ratio

i_{cr} = Critical hydraulic gradient

Thus, a soil deposit that is liquefied behaves like a better known phenomena: *"quicksand"*. Due to the forces exerted by gravity, soil particles naturally rest upon each other and, depending on the properties of the soil, form sort of grid that is relatively stable (or can be made so by compaction or other construction practices). During liquefaction the water pressures become high enough to counteract the gravitational pull on the soil particles and effectively '*float*', or suspend, the particles. The soil particles can then move freely with respect to each other. Since the soil is no longer behaving as an inactive grid of particles, the strength and stiffness of a liquefied soil is significantly decreased, often resulting in a variety of structural failures.

1.3 Which soils are likely to liquefy?

1.3.1 Loose Sand

A loose dry sand subjected to shaking (i.e cyclic shearing) would be expected to reduce in volume, as particles are given the energy to drop inter-particle voids (Fig 1.2a). If the soil is instead saturated and these voids are filled up with water, then the timescales are insufficient to allow the sand particles to drop into the gaps during shaking. In other words, an undrained response with no volume change occurs (Fig 1.2b). Soil particles lose contact and effective stress reduces. Excess pore pressure rises as the floating grains pressurize the fluid. At zero effective stress, looser soils are entirely in a state of sedimentation, as postulated by Florin & Ivanov (1961). Shear strength is reduced greatly and large settlements occur. This phenomenon is called complete liquefaction. Only after a period of time long enough to allow the fluid to drain away will the excess pore pressure dissipate and the grains regain contact.

The generation of pore pressure has been investigated by Seed et al. (1976) by cyclic laboratory tests. N/N_{liq} is the ratio between current cycle number to the number of cycles at the current shear stress level required to cause full liquefaction. r_u is the "excess pore pressure ratio", defined in Equation 1.5 as the ratio between excess pore pressure $\bar{u}$ and initial vertical effective stress σ_{v0}', and is a frequently used term in liquefaction problems because it equals 0 before shaking and 1 at complete liquefaction. The relationship between the two is given by Equation 1.6, which models a rapid initial rise and a rapid final rise in excess pore pressure. Parameter α should be approximately 0.7. A similar curve is used for design purposes in Japan, by the PHRI (1997).

$$r_u = \frac{\bar{u}}{\overline{\sigma_{v0}}} \qquad (1.5)$$

$$r_u = \frac{1}{2} + \frac{1}{\pi} \sin^{-1}\left[2\left(\frac{N}{N_l}\right)^{1/\alpha} - 1\right] \qquad (1.6)$$

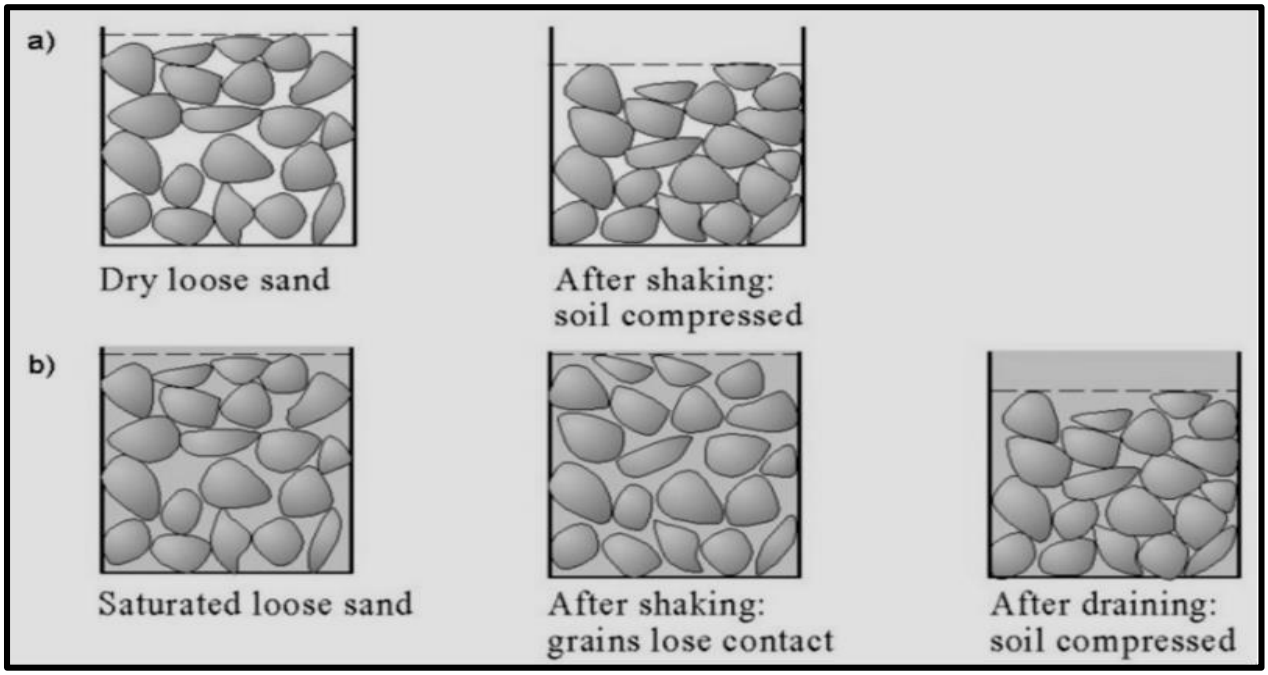

Fig 1.2 : Schematic behaviour of loose sand particles under rapid shaking

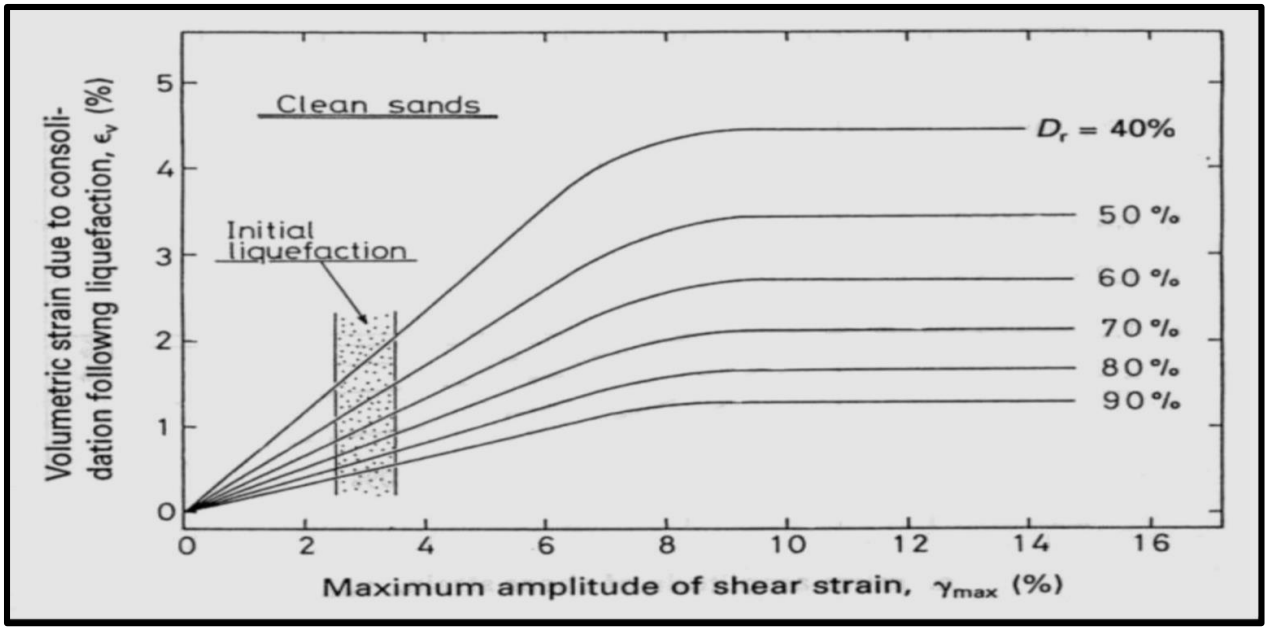

Fig 1.3 : Relationship between Shear Strain & Volumetric Strain in Liquefaction events, from Ishihara (1985)

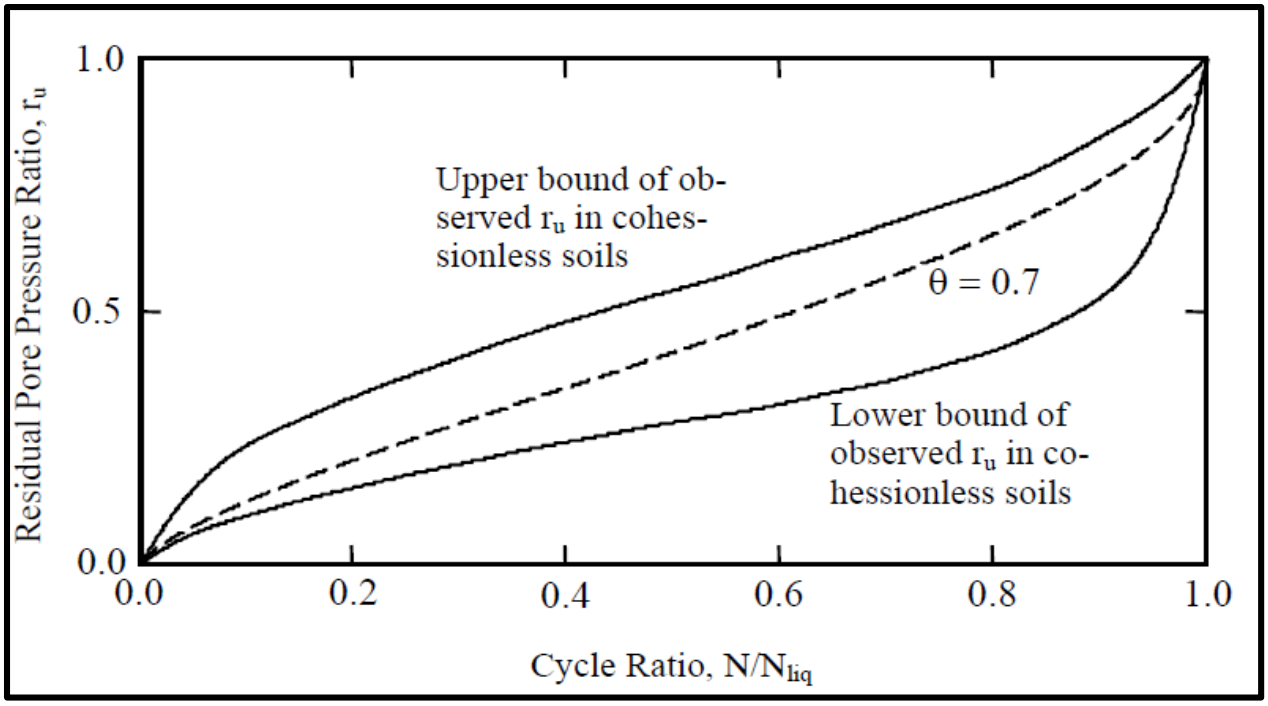

Fig 1.4 : Observed bounds of excess pore pressure generation as a function of cycle ratio and approximate average of bounds given by equation 1.6 when α = 0.7

1.3.2 Dense Sand

Dense sands under shearing experience an initial volume drop followed by an increase in volume as the particles ride over each other. The soil dilates. As demonstrated by Seed and Lee (1966) and others, dense saturated sands under shaking can also generate large excess pore pressures. A difference in behaviour is observed when shear is applied to the soil; attempting to shear dense sands in this condition causes the soil to dilate. This means that the soil attempts to increase in volume (rather than decrease), dropping the excess pore pressure and increasing the effective stress (and hence strength). Dense sands differ because, even when they generate these large excess pore pressures, they do not exhibit catastrophic failures as they regain strength rapidly when sheared. This state is therefore not called liquefaction but variously **"cyclic mobility"** (Castro, 1975) or **"liquefaction with limited strain potential"** (Seed, 1976).

1.4 Liquefaction Related Phenomena

1.4.1 Flow Liquefaction

Flow liquefaction produces most dramatic effects of all the liquefaction related phenomena— tremendous instabilities known as *flow failure*. Flow liquefaction can

occur when the shear stress required for static equilibrium of a soil mass (the static shear stress) is greater than the shear strength of the soil in its liquefied state. Once triggered the large deformations produced by Flow liquefaction are actually driven by static shear stresses. The cyclic stresses may simply bring the soil to an unstable state at which its strength drops sufficiently to allow the static stresses to produce the flow failure. Flow liquefaction failures are characterised by sudden nature of their origin, the speed of their development and the large distance over which the liquefiable materials often move. E.g. the flow-side failure of Sheffield Dam and Lower San Fernando Dam.

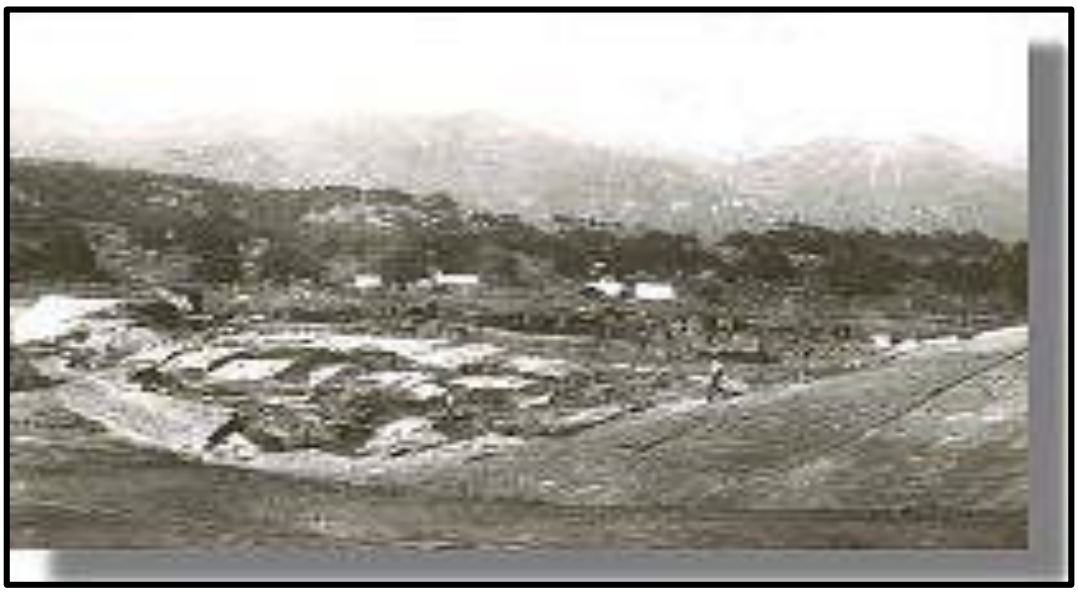

Fig 1.5 : Liquefaction failure of Sheffield Dam in the 1925 Santa Barbara Earthquake

Fig 1.6 : Liquefaction failure of upstream slope of lower San Fernando Dam in 1971 San Fernando earthquake

1.4.2 Cyclic Mobility

Cyclic Mobility is another phenomenon of Liquefaction that can produce unacceptably large permanent deformations during earthquake shaking. In contrast to flow liquefaction, cyclic mobility occurs when the static shear stress is less than the shear strength of the liquefied soil. The deformations produced by cyclic mobility failures develop incrementally during earthquake shaking. The deformations produced by cyclic mobility are driven by both cyclic and static shear stresses. These deformations, termed "*Lateral Spreading*", can occur on very gently sloping ground or on virtually flat ground adjacent to water bodies (Fig 1.6). When structures are present, lateral spreading can cause significant damage as in the case of Showa Bridge failure in Japan following to Niigata Earthquake of 1964 (Fig 1.7).

Fig 1.7 : Lateral spreading of very flat ground towards the Motagua River following the 1976 Guatemala Earthquake

Fig 1.8 : Failure of Showa bridge following the 1964 Niigata earthquake

A special case of cyclic mobility is **"level-ground liquefaction"**. Because static horizontal shear stresses that could drive lateral deformations do not exist, level-ground liquefaction can produce large, chaotic movement known as ground oscillation during earthquake shaking, but produces little permanent lateral soil movement. Level-ground liquefaction failures are caused by the upward flow of water that occurs when seismically induced excess pore pressure dissipate. Excessive vertical settlement and consequent flooding of low-lying land and the development of "*sand boils*" (Fig 1.8) are characteristics of level-ground liquefaction failure.

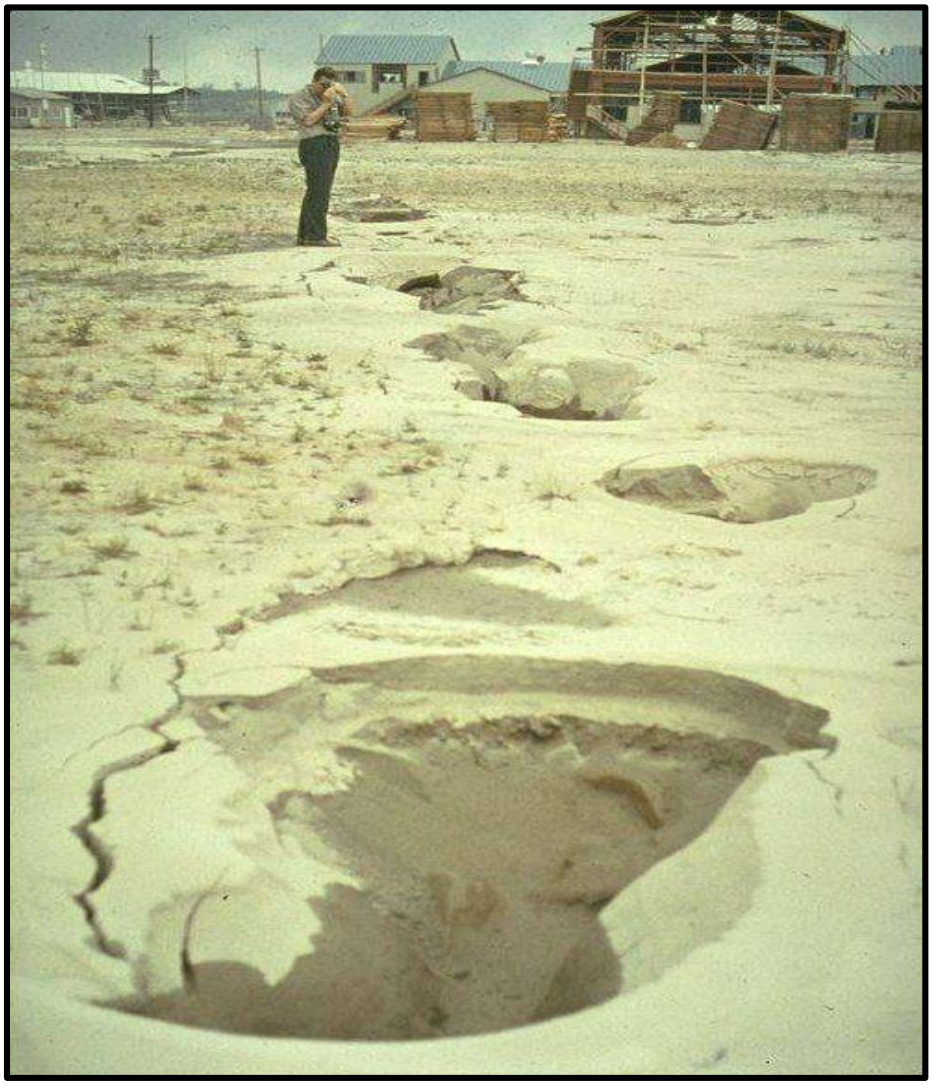

Fig 1.9 : Sand Boils near Niigata, Japan following 1964 Niigata Earthquake

1.5 Relevance of the Thesis Work

Now-a-days Kolkata is developing in a great pace. A huge number of skyscrapers requiring large length of piles, bridges which require pier foundation, well foundation and embankments are being constructed in and around Kolkata. The city of Kolkata is located on the left bank of river Hooghly. The city comes under the seismic zone III (IS-1893:2002 (part-I)) with its adjacent areas under a higher seismic zone IV. The soil deposit in Kolkata can be classified into 3 categories:

(1) **Normal Kolkata Deposit:** Soil contain mostly silty clay or clayey silt with lamination.
(2) **River Channel Deposit:** Soil contains silty fine sand down to considerable depth mainly along Adi Ganga channel / Tolly Nala.
(3) **Reclaimed Land:** Consists of fine sand in top layer and after a few metre, soil layer consists of silty soil. Salt Lake area is a kind of reclaimed land.

Chakraborti, Pandey, Mukherjee, Bhargava(2004) reported that soils down to a depth of 10.0m **in** some areas of the Southern parts of the city like Tollygunge, Behala, Kalighat have liquefaction potential of more than 1 at the PGA level of 0.2g. This indicates that liquefaction may cause damage to the structures during earthquake, if the effect of these are not incorporated in the analysis and design.

CHAPTER 2

REVIEW OF LITERATURE

2.1 General

A limited number of research works have been carried out by different investigators in the recent past to understand the effect of liquefaction on granular soil (sand and gravel) also granular soil mixed with fine content especially silt. Investigators have carried out laboratory tests (e.g. Cyclic Triaxial Test, Cyclic Simple Shear Test, Cyclic Torsional Shear Test, Shake Table Test etc.) and performed in-situ tests (e.g. Blasting Test, Shear Wave Velocity Test, Vibratory Pile Driving Test etc.) to understand the changes in soil properties, the interaction mechanism of liquefaction and possible remediation techniques to either limit the problem or completely remove from the soil. Internationally accepted calculation for liquefaction potential of soil has been proposed by Seed and Idriss, 1971.

2.2 Liquefaction Susceptibility

2.2.1 Historical Criteria

From post-earthquake field investigations, it is seen that liquefaction often recurs at the same location when soil and ground water condition remain unchanged (Youd, 1984a). Youd (1991) described a number of instances where historical evidence of liquefaction has been used to map liquefaction susceptibility.

Post-earthquake field investigations have also shown that liquefaction effects have historically been confined to a zone within a particular distance of the seismic source. The distance to which liquefaction can be expected increases dramatically with increasing magnitude. Ambraseys (1988) compiled worldwide data for shallow earthquakes and developed a chart showing the limiting epicentral distances beyond which liquefaction has not been observed vs earthquakes of different magnitude (Fig 2.1).

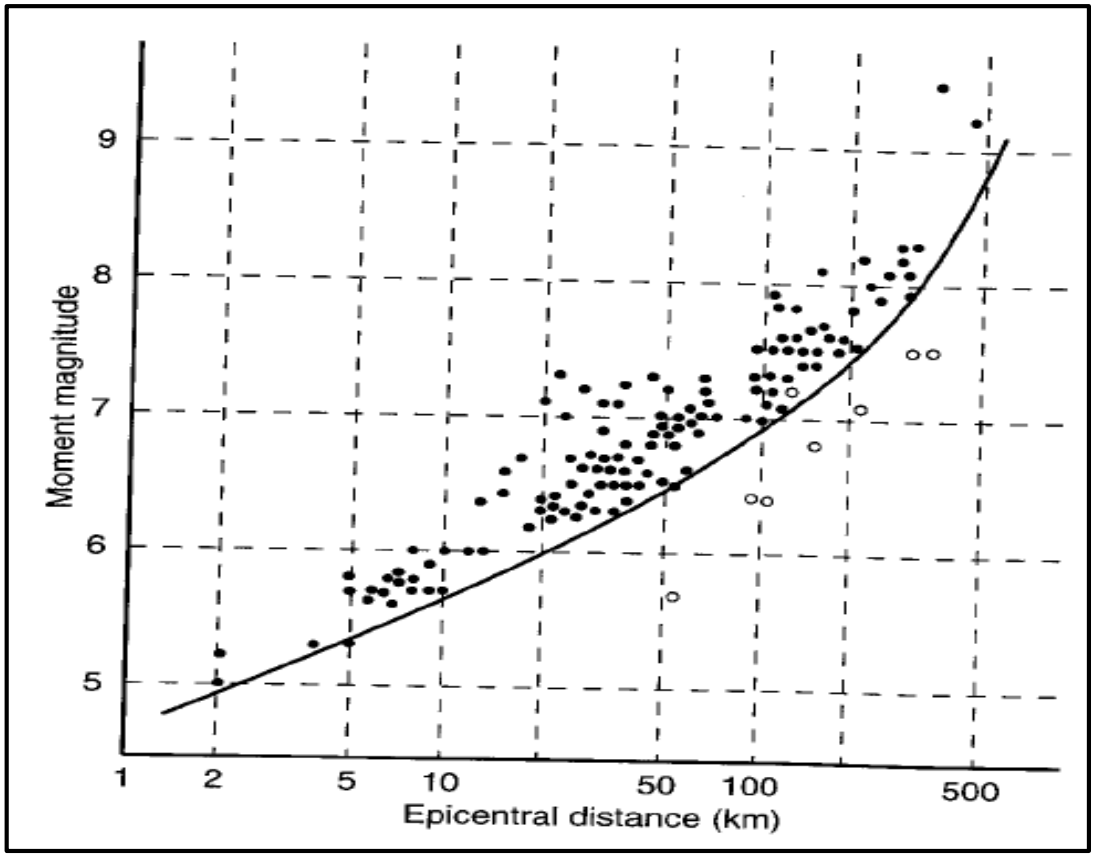

Fig 2.1 : Limiting Epicentral Distance vs Earthquake Magnitude, Ambraseys (1988)

2.2.2 Geologic Criteria

The depositional environment, hydrologic environment and age of a soil deposit contribute to its liquefaction susceptibility (Youd and Hoose, 1977).

Geologic processes that sort soils into uniform grain size distributions and deposit them in loose states produce high liquefaction susceptibility. Consequently, fluvial deposits, and colluvial & aeolin deposits when saturated, are likely to be susceptible to liquefaction.

Liquefaction occurs only in case of saturated soils, so the depth to ground water influences liquefaction susceptibility. Liquefaction susceptibility decreases with increasing ground water depth.

2.2.3 Compositional Criteria

Since liquefaction requires the development of excess pore pressure, liquefaction susceptibility is influenced by the compositional characteristics that influence volume change behavior. Compositional characteristics associated with high volume

change potential tend to be associated with high liquefaction susceptibility. These characteristics include particle size, shape and gradation.

For many years, the liquefaction related phenomena were thought to be limited to sands. Fine grained soil is considered incapable of generating the high pore pressure associated with liquefaction; and coarser grained soils were considered too permeable to sustain any excess pore pressure long enough for liquefaction to develop. But more recently, the bounds of gradation criteria for liquefaction susceptibility has been extended.

Liquefaction of non-plastic silts has been observed (Ishihara, 1984) in the laboratory and the field, indicating plasticity characteristics rather than grain size alone influence the liquefaction susceptibility of fine-grained soil. Coarse silt which are nonplastic & cohesionless are fully susceptible to liquefaction (Ishihara, 1993). Finer silts with flaky particles generally exhibit sufficient cohesion to inhibit liquefaction. Clays remain non susceptible to liquefaction, although sensitive clays can exhibit strain-softening behavior similar to that of a liquefied soil.

Fine grained soil which satisfy the following four Chinese criteria (Wang, 1979) may be considered susceptible to liquefaction.

- Fraction finer than 0.005mm ≤ 15%
- Liquid limit (LL) ≤ 35%
- Natural water content (NMC) ≥ 0.9LL
- Liquidity index ≤ 0.75

2.2.4 State Criteria

Even if a soil meets all the preceding criteria for liquefaction susceptibility, it still may not be susceptible to liquefaction as it also depends upon the initial state of the soil *i.e.* its stress and density characteristics at the time of the earthquake.

Casagrande (1936) performed drained, strain-controlled triaxial tests on initially loose & dense sand specimens. The results showed that at large strains, all specimens approached the same density and continued to shear with constant shearing resistance. The void ratio corresponding to this constant density is termed as the "*Critical Void Ratio (CVR)*". By performing the test at different confining pressure, Casagrande found that the CVR was uniquely related to the effective confining pressure, and called the locus of the "*Critical Void Ratio Line*".

By defining the state of the soil in terms of void ratio and effective confining pressure, the CVR line could be used to mark the boundary between loose (contractive) and dense (dilative) states.

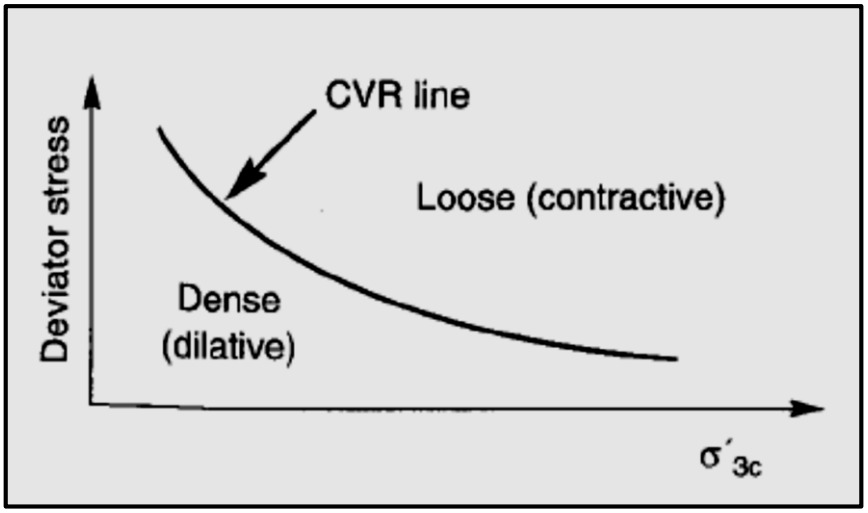

Fig 2.2 : CVR line as a boundary between Contractive & Dilative state of soil

Since the CVR line marked the boundary between the contractive and dilative behavior, it was considered to mark the boundary between states in which a particular soil was or was not susceptible to flow liquefaction. Saturated soils with initial void ratios high enough to plot above CVR line were considered susceptible to flow liquefaction and soils with initial states plotting below the CVR line were considered non-susceptible.

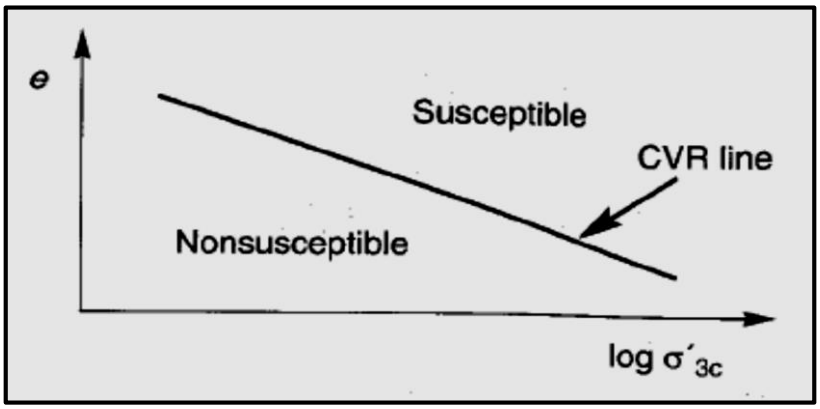

Fig 2.3 : CVR line as boundary between liquefaction susceptibility & non-susceptibility

2.3 Evaluation of Liquefaction Potential

2.3.1 H.B. Seed & I.M. Idriss (1971) Method

The steps for determining the Liquefaction Potential of cohesionless soil are given as below:

(i) The evaluation of Vertical Stress σ_{v0} & effective vertical stress σ'_{v0} at the desired depth.

(ii) Calculation of stress reduction coefficient r_d as per Blake (1996) for any depth z by the following equation:

$$r_d = \frac{1-0.4113Z^{0.5}+0.04052Z+0.001753Z^{1.5}}{1-0.4177Z^{0.5}+0.05729Z-0.006205Z^{1.5}+0.00121Z^{2}}$$

(iii) Calculation of equivalent uniform cyclic shear stress (τ_{avg}) induced by earthquake using "Simplified Procedure" by Seed & Idriss (1971)

$$\tau_{avg} = 0.65 \times \sigma_0 \times (a_{max}/g) \times r_d$$

Where, σ_0 = Total vertical Stress

r_d = Stress reduction factor

a_{max} = Maximum ground acceleration

g = Acceleration due to gravity.

(iv) Estimation of Cyclic Stress Ratio (CSR) as below:

$CSR = \tau_{avg}/\sigma_0'$ Where, σ_0' is the effective vertical stress.

(v) Evaluation of $(N_1)_{60}$ from available N_m (SPT) value by application of the following correction factors proposed by Youd et al. (2001)

$$(N_1)_{60} = N_m\, C_N\, C_E\, C_B\, C_R\, C_S$$

These correction factors are given in table 2.1 by Idriss (2001)

Table : 2.1 Corrections as per Idriss, I.M (2001)

Factor	Equipment Variable	Term Correction
Overburden Pressure		$C_N = 0.77\log_{10}(2000/\sigma_0')$ σ_0' is in KN/m^2
Energy Ratio	Donut hammer	C_E = 0.50 to 1.00
	Safety hammer	C_E = 0.70 to 1.20
	Automatic-trip Donut	C_E = 0.80 to 1.30
Borehole Diameter	65-115 mm	C_B = 1.00
	150 mm	C_B = 1.05
	200 mm	C_B = 1.15
Factor	**Equipment Variable**	**Term Correction**
Rod Length	< 3m	C_R = 0.75
	3 - 4m	C_R = 0.80
	4 - 6m	C_R = 0.85
	6 – 10m	C_R = 0.95
	10 – 30m	C_R = 1.00
Sampling Method	Standard Sampler	C_S = 1.00
	Sampler without liner	C_S = 1.10 to 1.30

(vi) Estimation of Cyclic Resistance Ratio (CRR) using the Formula suggested by Roach (1998) for earthquake magnitude of 7.5

$$CRR\,|\,M=7.5 = \frac{1}{34-(N1)_{60CS}} + \frac{(N1)_{60CS}}{135} + \frac{50}{[10\times(N1)_{60CS}+45]^2} - \frac{1}{200}$$

Where, $(N1)_{60CS}$ = Equivalent clean sand value of $(N1)_{60}$

$$(N1)_{60CS} = \alpha + \beta(N1)_{60}$$

Where, α & β are determined as mentioned below:

α = 0 for fine content (FC) < 5%

α = exp [1.76-(190/FC^2)] for 5% < FC < 35%

α = 5.0 for FC > 35%

β = 1 for FC < 5%

β = [0.99 + $(FC)^{1.5}$/1000] for 5% < FC < 35%

β = 1.2 for FC > 35%

For earthquakes of magnitude other than 7.5, this value of CRR to be multiplied by a Magnitude Scaling Factor (MSF)

[CRR | for any M] = [CRR | M=7.5 × MSF]

These factors are proposed by Seed & Idriss and given in Table 2.2.

Table 2.2: Magnitude Scaling Factor Values

Magnitude	Seed and Idriss (1982)	Idriss (1998)
5.5	1.43	2.2
6	1.32	1.76
6.5	1.19	1.44
7	1.08	1.19
7.5	1	1
8	0.94	0.84
8.5	0.89	0.72

(vii) Correction (K_a) due to effective overburden pressure applied to CRR | M=7.5

If effective overburden pressure is less than 100 KN/m^2, the correction is unity. But it decreases with increase in effective overburden pressure. The correction factor (K_a) is taken as:

$$(K_a) = [(\sigma_{vo}')/100]^{(f-1)}$$

Where, f is an exponent and assumes the value of 0.6 to 0.8 for R_D = 80% to 60%

$CRR \mid M=7.5_{(corrected)} = K_a\ (CRR \mid M=7.5)$

(viii) The last step is to find the Factor of Safety against liquefaction using the relation; FS = (CRR)/(CSR)

If this FS becomes < 1, the soil is susceptible to liquefaction.

2.3.2 Euro code-8 Approach

Step-1: The cyclic shear stress is calculated as:

$$\tau_e = 0.65\times(a_{max}/g)\times S\times\sigma_v$$

Where, S is the soil parameter defined in clause 4.2.2 of Part 1-1 which depends upon the soil types (A,B,C or D). [given in Table 2.3]

The other notations bear the same meaning as that of Seed & Idriss Method.

Table 2.3: Different types of ground (Eurocode 8)

Ground type	Description of stratigraphic profile	Parameters		
		$v_{s,30}$ (m/s)	N_{SPT} (blows/30cm)	c_u (kPa)
A	Rock or other rock-like geological formation, including at most 5 m of weaker material at the surface.	> 800	–	–
B	Deposits of very dense sand, gravel, or very stiff clay, at least several tens of metres in thickness, characterised by a gradual increase of mechanical properties with depth.	360 – 800	> 50	> 250
C	Deep deposits of dense or medium-dense sand, gravel or stiff clay with thickness from several tens to many hundreds of metres.	180 – 360	15 - 50	70 - 250
D	Deposits of loose-to-medium cohesionless soil (with or without some soft cohesive layers), or of predominantly soft-to-firm cohesive soil.	< 180	< 15	< 70
E	A soil profile consisting of a surface alluvium layer with v_s values of type C or D and thickness varying between about 5 m and 20 m, underlain by stiffer material with v_s > 800 m/s.			
S_1	Deposits consisting, or containing a layer at least 10 m thick, of soft clays/silts with a high plasticity index (PI > 40) and high water content	< 100 (indicative)	–	10 - 20
S_2	Deposits of liquefiable soils, of sensitive clays, or any other soil profile not included in types A – E or S_1			

The values of S parameters are defined based on types of response spectra.

For type 1 : for larger events > 5.5 M_L and unknown deep geology

For type 2 : for smaller events < 5.5 M_L and unknown deep geology

Table 2.4: Values of S parameter for type 1 elastic response spectra

Ground type	S	T_B (s)	T_C (s)	T_D (s)
A	1,0	0,15	0,4	2,0
B	1,2	0,15	0,5	2,0
C	1,15	0,20	0,6	2,0
D	1,35	0,20	0,8	2,0
E	1,4	0,15	0,5	2,0

Table 2.5: Values of S parameter for type 2 elastic response spectra

Ground type	S	T_B (s)	T_C (s)	T_D (s)
A	1,0	0,05	0,25	1,2
B	1,35	0,05	0,25	1,2
C	1,5	0,10	0,25	1,2
D	1,8	0,10	0,30	1,2
E	1,6	0,05	0,25	1,2

Step-2: The SPT data to be normalized to a reference effective overburden pressure of 100 kPa and to a 60% ratio of impact energy over theoretical free fall energy. For depth less than 3m, the measured SPT value should be reduced by 25%. To normalize with respect to the effective overburden pressure, the measured SPT data needs to be multiplied by a factor of $(\frac{100}{\sigma_{v'}})^{0.5}$ where σ'v (kPa) is the effective overburden pressure acting at a depth where SPT measurement has been carried out.

Step3: Energy normalization must be carried out by multiplying the measured SPT data by the factor of ER/60, where ER= (Measured Energy Ratio)×100% and the normalized SPT data has been denoted by $N_{1(60)}$. In Europe, ER is typically 70%.

Step 2 & Step 3 can be written as:

$$(N_1)_{60} = N_{SPT}\sqrt{\frac{100}{\sigma_{v'}}}\left(\frac{ER}{60}\right)$$

Step-4: Determination of Cyclic Stress Ratio (CSR)= (τ_c/σ_v') from the chart (Fig 2.4) given in Euro code 8 (CSR vs $(N_1)_{60}$) for earthquake magnitude of 7.5. Thereby the critical shear stress (τ_c) is calculated. For other magnitudes of earthquake, this value of CSR needs to be multiplied by a factor CM.

Table 2.6: Multiplication factor (CM) for CSR determination

M_S	CM
5.5	2.86
6.0	2.20
6.5	1.69
7.0	1.30
8.0	0.67

Step-5: A soil has been considered susceptible to liquefaction whenever the earthquake-induced shear stress (from Step1) exceeds 80% of the critical stress (from Step 4). In other words, the recommended Factor of Safety is 1.25.

i.e. $\tau_c/\tau_e = 1.25$ for non-susceptibility of liquefaction.

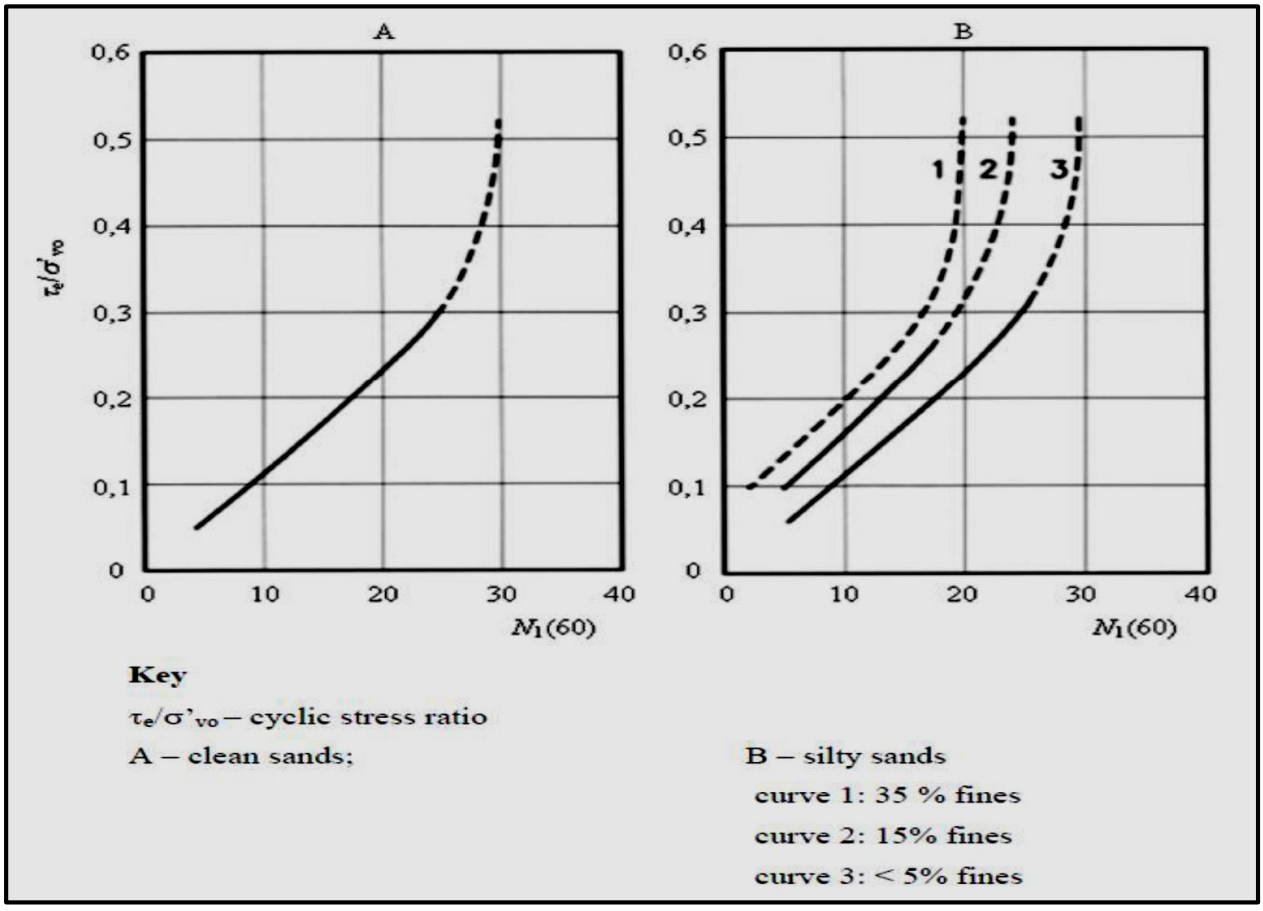

Fig 2.4 : Stress Ratio causing Liquefaction and N_{60} relationship (Euro code 8)

2.4 Literature Review

Several research works have been carried out in past years about geotechnical earthquake engineering, especially liquefaction. Some of previous works of some renowned researchers have been discussed below:

2.4.1 Theoretical Work

2.4.1.1 Kenji Ishihara (1974)

Ishihara (1974) studied case history of some major earthquakes in Japan viz, The Great Kanto Earthquake of 1923; Fukui Earthquake of 1948; Niigata Earthquake of 1964 and then three soil profiles most prone to liquefaction were suggested by him. These three types of soil deposits are:

i) Sand deposits

ii) Sandwiched sand deposits on top of and underneath this sand layer are silt or clay strata.

iii) Thin sand layer lying on gravelly sand

From the test data using triaxial test, the simple shear test and the torsional shear test the results obtained are discussed below:

1. The maximum stress ratio, τ_{max}/σ_0 at each depth, to which the soil elements have been subjected was determined where τ_{max} is maximum shear stress and σ_0 overburden pressure.

2. Resistance to liquefaction at any relative density can be evaluated.

3. The data shown in **Figure 2.5** not only yield the resistance to liquefaction, but more generally, the stress ratios which are required to cause a certain magnitude of residual pore pressure.

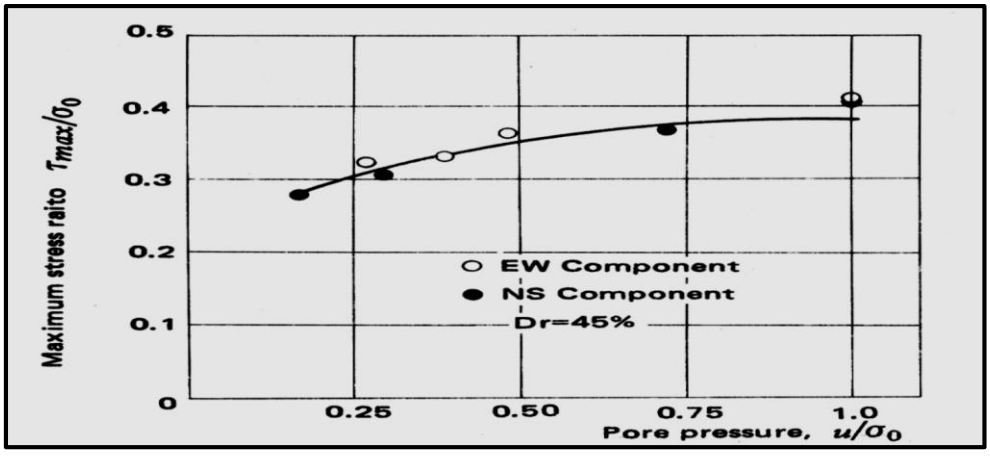

Fig 2.5 : Relation between the maximum stress ratio and residual pore pressure using the records of the Niigata Earthquake (Kawagishi-cho apartment).

2.4.1.2 Andrews et al. (2000)

Desmond C A Andrews & Geoffrey R Martin investigated simple criteria based on "key" soil parameters that help partition liquefiable and non-liquefiable silty soils. Silt can be seen as a very fine sand of size finer 0.074mm. That's why silt cannot be seen in naked eye and for this it is assumed that there is not very significantly different physical properties between sand and silt.
Clay bears little resemblance to sand and silt. The grain size boundary between silt and clay is taken as 0.002mm. In China and Japan, this boundary is set at 0.005mm. Significantly most grains finer than 0.002mm tend to comprise of clay minerals and most grains coarser than 0.002mm tend to comprise of rock-forming mineral.

Seed et al.(1983) outlined the criteria based on case histories in China, Wang (1979) for the liquefaction susceptibility of fine grained soil.

- Clay Content (finer than 0.005mm) < 15%
- Liquid limit (LL) < 35%
- Water Content > 0.9×LL

Andrews et al. modified the above criteria as:

- If clay is to be defined as finer than 0.002mm, then the cut off for liquefaction susceptibility stands at 10%
- Also liquid limit should be < 32%

Clay content can be regarded as a "key" soil parameter that partitions a liquefiable and non-liquefiable silty soil.
Liquid limit can be regarded as a "key" soil parameter that partitions a liquefiable and non-liquefiable silty soil.
Water content is not considered as a "key" soil parameter due to its sensitivity to fluctuating environmental factors and errors arising during soil sampling.

Table 2.7: Liquefaction Susceptibility of Silty Soil

	Liquid Limit < 32%	Liquid Limit ≥ 32%
Clay Content < 10%	Susceptible	Further studies required (Considering plastic non-clay sized grains- such as mica)
Clay Content ≥ 10%	Further studies required (Considering non plastic clay sized grains – such as mine & quarry tailings)	Not Susceptible

2.4.1.3 Chakraborty et al. (2004)

Chakraborty, Pandey, Mukherjee & Bhargava had done extensive analysis using Artificial Neural Network (ANN) technique for determination of liquefaction potential at different locations in and around Kolkata city for different PGA levels. From the analysis, it was seen that the river channel deposits are the most vulnerable to liquefaction.

They had divided the city deposits into 3 broad categories:

(1) **Normal Kolkata Deposit:** Soil contain mostly silty clay or clayey silt with lamination.

(2) **River Channel Deposit:** Soil contains fine sand in top layer.

(3) **Reclaimed Land:** Consists of fine sand in top layer and after a few metre, soil layer consists of silty soil. Salt Lake area is a kind of reclaimed land.

They have divided Kolkata into several equipotential contour zones (liquefaction lines) for different depths with different PGA levels.

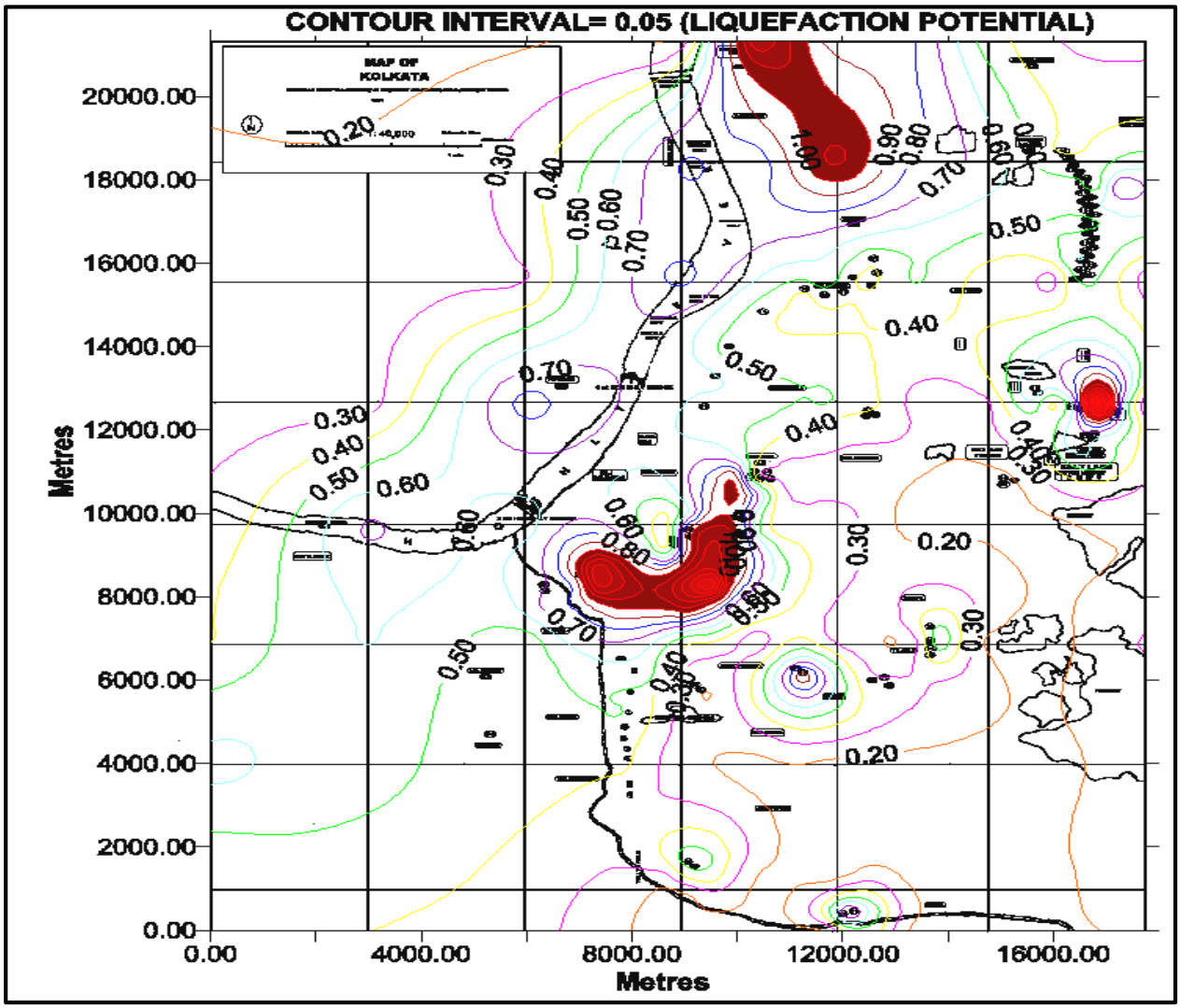

Fig 2.6 : Liquefaction potential map of Kolkata at 2.5m depth for PGA of 0.15g

As per their analysis, the assessment regarding the liquefaction potential for different Kolkata deposit is that:

- River Channel deposit in South Kolkata area like Tollygunge, Kasba are found to be most susceptible to liquefaction. Extra care should be taken against liquefaction during construction of a structure upon this type of deposit.

- The Salt Lake region being a reclaimed area has a top layer of very loose fine sand followed by soft to medium stiff / loose sandy silt or clayey silt mixed with decayed vegetation and this soil is also susceptible to liquefaction.

- The Normal Kolkata deposit in central Kolkata areas like Beliaghata, Sealdah generally are less susceptible to liquefaction.

- From the study it is also concluded that if an earthquake of magnitude more than or equal to 7 on Richter Scale occurs in Kolkata or adjacent region then most of the areas will be extensively damaged due to liquefaction while only some part of Central Kolkata will be marginally damaged due to liquefaction at that magnitude.

2.4.2 Laboratory based Experimental Work

2.4.2.1 Chen et al. (1992)

Chen and Liao (1992) obtained the effects of stress path, fines content, and over-consolidation ratio (OCR) on the steady state line by performing undrained cyclic triaxial tests.

The results obtained from the tests are discussed below:

A) Results of Steady State Tests

i) The steady state shear strength from compression tests is slightly larger than that from extension tests.

ii) The steady state line shifts leftward and downward with increasing fines content. The slope of the steady state line decreases with increasing fines content (FC).

iii) Over consolidation ratio has no effects on the steady state line.

B) Results of liquefaction resistance

i) Liquefaction resistance increases with increasing relative density more or less linearly for the range of 40 to 70%.

ii) Samples with higher OCR would have higher liquefaction resistance.

iii) Increasing fines content would decrease the liquefaction resistance.

C) Relation between state parameter and liquefaction resistance

i) Liquefaction resistance decreases more or less linearly with increasing state parameter.

ii) Over consolidation has no effect on the steady state line but affects the liquefaction resistance a lot.

2.4.2.2 Chien et al.(2000)

Lien-Kwei Chien, Yan-Nam Oh and Chih-Hsin Chang experimented with filled material in Yun-Lin near shore in west Taiwan and obtained the liquefaction resistance and liquefaction induced settlement for reclaimed soil.

The experimental analysis & results are given below:

A) Influence of Fines content on liquefaction resistance of reclaimed soil.

Fines content of reclaimed soil is one of most influence factors. Therefore, in this study, in order to understand the influence of fines content, a series of liquefaction test was performed with different fine contents (as FC = 0% to 30%) and different relative densities (as Dr 35%, 55%, and 75%).

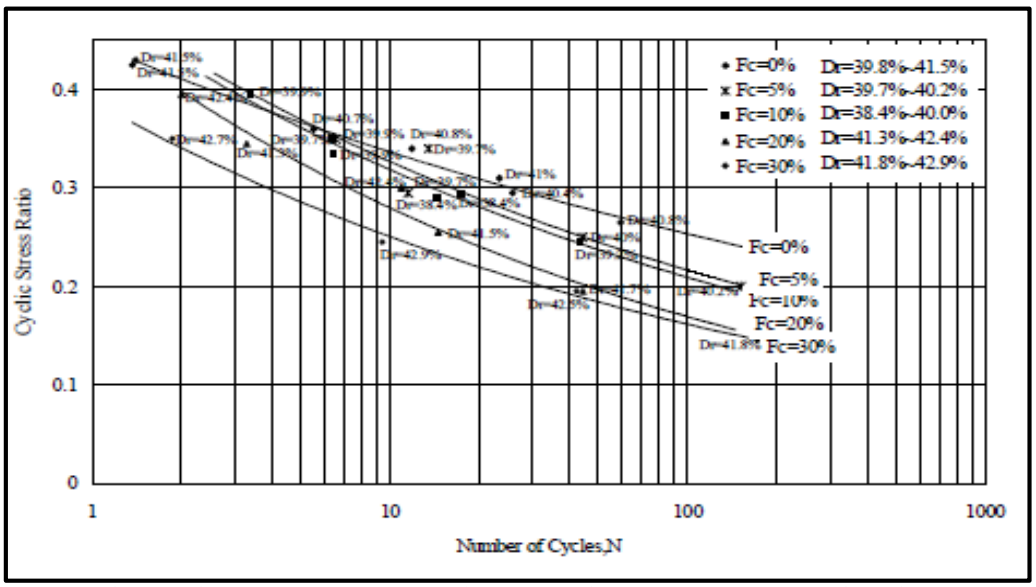

Fig 2.7 : Relation between no. of cycles & Cyclic Stress Ratio under different fines content (Initial D_r= 35%)

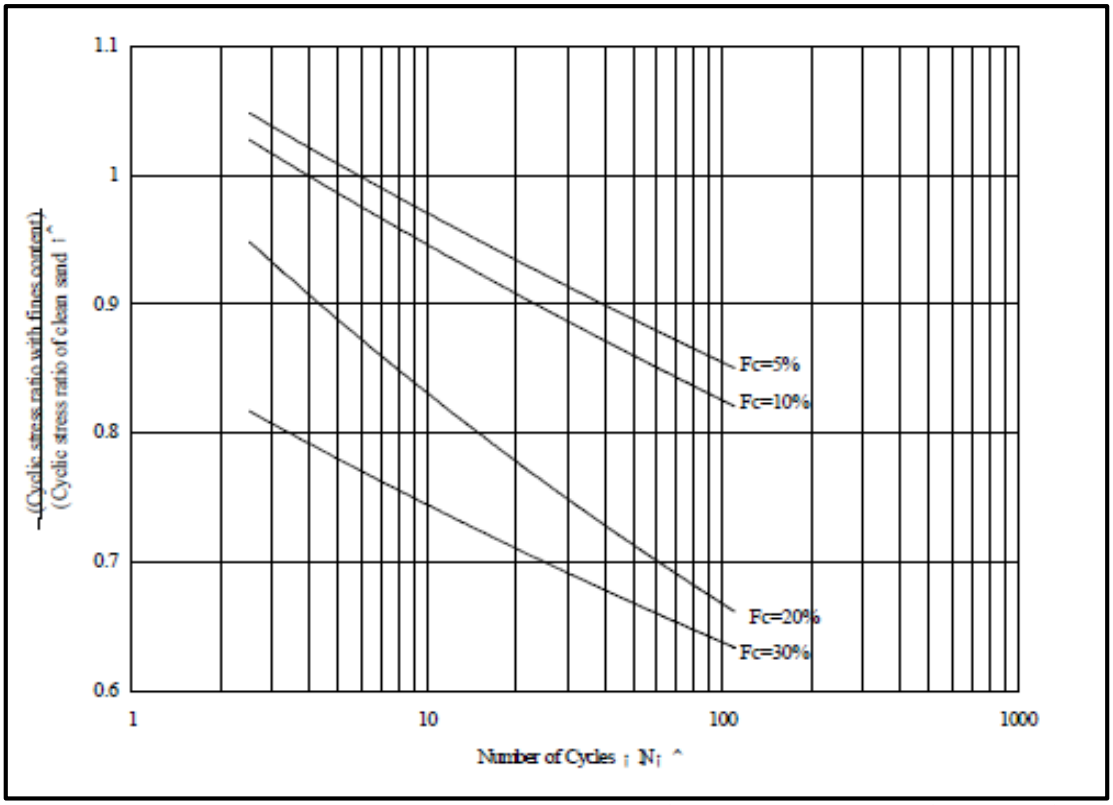

Fig 2.8 : Comparison curve for specimen with fines content & clean sand (D_r= 38.4%~42.9%)

B) The liquefaction resistance of reclaimed soil

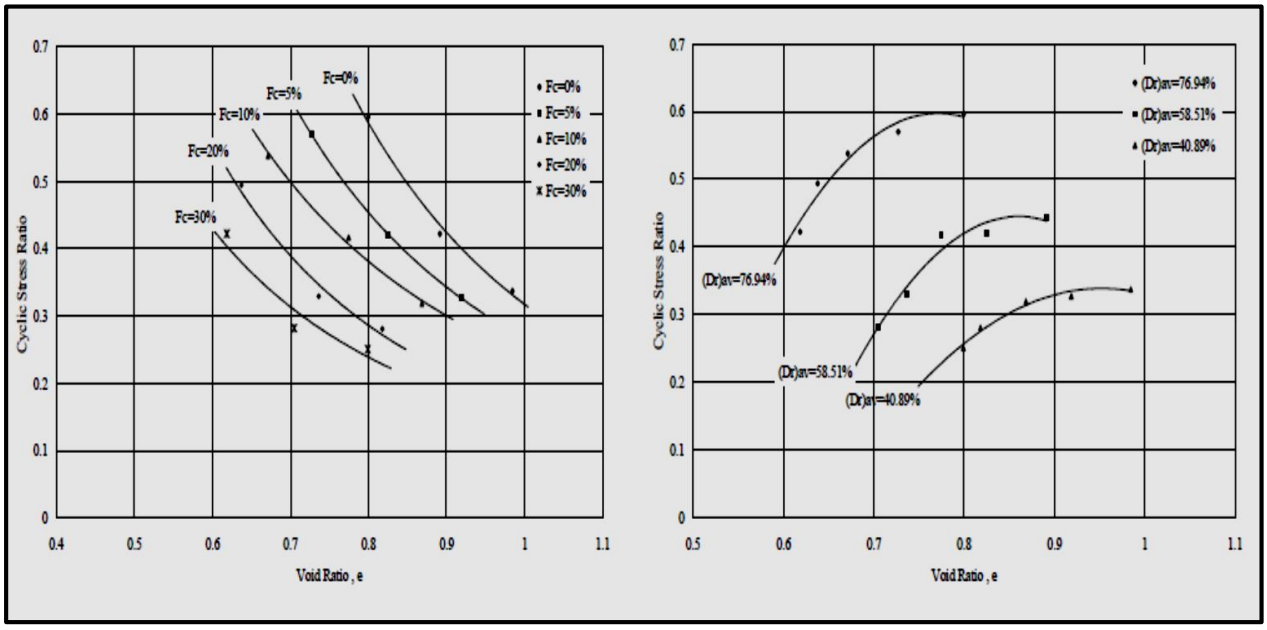

(A) (B)

Fig 2.9: Relation between void ratio & cyclic stress Ratio under different fines content (A) & different Relative Density (B) with No. of cycle=10

C) Liquefaction induced settlement for reclaimed soil

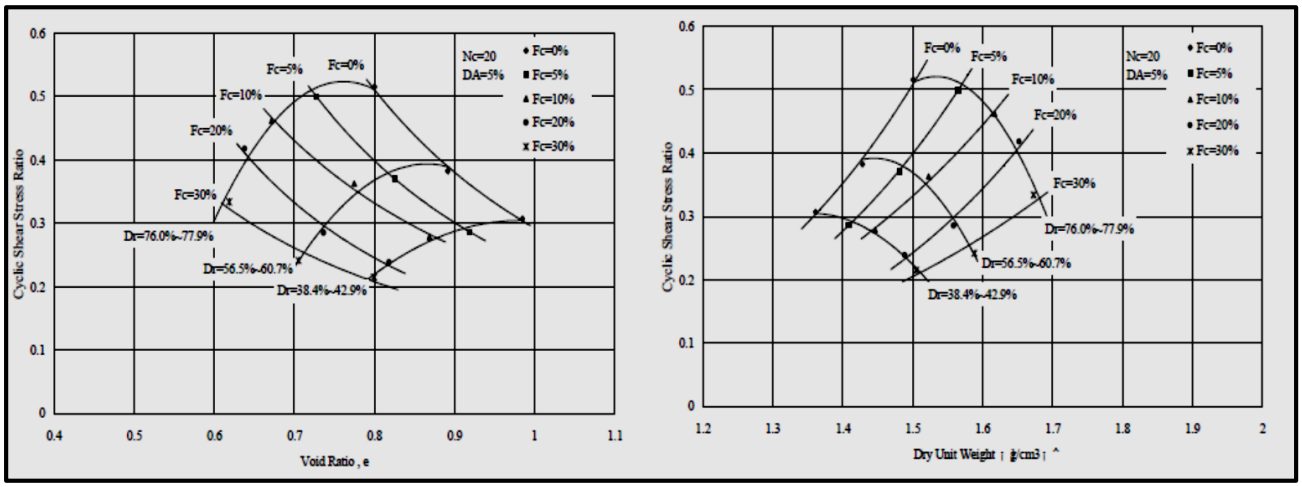

(A) **(B)**

Fig 2.10 : Void Ratio (A)/ Dry unit weight (B) vs Cyclic Stress Ratio under different fines content and Relative densities (No. of cycle=20; DA= 5%)

2.4.2.3 Arab et al. (2002)

Arab and Belkhatir (2002) studied the influence of low plastic fines and preloading on the cyclic behavior of silty sand. The study was based on cyclic undrained triaxial tests which were carried out for fines content ranging from 0 to 40% on reconstituted uniform sand samples of Rass (Algeria) mixed with the silt having a plasticity index of 2.33 (classified as low plastic silt). The dimensions of the samples were 70 mm in diameter and 70 mm in height in order to avoid the appearance of the instability (sliding surfaces) and buckling.

The results obtained from the cyclic triaxial tests are discussed below:

A) Effect of Loading Level

i) The rate of the water pore pressure increases with the increasing amplitude of cyclic loading.

ii) An increase in the amplitude of cyclic loading (q_m) accelerates the liquefaction process.

B) Effect of Fines on the Liquefaction Potential

i) The resistance of liquefaction of the mixture Rass sand-SM silt decreases with an increase in the amount of fines until the fines content, FC = 20%; and a small increase in the liquefaction potential with the fines content, FC = 40%.

ii) The cyclic liquefaction resistance decreases with an increase in the fines content up to 20% having RLC = 0.14, then it re-increases slightly to reach the value of RLC = 0.15 for the fines content, FC = 40%.

[Where RLC = Resistance to liquefaction which is defined by the cyclic stress ratio giving liquefaction for 15 cycles (Ishihara 1993)]

C) Effect of Preloading on the Resistance of Liquefaction

The over-consolidation and the cyclic drained preloading of low stress amplitude improve the liquefaction resistance of the sand-silt mixtures.

2.4.2.4 Xenaki V.C. and Athanasopoulos G.A (2002)

They proposed a new concept of threshold fine content (FC_{th}). FC_{th} comes out approximately as 44% though it is not unique and depends upon the characteristics of coarse and fine grains.

(a) For FC < FC_{th} , for same intergranular void ratio, an increase in fine content increases liquefaction resistance. For FC > FC_{th} , the liquefaction resistance decreases with increase in fine content.

(b) For a constant value of global void ratio, an increase in pore pressure generation rate with increasing fine content is observed upto the threshold value whereas beyond this value, the trend is reversed.

2.4.2.5 Ravishankar et al. (2005)

Ravishankar et. al. (2005) did extensive analysis with Ahmedabad sands at large strains and presented the paper on their test results at IGC, 2005 in Ahmedabad, Gujarat.

Representative soil samples were collected from the right bank of Savarmati River bed at different depths in Ahmedabad city of the Indian State of Gujarat. As it is mostly a River channel deposit, the Ahmedabad sand falls in the liquefiable zone. The index properties of the collected sand sample are:

Index Properties	Values
Specific gravity	2.66
Medium sand	37%
Fine sand	53.4%
Silt content	9.6%
Maximum void ratio	0.67
Minimum void ratio	0.54

The following inferences were drawn from the experimental results:

i) It is evident that the shear modulus decreases with increase in shear strain for the range of strains tested (0.27% to 3.2%).

ii) The sample with higher relative density exhibits higher modulus in the range of shear strain 0.27% to 0.80% and thereafter the relative density effects on shear modulus becomes insignificant.

iii) The damping ratio is increasing with increase in shear strain amplitude.

iv) Saturated sand behaves very similar to dry sand. The reduction in shear modulus and increase in damping are significant over a range of shear strains 0.053 to 5%. The increase in relative density results in increase in shear modulus at low level of shear strains of 0.5%. Beyond 0.5% of shear strain, shear modulus value falls in a narrow band and the effect of Relative density on damping is not very significant.

v) Shear modulus decreases with increase in shear strain for both dry & saturated sands and the value falls in a narrow band. The damping ratios for dry & saturated sands are not different but fall in a narrow band over a range of shear strain tested.

vi) The shear modulus is decreasing with increase in shear strain irrespective of frequency of cyclic loading. But it has been noticed that the damping ratios are affected to some extent by the frequency of loading with higher damping ratios are noticed for higher frequencies.

2.4.2.6 Paul et al. (2007)

Paul et al. presented a paper in 4th ICEGC based on cyclic triaxial testing of fully and partially saturated soil at Silchar. The following conclusions may be drawn from their findings:

(i) For fully saturated condition

(a) At a particular shear strain the G value remains higher for a denser sample and the D value remains higher for a loose sample when confining pressure remains constant. Again at a particular shear strain the G value remains higher for higher confining pressure and the D value remains higher for lower confining pressure when relative density of sample remains constant.

(b) When a cyclic load is applied on the soil, pore water pressure builds up steadily and reaches initially applied confining pressure depending on the magnitude of cyclic shear strain as well as on the density of the soil.

(c) The amplitude of cyclic shear strain governs the liquefaction resistance of a soil characterized by the cyclic strain approach. A threshold strain of approximately 0.015 % is obtained in the present analysis.

(ii) For unsaturated condition

(a) With increase in number of cycles, pore pressure increases gradually and then decreases suddenly. The samples failed in shear along a diagonal plane.

(b) Irrespective of confining pressure, shear modulus decreases and damping ratio increases with strain.

(c) The rise of pore pressure with number of cycles is more for low relative density.
(d) With the increase in degree of saturation, the shear modulus of soil increases, reaches an optimum value and then decreases at a particular strain level.

(e) Damping ratio reduces with the increase in degree of saturation, as the area of hysteresis loop increases with the increase of the degree of saturation at a particular strain level.

(f) The change in pore pressure during cyclic load application is not constant for loading and unloading operations. This change is more prominent for higher degree of saturation.

2.4.2.7 Kumar et al. (2014)

Kumar et al. did extensive investigation on dynamic soil properties of Bhramhaputra sand. Based on the cyclic triaxial studies, it has been observed that the dynamic soil properties, as obtained from the first loading cycle, are strongly influenced by confining pressure and shear strain. High shear strains (γ>1%) has been found to produce a quasi-liquefaction state manifested by the rise of first-cycle peak excess pore-water pressure ratio near to or greater than 1 (one), which results in a decrease in the damping ratio. For a particular shear strain, an optimum loading frequency has been observed (f~2Hz) beyond which the dynamic response of the soil is substantially affected.

2.4.3 Field Based Experimental Work

2.4.3.1 Youd et al. (2001)

Idriss and Youd (2001) with 20 experts convened a workshop sponsored by the National Center for Earthquake Engineering Research (NCEER) in 1996 to review developments for evaluating liquefaction resistance of soils over the previous 10 years.

The following topics were reviewed and recommendations developed given below:

(1) Criteria based on standard penetration tests;

(2) Criteria based on cone penetration tests;

(3) Criteria based on shear-wave velocity measurements;

(4) Use of the Becker penetration test for gravelly soil;

(5) Magnitude scaling factors;

(6) Correction factors for overburden pressures and sloping ground; and

(7) Input values for earthquake magnitude and peak acceleration.

The conclusions obtained from the workshop are:

1. Four field tests were recommended for routine evaluation of liquefaction resistance: the cone penetration test (CPT), the standard penetration test (SPT), shear-wave velocity (Vs) measurements, and for gravelly sites the Becker penetration test (BPT). Advantage and disadvantages of each test is given in **Table 2.8.**

2. Moment magnitude M_w should be used for liquefaction resistance calculations. Magnitude, as used in the simplified procedure introduced by Seed and Idriss was a measure of the duration of strong ground shaking.

3. The workshop participants recommended correction factor for overburden pressure over (or below) 100kPa, Kσ values defined by the curves in **Figure 2.11**. Because Kσ values are usually applied to depths greater than those verified for the simplified procedure, special expertise is generally required for their application.

4. The magnitude scaling factors originally derived by Seed and Idriss (1982) are overly conservative for earthquakes with magnitudes <7.5. A range of scaling factors is recommended for engineering practice. The new MSF recommended by Idriss shown in **Table 2.8**

Table 2.8: Magnitude Scaling Factor Values (Idriss, 1998)

Magnitude	Seed and Idriss (1982)	Idriss
5.5	1.43	2.2
6	1.32	1.76
6.5	1.19	1.44
7	1.08	1.19
7.5	1.00	1.00
8	0.94	0.84
8.5	0.89	0.72

Table 2.9: Comparison of Advantages and Disadvantages of Various Field Tests for Assessment of Liquefaction Resistance (Idriss and Youd, 2001)

Feature (1)	Test Type			
	SPT (2)	CPT (3)	Vs (4)	BPT (5)
Past measurements at liquefaction sites	Abundant	Abundant	Limited	Sparse
Type of stress-strain behavior influencing test	Partially drained, large strain	Drained, large strain	Small strain	Partially drained, large strain
Quality control and repeatability	Poor to good	Very good	Good	Poor
Detection of variability of soil deposits	Good for closely spaced tests	Very good	Fair	Fair
Soil types in which test is recommended	Non-gravel	Non-gravel	All	Primarily gravel
Soil samples retrieved	Yes	No	No	No
Test measure index or engineering property	Index	Index	Engineering	Index

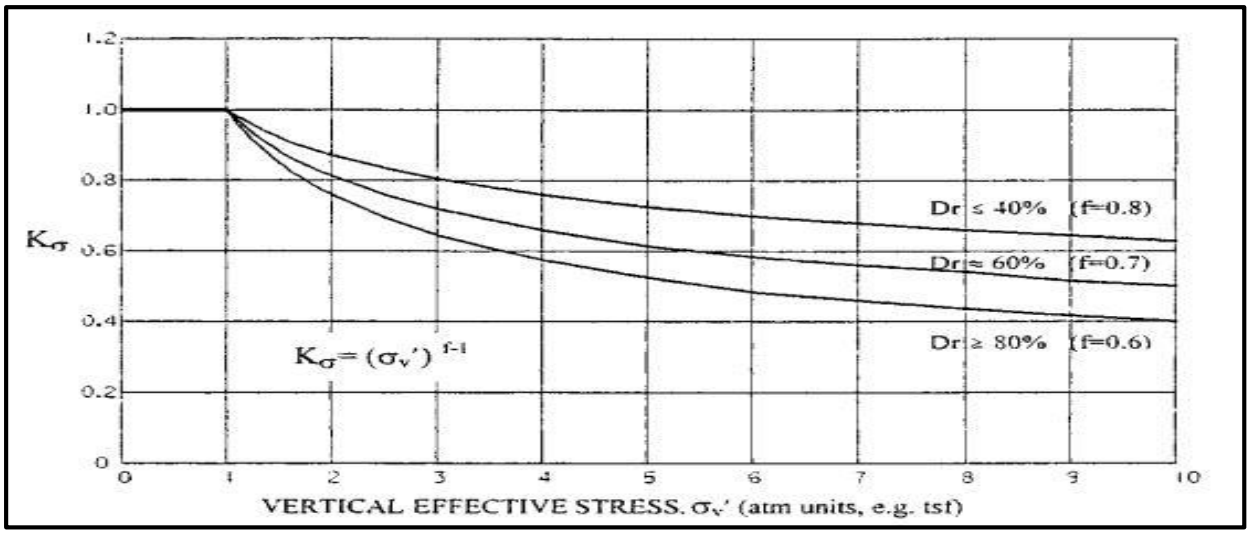

Figure 2.11: Recommended Curves for Estimating Kσ for Engineering Practice (Idriss and Youd, 2001)

CHAPTER 3

OBJECTIVES AND SCOPE OF WORK

3.1 Objectives

The objectives of the present investigation are as follows:

- To determine the liquefaction susceptibility of a typical silty sand collected from upper region of river channel deposit in Kolkata region
- To investigate the effect of various parameters influencing the liquefaction resistance of the deposit and pore water pressure generation characteristics.

3.2 Scope of Work

The scope of present investigation is given below:

1. Collection of disturbed and undisturbed samples from a depth of 1.5 – 4.0m below ground surface in the compound of ITI, Tollygunge, Kolkata having latitude 22.4953°N and longitude 88.3555°E.

2. Determination of physical properties of the collected soil sample (e.g. grain size distribution, maximum and minimum density, specific gravity etc.)

3. Performance of cyclic triaxial tests at three relative densities with three different confining pressures at three different displacement amplitudes to obtain the liquefaction susceptibility of soil with respect to these three parameters.

4. Investigation of pore pressure generation characteristics of soils.

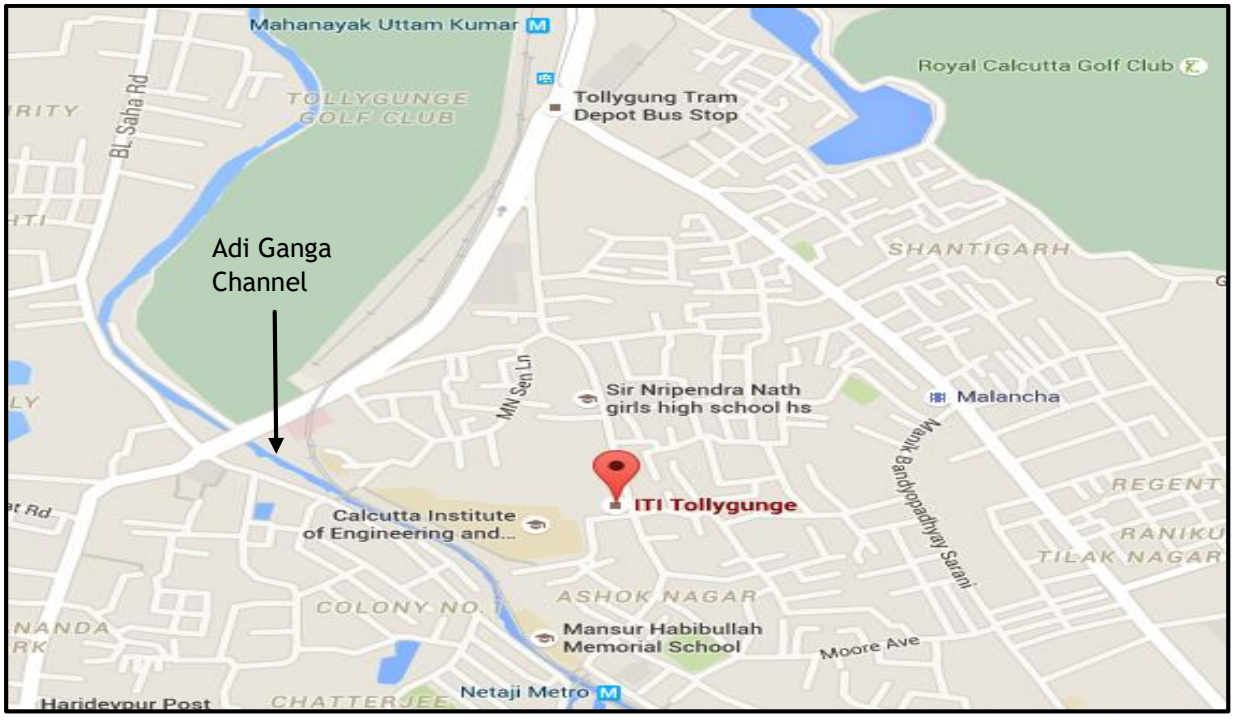

Fig 3.1 Location of the sampling point (ITI Tollygunge)

Chapter 4

EXPERIMENTAL WORK

4.1 Test Programme

Sample was collected from the compound of ITI, Tollygunge, Kolkata by boring process. (Ref Fig 4.1). Total 27 numbers of strain controlled cyclic triaxial tests have been performed. Three target relative densities are chosen i.e. 25%, 50% and 75%. These densities are achieved by moist tamping method.

For each of these relative densities, three effective confining pressures (σ_{3c}') were chosen, viz, 50, 100, 150 kPa

Now for each relative density and confining pressure, three cyclic shear strains have been chosen i.e. 0.5%, 0.67% and 0.83% (or displacement amplitude ±0.75mm, ±1.00mm and ±1.25mm respectively).

So total 3×3×3 = 27 numbers of tests have been performed. The test program has been given in **Table 4.1**:

Fig 4.1 Boring work is going on for collection of sample

Table 4.1 : Cyclic Triaxial Test Programme

Test No.	Target WC. (%)	Target Dry Density (gm/CC)	Target Relative Density (%)	Cell Pressure (KPa)	Back Pressure (KPa)	Effective Confining Pressure (KPa)	Cyclic Shear Strain (%)	Frequency (Hz)
1	5	1.557	75	350	300	50	0.50	1
2	5	1.557	75	350	300	50	0.67	1
3	5	1.557	75	350	300	50	0.83	1
4	5	1.557	75	400	300	100	0.50	1
5	5	1.557	75	400	300	100	0.67	1
6	5	1.557	75	400	300	100	0.83	1
7	5	1.557	75	450	300	150	0.50	1
8	5	1.557	75	450	300	150	0.67	1
9	5	1.557	75	450	300	150	0.83	1
10	10	1.506	50	350	300	50	0.50	1
11	10	1.506	50	350	300	50	0.67	1
12	10	1.506	50	350	300	50	0.83	1
13	10	1.506	50	400	300	100	0.50	1
14	10	1.506	50	400	300	100	0.67	1
15	10	1.506	50	400	300	100	0.83	1
16	10	1.506	50	450	300	150	0.50	1
17	10	1.506	50	450	300	150	0.67	1
18	10	1.506	50	450	300	150	0.83	1
19	10	1.424	25	350	300	50	0.50	1
20	10	1.424	25	350	300	50	0.67	1
21	10	1.424	25	350	300	50	0.83	1
22	10	1.424	25	400	300	100	0.50	1
23	10	1.424	25	400	300	100	0.67	1
24	10	1.424	25	400	300	100	0.83	1
25	10	1.424	25	450	300	150	0.50	1
26	10	1.424	25	450	300	150	0.67	1
27	10	1.424	25	450	300	150	0.83	1

4.2 Test Material

The test sample was collected from the Industrial Training Institute, Tollygunge. It is mostly the river channel deposit of Adi Ganga Channel. It was collected from a depth of 1.5 to 4m BGL.

Fig 4.2 Sand sample used in testing

After collecting the soil samples the following physical properties have been determined:

1. Specific gravity of soil solid, G_s
2. Mean grain size, D_{50}
3. Coefficient of uniformity (C_u) and Coefficient of curvature (C_c)
4. Maximum and minimum dry density, γ_{dmax} and γ_{dmin}
5. Relative density, R_d

The specimen used in the test was mostly a sand-silt mixture with a higher percentage of silt. The grain size distribution curve is given below:

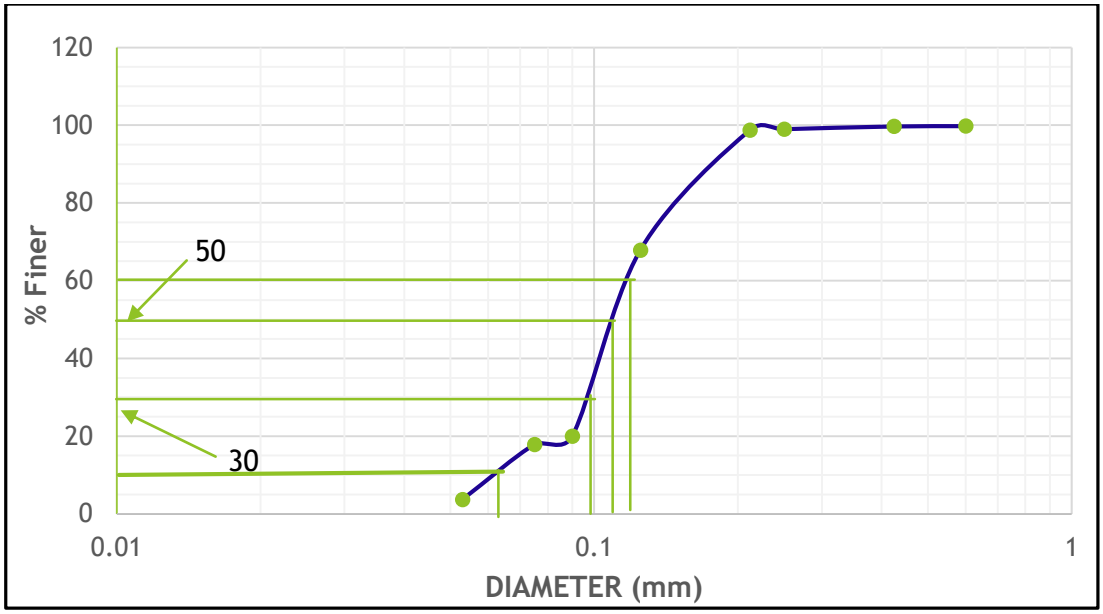

Fig 4.3 Grain Size Distribution Curve

The portion of silt in this soil is coming out as 17.82% (percent finer than 75μm)

From the GSD curve, we get the mean particle size D_{50} = 0.12 mm

Also, D_{30} = 0.1 mm , D_{60} = 0.14 mm , D_{10} = 0.065 mm

Hence, uniformity coefficient (C_u) = D_{60}/D_{10} = 0.14/0.065 = 2.15

And coefficient of curvature (C_c) = D_{30}^2 / ($D_{60} \times D_{10}$) = 1.099

The specific gravity is determined by Pycnometer and it comes out to be 2.39

The maximum dry density obtained from Relative Density test and Modified Proctor Test comes out as γ_{dmax} = 1.525 and 1.715 gm/cc respectively we have chosen the higher value, i.e. 1.715 gm/cc for calculation purpose.

The minimum dry density by Relative Density test comes out as, γ_{dmin} = 1.157 gm/cc.

Three different types of relative densities, Rd: 25%, 50% and 75% have been targeted to be obtained with the help of 'Moist Tamping Method' (which has been discussed in Article 4.4). For Rd =25% the sand is in the loosest state and for Rd = 75% the sand is in the densest state.

4.3 Relative Density Control

To ensure that representative and accurate results to be obtained from the triaxial test, a specified procedure was determined and followed:

Relative density is expressed as:

$$R_d = \gamma_{dmax} / \gamma_d \times (\gamma_d - \gamma_{dmin}) / (\gamma_{dmax} - \gamma_{dmin}) \times 100\% \quad (4.1)$$

Where:

R_d = relative density (in percent)

γ_{dmax} = maximum dry density of the soil (gm/cc)

γ_{dmin} = minimum dry density of the soil (gm/cc)

γ_d = dry density of the soil (gm/cc)

To determine the air dry weight of soil necessary to create the sample, the following equation was used:

$$\gamma = W/V \quad (4.2)$$

Where:

W = Weight of the sample at a particular moisture content (Say w %) (gm)

V = Volume of the sample in cc = $\pi . (Ds^2) . (Hs)/ 4$

Ds = diameter of specimen = 7.5 cm

Hs = height of specimen =15 cm

Finally, $\gamma d = \gamma/ (1+ (w/100))$ (4.3)

4.4 Sample Preparation Method

Moist tamping (MT) sample preparation method was adopted. This method is described below:

Moist Tamping Method

An oven-dried batch of sand has been mixed thoroughly with de-aired water to achieve certain percentage of moisture content. This small amount of water has been added (5% to 10% by weight) to the dry sand sample to make the sample much more densify as water acts as lubricating agent between sand particles. If water beyond 10% is added, it will be difficult to construct a sample in the mould. If dry sand was compacted then the friction between the sand particles would not allow the sand sample for much more densification. So targeted relative density would never been achieved. The moist sand has been compacted in 3 layers to achieve the required relative density forming a specimen with 75 mm diameter and 150 mm height. Each batch was dumped onto two membrane-lined pedestal encapsulated inside a spilt mould. Compaction has been made by a tamper on each layer until the prescribed height would be reached. Porous stone with filter paper at bottom and top of split mould was given before placing it to cyclic triaxial testing machine.

To obtain three target relative densities i.e. 25%, 50% and 75% how much percentage of water has been added and how many numbers of tamping have been done for trial sample preparation have been described in Table 4.2 given below:

Table 4.2: Trial Sample Preparation by Moist Tamping Method

No. of Layer	No. of tamping for each layer	Target dry Density (gm/cc)	Weight of sample achieved (gm)	Volume of sample (cc)	Actual unit weight obtained (gm/cc)	Actual dry density obtained (gm/cc)	Target Moisture Content (%)	Actual Moisture Content achieved (%)	Target Relative density(%)	Actual Relative Density achieved (%)
3	10	1.259	886.64	662.7	1.338	1.274	5	4.98	25	28.426
3	30	1.382	970.64	662.7	1.464	1.396	5	4.86	50	52.607
3	55	1.530	1052.64	662.7	1.588	1.515	5	4.82	75	72.617

4.5 Test System

HS28.610 Cyclic Triaxial Test System manufactured by HEICO has been used which is a highly advanced combination of hydraulic and pneumatic technology where major principal stress, σ1 is applied through hydraulic system in dynamic tests and minor principal stress, σ3 is applied through pneumatic system. It is totally based on Closed Loop principle. The processing of the pre-programmed signal and machine responsible signal in the Controller is at the speed of 10 KHz. This keeps the machine working within the limits of ± 2.5% of the programmed signal. Confining pressure & Back pressure are also controlled through computer and operates on closed loop control mechanism.

Broad specification of each componet is given below:-

4.5.1 Load Frame

Loading Frame is a free standing two pillar type unit. It has a base and a cross head with fitted actuator along with servo valve. Cross head carrying the Hydraulic Actuator for conducting dynamic tests is movable on threaded columns to adjust the height of the sample. Arrangement is also provided for locking of the crosshead at any desired position. Static and dynamic loading would be fully computer controlled. It can accommodate triaxial cell for sample sizes up to 100mm diameter & 200mm height.

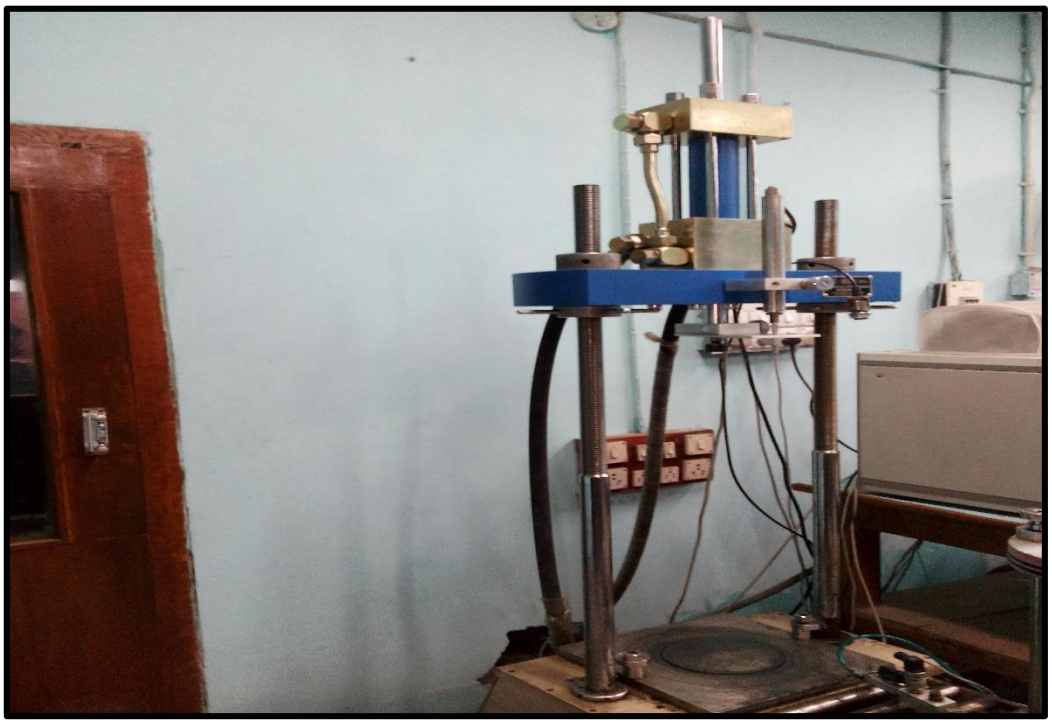

Fig 4.4 Loading Frame

4.5.2 Hydraulic Actuator and Hydraulic Power Supply

Actuator is a linear motion device, which gives a controlled motion either on stress basis or strain basis. It is a precision piece of equipment which follows the command from the wave generator through the servo valve. It is an equal area ram and piston with surface finish of 0.2 microns. End plates have metallic seals for side thrust. Servo valve is fixed to the actuator. These valves are high performance two stage valves with a pressure drop of @ 70 bars.

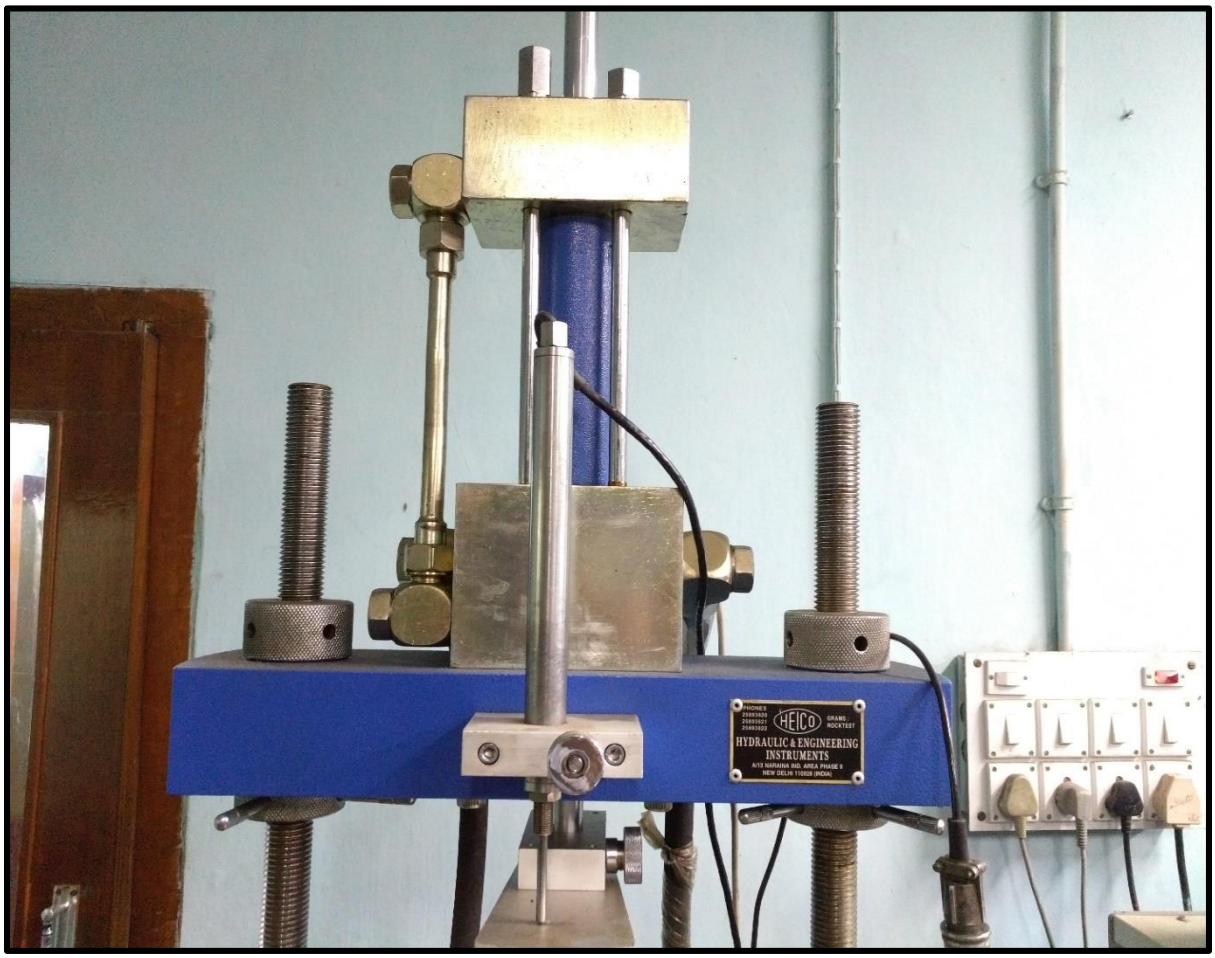

Fig 4.5 Hydraulic Actuator

Hydraulic power supplies are compacted in design and are suitable for the supply of required flow and pressure for the movement of the actuator. It has an oil tank of adequate capacity, vane type pump powered by a three phase motor. All the electrical controls including the temperature controller are fixed on one side of the tank. It includes all the accessories like pressure line filter, return line filter, oil level, relief valve, pressure gauge and shell & tube type heat exchanger. Anti-vibration mountings are provided as standard along with the Hydraulic Power Supply.

4.5.3 Triaxial Cell

Standard Triaxial Cell can accommodate sample size, ranging from 38mm to 100mm diameter with L/D ratio of 1:2. It is suitable for both Static and Dynamic tests (Compression & Extension). It has a submersible load cell connected to the transfer bar. Linear bearings ensure smooth movement of the transfer bar (plunger). Sensors for pore pressure and back pressure are attached to the stainless steel base. It would have a facility for on sample transducer.

Tests Possible : Static & Dynamic (Compression/ Extension or both)

Confining Pressure : Up to 1000 kPa

Specimen Size : Up to 100mm diameter & 200mm height

Submersible Load cell : 500Kg

Fig 4.6 Triaxial Cell

4.5.4 Digitally Controlled Pressure System

HEICO Pneumatic Pressure system has two line pressures distribution systems for both Confining and Back pressure up to 100 kPa with air/water bladder system with a panel complete with pressure gauge and outlets for two pressures. Control panel is a combination of Electro pneumatic regulators. There are two independent lines one for confining pressure and the other for back pressure. A separate Vacuum line with vacuum regulator and gauge is also provided for de-airing of water and vacuum application. A de-airing chamber of 15Liters is also provided. Both pressures can be set and controlled digitally through computer. A sensitive volume change sensor fitted with differential pressure transducer is fixed on one side to measure the change in volume during the test.

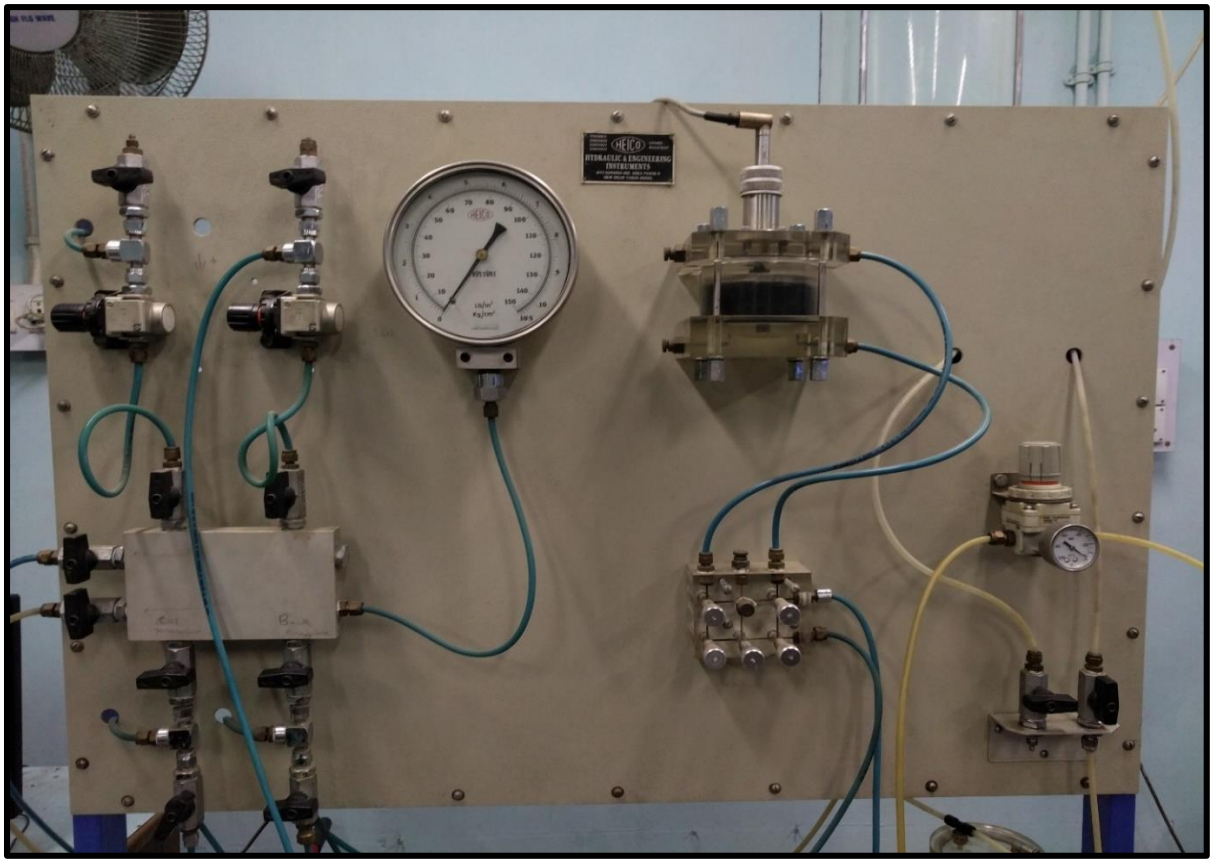

Fig 4.7 Pressure System

4.5.5 Transducers

The following transducers are supplied with the system for the accurate measurement of various parameters (the values given bracket indicate the least unit value which can be measured):

1. Submersible Load Cell: ±500Kg (0.1Kg)
2. Displacement Transducer: ±25mm (0.01mm)
3. Confining Pressure Transducer: 1000 kPa (1 kPa)
4. Pore Pressure Transducer: 1000 kPa (1 kPa)
5. Back Pressure Transducer: 1000 kPa (1 kPa)
6. Volume Change Transducer: 200cc (0.1cc)

4.5.6 Computer Based Control System and Application Software

HEICO controller basically consists of signal conditioning and controlling unit and operates on closed loop Servo Hydraulic Control for axial loading on Load/displacement basis. Cell pressure & back pressure are also controlled through computer and operates on closed loop control mechanism. Signal conditioning unit receives the output signal from the various transducers and amplifies and process that signal as per the requirement and transfer it to computer through connecting cables where it is accepted by the data acquisition system. A system is provided with dedicated computer with built in data acquisition card and wave generator. Control software is the integral part of the system for precise controlling & Data Acquisition and analysis.

Fig 4.8 Computer with data acquisition software

4.6 Test Procedure

After preparing the soil sample by Moist Tamping method the following steps have been followed to perform cyclic triaxial test:

1. First the sample has been prepared for a particular relative density by Moist Tamping method in a split mould wrapped by double membrane shown in Figure 4.9.

Fig 4.9 Split Mould

2. One 'O' Ring of diameter 65mm has been placed on the split mould and another 'O' Ring of same diameter has been placed at the top of load cell. The 'O' Ring at the split mould is used to tighten the soil sample with the membrane at the bottom of the base pedestal and the 'O' Ring at the top of load cell is used to tighten the sample at the top of load cell.

3. The mould is placed around the base pedestal.

4. After placing the mould the bottom portion of the membrane is wrapped over the bottom of the mould and the excess membrane has been folded outside of the mould to ensure a smooth surface. This step involves stretching membrane with four fingers, two from each hand. The rubber membrane should be stretched equally outward, and wrapped around the bottom of the mould. Then the 'O' Ring at the split mould is placed on the base pedestal.

5. Next the split mould is removed without disturbing the sample.

6. The load cell is placed on the sample and its three legs have been tightened by three screws on the base pedestal and the load cell is lowered and placed tightly on the top of the sample by a fastener.

7. Next the top portion of the membrane has been tightened with top portion of the load cell by the 'O' Ring at the top portion of load cell.

8. The large 'O' rings at the load cell have been greased on the triaxial cell base to provide good seal between the chamber and the base.

9. The interface area between the chamber and the cell base has been cleaned and a thin layer of grease sealant has been applied.

10. An open tube to the top of the triaxial cell chamber has been plugged to prevent any pressure building-up, carefully placing the chamber over the sample it has been locked onto the triaxial cell base using a rim locking band.

11. The chamber has been filled with water, until water flows out of the top of the chamber through the open valve.

12. After the chamber is properly filled, the valve leading to the filling chamber is closed and the open tube has been removed from the top of the chamber (Figure 4.10).

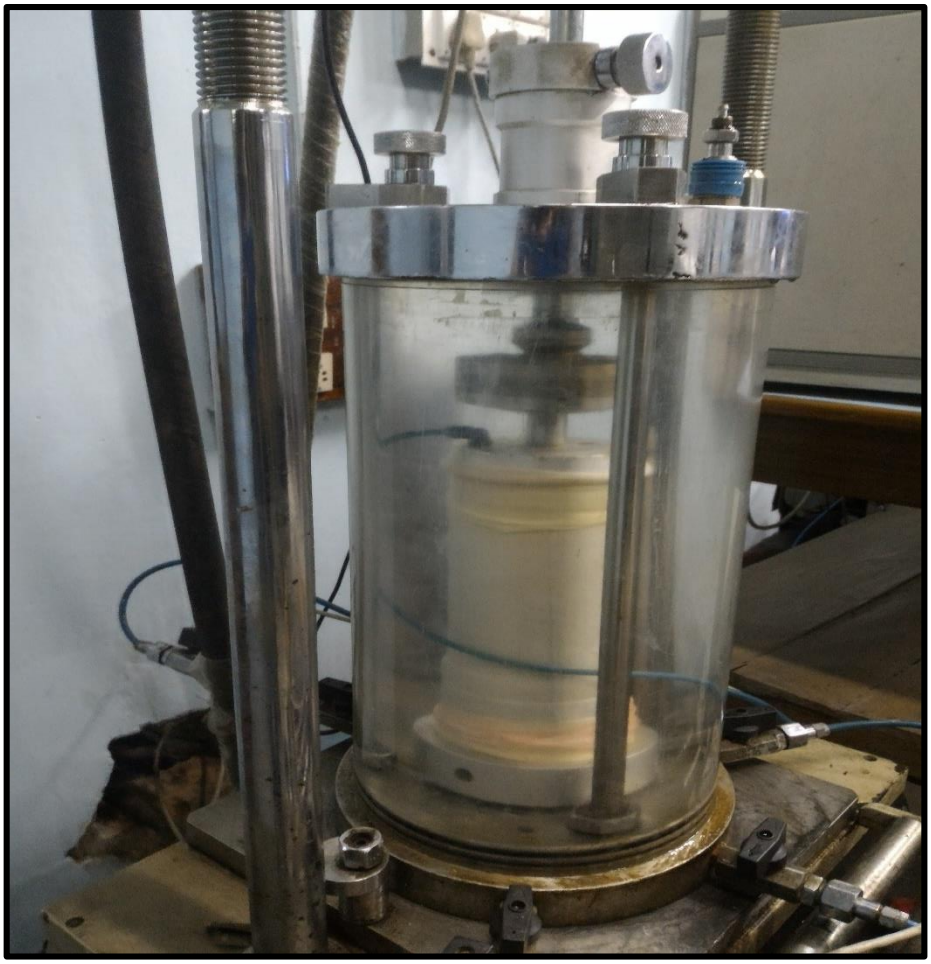

Fig 4.10 Soil sample in the cell after filling with water

13. Next the sand sample is saturated by applying cell pressure 280 kPa and back pressure 250 kPa about two and half hours for target relative density 75%, for two hours for Rd = 50% and for one and half hours for Rd = 25%.

14. Next the sand sample has been consolidated by applying cell pressure 350 kPa and back pressure 250 kPa during half an hour.

15. The triaxial cell is then transferred to the HEICO cyclic triaxial machine; it is then centered and locked on the triaxial cell base to the HEICO loading platform using two C clamps.

16. Then cell pressure and back pressure have been changed to provide the desired effective confining pressure (σ_{3c}') e.g. when σ_{3c}' is 100 kPa then cell pressure would be 350 kPa and back pressure would be 250 kPa. One thing has been cared that back pressure should not fall below 250 kPa during or after saturation. It is because the sand sample has been saturated with a back pressure of 250 kPa, so if the back pressure is reduced below 250 kPa then the water from the sand sample will be drained out from the sample and the sample will become partially saturated sand.

17. After providing the effective confining pressure the hammer has been lowered and it is then allowed to just touch the top of load cell. Whether the hammer has touched the load cell can be recognized by observing the 'Load' reading in the computer screen shown in Figure 4.7.

18. Then the hammer has been clamped on the load cell tightly to provide two way cyclic load e.g. compression and tension and the load cell has been loosened on the sand sample by the fastener and the back pressure line has been closed.

19. Finally in the computer (shown in Figure 4.7) number of cycle of the test has been selected. Then the 'Load' is tarred before clicking on 'Load/Base' option. Finally the cyclic triaxial test is started after clicking on 'Start' option. One thing should be kept in mind that as displacement controlled cyclic triaxial test has been performed so for every time before starting the test the load should be tarred. If the test is load controlled test then the displacement should be tarred.

20. The data file for each test has been saved in a folder named 'ABHISHEK' in the computer provided.

21. The test has been terminated when the sample has been liquefied during cyclic loading, or when the excess pore pressure generation has been stabilized and become constant and change in load becomes zero.

22. The triaxial cell from the HEICO Triaxial Testing machine has been removed after releasing back pressure and cell pressure from pressure control system. Next the water from the cell is extracted by a suction pipe operated by a pump to the de-airing chamber after the valve leading to the filling chamber is opened and the open tube is placed on the top of the chamber.

23. But the back pressure line is not opened as we have to calculate the degree of saturation of the sample. It it was opened, the pore water from the sand sample will be drained out.

24. At last the tested soil has been removed from the triaxial cell and before recycling the weight of wet sample has been recorded and a few amount of soil sample is taken from the middle portion of the sand sample to measure water content and the cell has been cleaned for subsequent use.

CHAPTER 5

TEST RESULTS

5.1 Introduction

Total 27 numbers of cyclic triaxial tests were performed. For each test relative density, Rd (%) of the sample, effective confining pressure, σ_{3c}' (kPa) and displacement amplitude (mm), has been decided, listed in **Table 4.1**. All samples were tested at 1 Hz frequency. For each test the test data has been saved as '.Txt' file. Each of this file has been converted into Microsoft excel worksheet. For each test a huge numbers of data (approximately 6000 to 18000 data) has been obtained in excel sheet. From those data for each test total three numbers of graphs have been generated. These graphs are:

1. Displacement (mm) vs. Number of Cycles
2. Load (Kg) vs. Displacement (mm)
3. Pore Pressure (kPa) vs. Number of Cycles

So from all the 27 numbers of tests total 27×3 = 81 numbers of graphs have been generated. After analyzing all the data obtained from the tests and all the graphs generated the following relationships of different parameters related to cyclic strength of soil have been obtained:

(i) Effect of Relative Density with Number of Cycles of Failure

(ii) Effect of Confining Pressure with Number of Cycles of Failure

(iii) Relationship of Cyclic Shear Strain with Number of Cycles of Failure

(iv) Pore water pressure generation characteristics

5.2 Test Results

The entire 27 test results are given below in **Table 5.1**:

Table 5.1 Cyclic Triaxial Test Results

Sample No	Achieved dry density after sample preparation (γ_d) (gm/cc)	Achieved density after saturation (γ) (gm/cc)	Actual water content after saturation (w) (%)	Degree of saturation obtained (s) (%)	Target Relative Density (R_d) (%)	Achieved Relative Density (R_d) (%)	Effective Confining Pressure (σ_3') (KPa)	Displacement Amplitude (d_e) (mm)	Frequency (f) (Hz)	Number of Cycles to Failure	Cyclic Shear Strain (%)	Failure pore water pressure (KPa)
1	1.263	1.692	33.95	90.93	25	25.79	50	0.75	1	26	0.50	300
2	1.384	1.803	30.24	99.43	50	50.40	50	0.75	1	61	0.50	300
3	1.54	1.893	22.95	99.38	75	76.43	50	0.75	1	79	0.50	300
4	1.255	1.696	35.16	92.92	25	24.00	100	0.75	1	58	0.50	350
5	1.381	1.798	30.19	98.76	50	49.84	100	0.75	1	90	0.50	350
6	1.515	1.879	24.05	99.52	75	72.62	100	0.75	1	100	0.50	350
7	1.261	1.694	34.32	91.61	25	25.34	150	0.75	1	86	0.50	400
8	1.38	1.793	29.95	97.80	50	49.66	150	0.75	1	98	0.50	400
9	1.545	1.896	22.75	99.41	75	77.17	150	0.75	1	112	0.50	400
10	1.257	1.705	35.68	94.61	25	24.45	50	1.00	1	16	0.67	300
11	1.382	1.800	30.25	99.12	50	50.03	50	1.00	1	24	0.67	300
12	1.524	1.883	23.56	99.09	75	74.00	50	1.00	1	33	0.67	300
13	1.262	1.718	36.15	96.66	25	25.57	100	1.00	1	31	0.67	350
14	1.384	1.790	29.32	96.41	50	50.40	100	1.00	1	34	0.67	350
15	1.529	1.889	23.53	99.87	75	74.76	100	1.00	1	57	0.67	350

Sample No	Achieved dry density after sample preparation (γ_d) (gm/cc)	Achieved density after saturation (γ) (gm/cc)	Actual water content after saturation (w) (%)	Degree of saturation obtained (s) (%)	Target Relative Density (R_d) (%)	Achieved Relative Density (R_d) (%)	Effective Confining Pressure (σ_3') (KPa)	Displacement Amplitude (d_e) (mm)	Frequency (f) (Hz)	Number of Cycles to Failure	Cyclic Shear Strain (%)	Failure pore water pressure (KPa)
16	1.258	1.694	34.65	92.03	25	24.67	150	1.00	1	45	0.67	400
17	1.381	1.792	29.77	97.38	50	49.84	150	1.00	1	54	0.67	400
18	1.537	1.893	23.14	99.65	75	75.98	150	1.00	1	68	0.67	400
19	1.259	1.710	35.84	95.35	25	24.90	50	1.25	1	14	0.83	300
20	1.38	1.802	30.57	99.83	50	49.66	50	1.25	1	18	0.83	300
21	1.541	1.895	22.98	99.69	75	76.58	50	1.25	1	24	0.83	300
22	1.26	1.709	35.65	95.01	25	25.12	100	1.25	1	25	0.83	350
23	1.379	1.796	30.25	98.61	50	49.47	100	1.25	1	32	0.83	350
24	1.532	1.890	23.38	99.77	75	75.22	100	1.25	1	50	0.83	350
25	1.259	1.699	34.97	93.04	25	24.90	150	1.25	1	34	0.83	400
26	1.382	1.800	30.21	98.99	50	50.03	150	1.25	1	41	0.83	400
27	1.528	1.888	23.56	99.81	75	74.61	150	1.25	1	57	0.83	400

5.2.1 Calculation for Degree of saturation, (s):

After performing the test, the saturated sand sample was removed from the triaxial cell. Then immediately after removing the sample, the weight of the sample was taken. From the weight obtained, the weight of the two porous stones with filter paper and weight of the two membranes have been subtracted. Thus the final weight of the sample is obtained, say W gm. As the height and diameter of the sample is known, the volume, V can be calculated easily.

So wet density of the sample is, γ (gm/cc) = W/V (5.1)

After that water content of the sample is measured by taking a few amount of sample from the middle of entire sand sample.

Water content, w = (wt. of wet sand – wt. of dry sand)/ (wt. of dry sand - wt. of container)

But $\gamma = (Gs + w.Gs) * \gamma_w / (1+e)$ (5.2)

Where, Gs = Specific gravity of sand sample = 2.39

e = Void ratio of the sample

γ_w = density of water = 1gm/cc

From **Eq. (5.2)** void ratio, e can be obtained.

Finally degree of saturation, s can be obtained as:

$s = w.Gs/e$ (5.3)

5.2.1.1 Sample Calculation:

After performing triaxial test the weight of wet of sample no. 1 obtained is, W = 1068.94 gm

Volume of sample = $\Pi/4 * 7.5^2 * 15$ =662.68 cc

So, wet density, γ = 1121.25/662.68 = 1.692 gm/cc

After oven drying the sample the water content obtained is, w = 33.95%

Using **Eq. (5.2)** the void ratio of the sample obtained is, e = 0.892

Again using **Eq. (5.3)** degree of saturation obtained is, s = 0.9093 = 90.93 %

The value of dry density is obtained by, γ_d = Bulk Density/ (1+ water content) = 1.692/ (1+0.3395) = 1.263gm/cc.

Now from the value of dry density using **Eq. (4.1) (Article 4.3)** relative density for the soil sample can be calculated.

Rd = γ_{dmax} / γ_d × (γ_d - γ_{dmin}) / (γ_{dmax} - γ_{dmin}) ×100%. For this type of sand γ_{dmax} = 1.715 gm/cc and γ_{dmin} = 1.157 gm/cc.

For, γ_d = 1.263 gm/cc, R_d = 24.67%.

For each test the three sets of graphs obtained (discussed in **Article 5.1**) have been given in **Figure 5.1** to **Figure 5.27**:

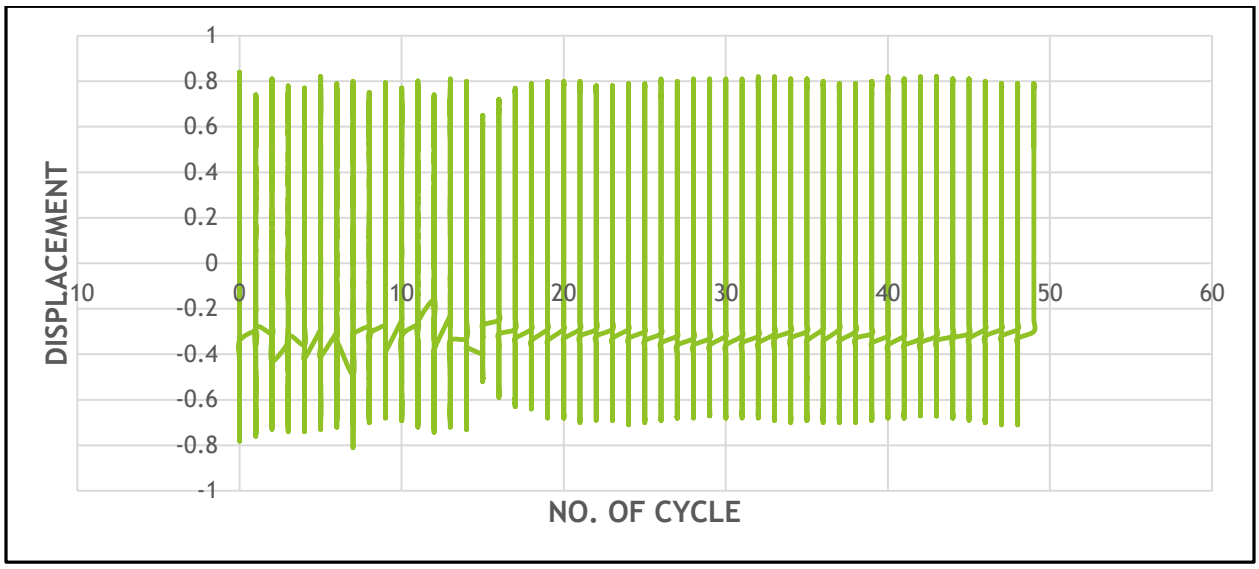

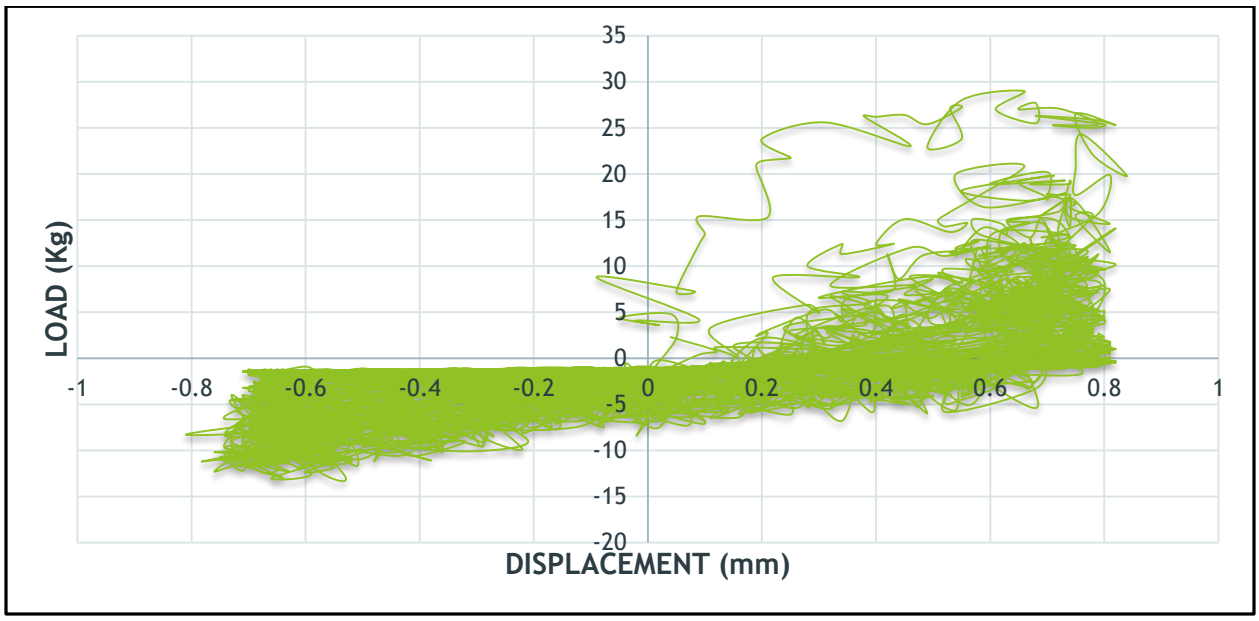

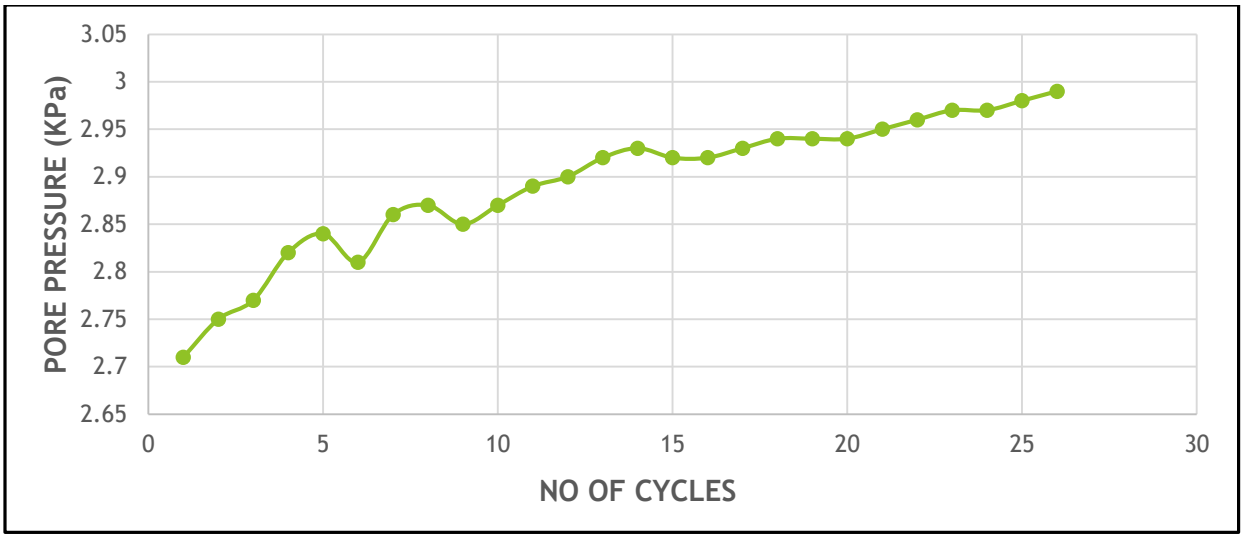

Fig 5.1 Relative Density 25% ; Effective confining pressure 50 KPa ; Amplitude 0.75mm

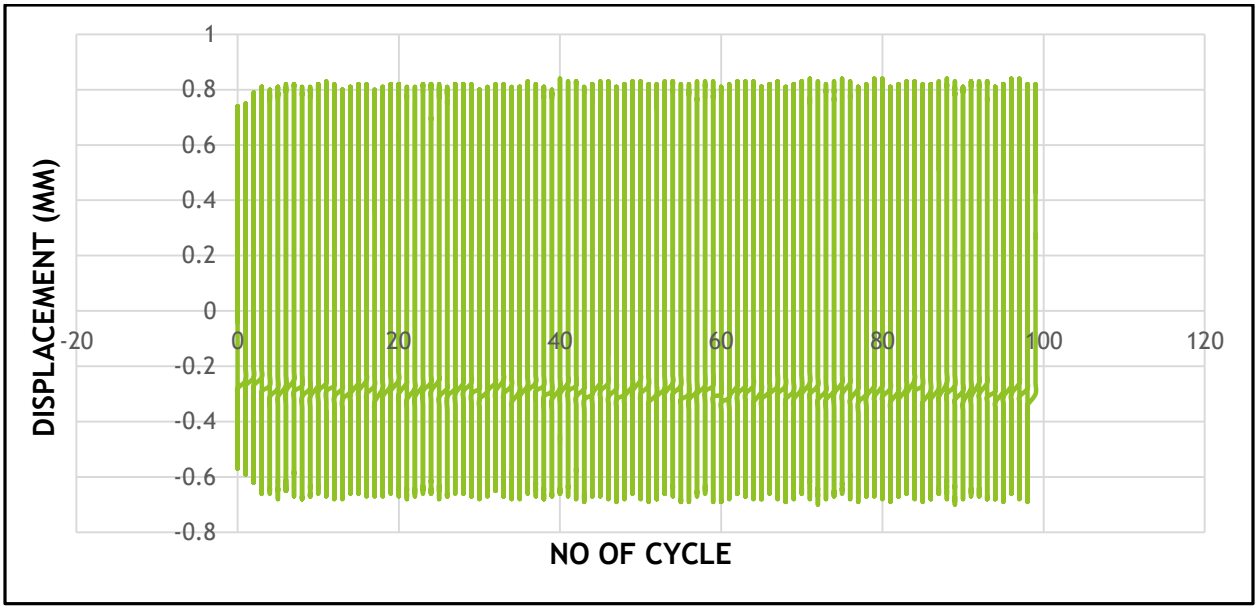

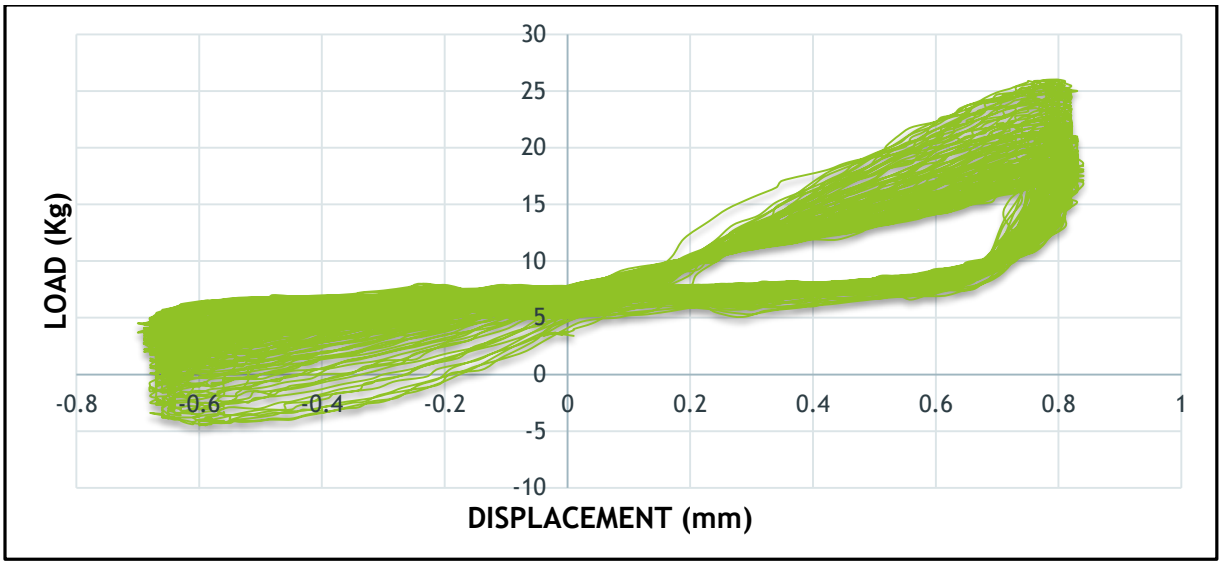

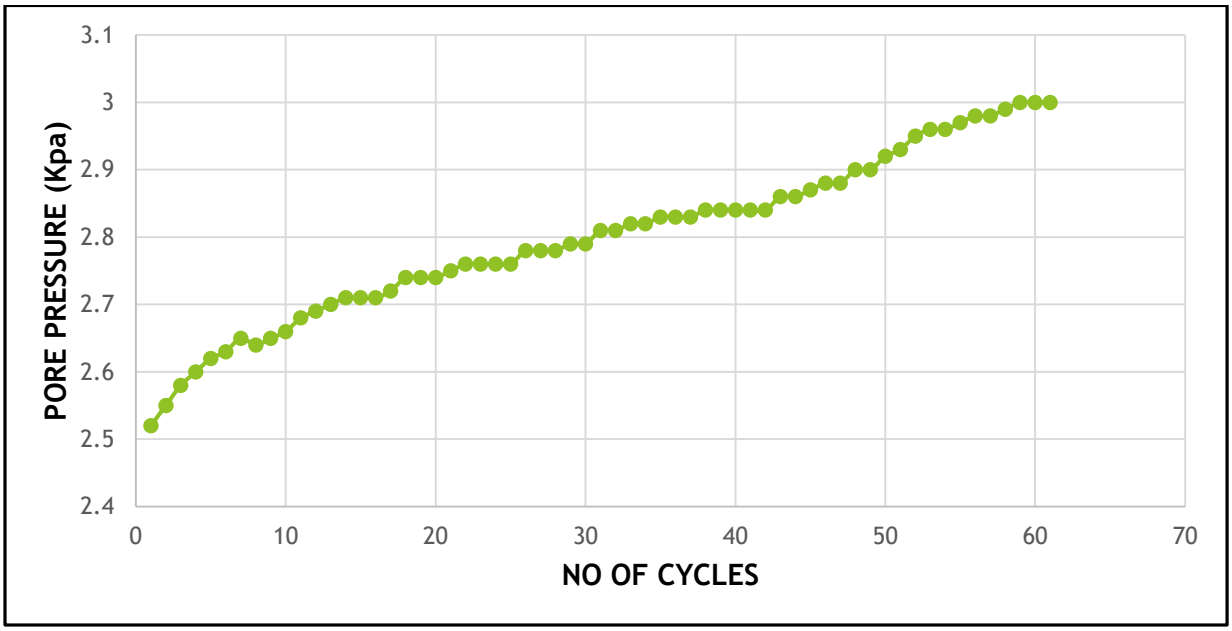

Fig 5.2 Relative Density 50% ; Effective confining pressure 50 KPa ; Amplitude 0.75mm

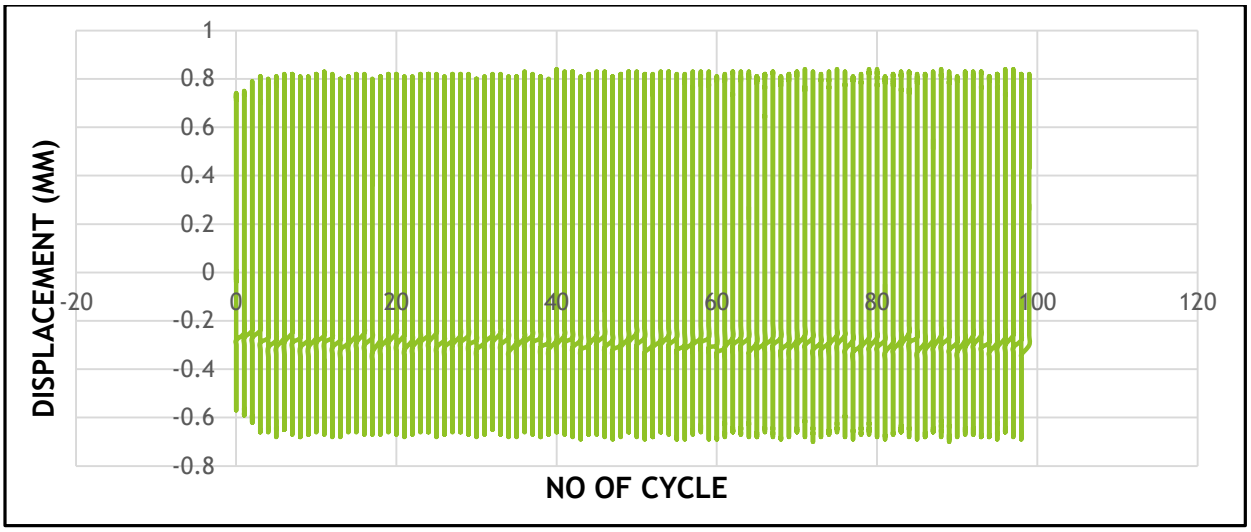

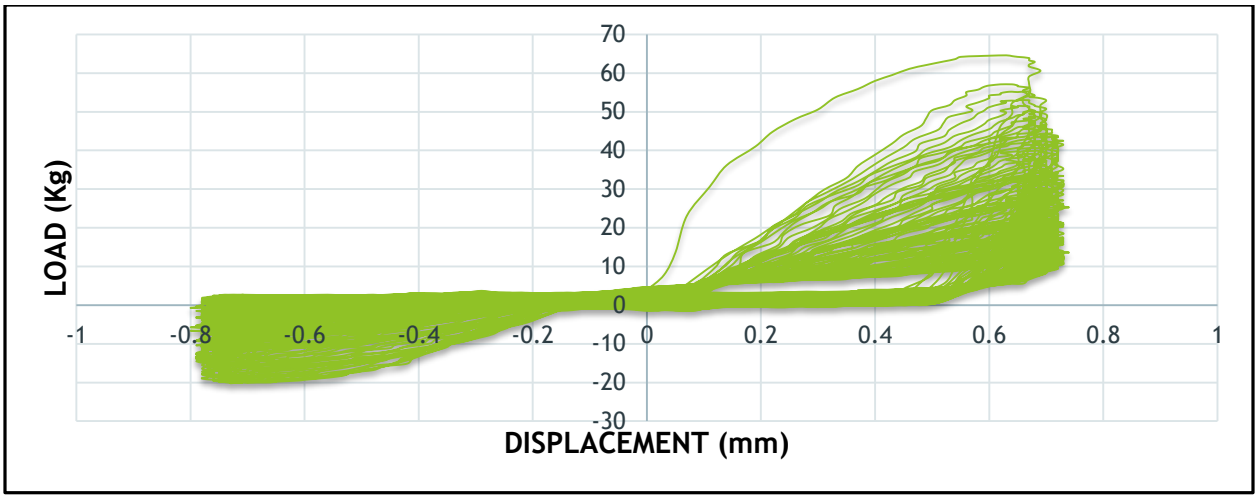

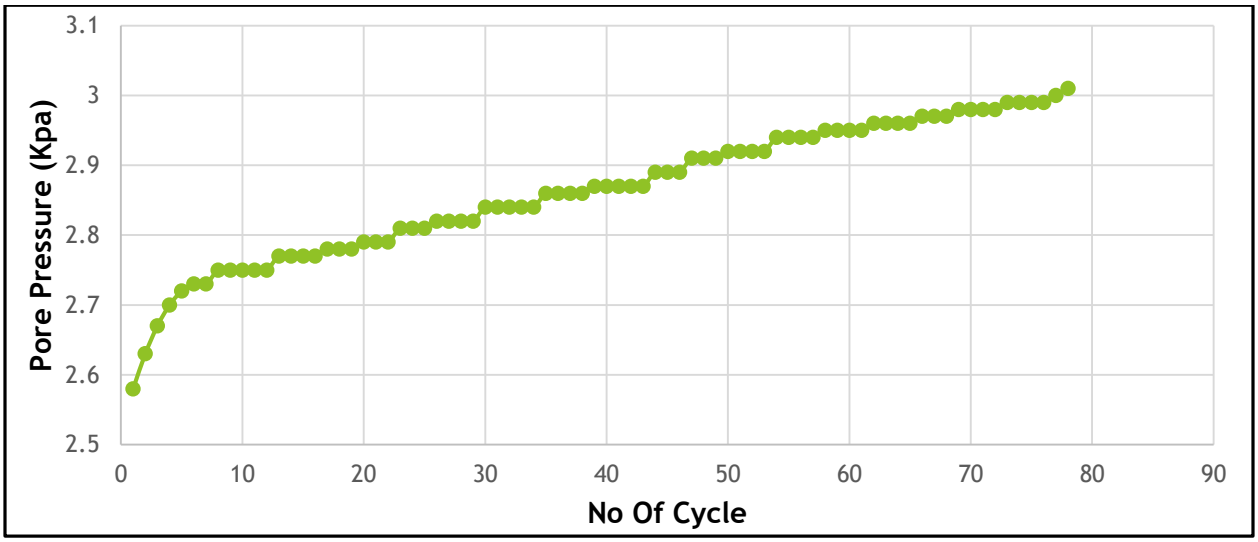

Fig 5.3 Relative Density 75% ; Effective confining pressure 50 KPa ; Amplitude 0.75mm

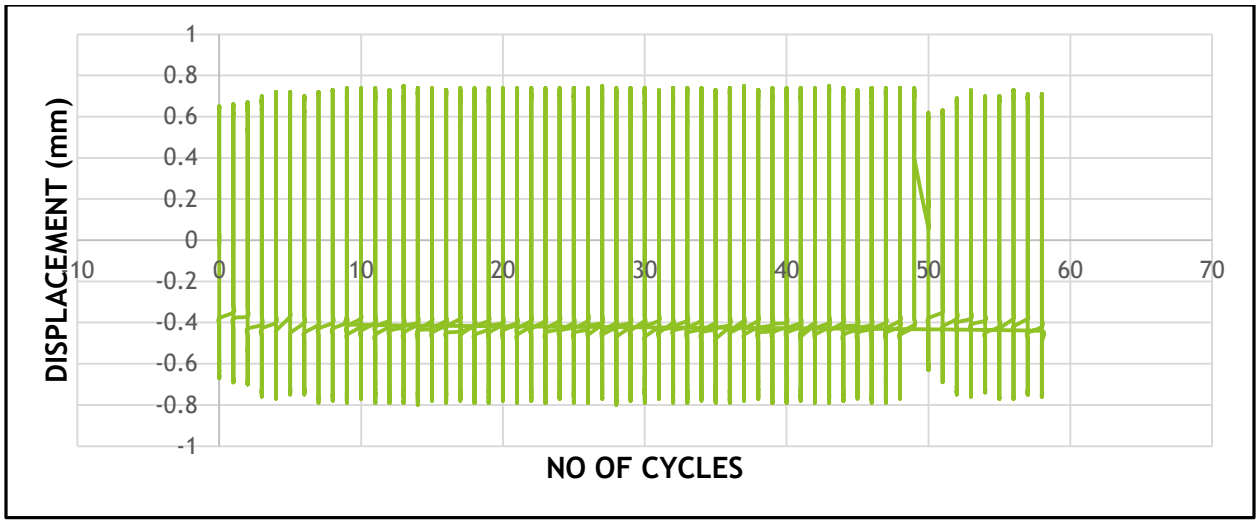

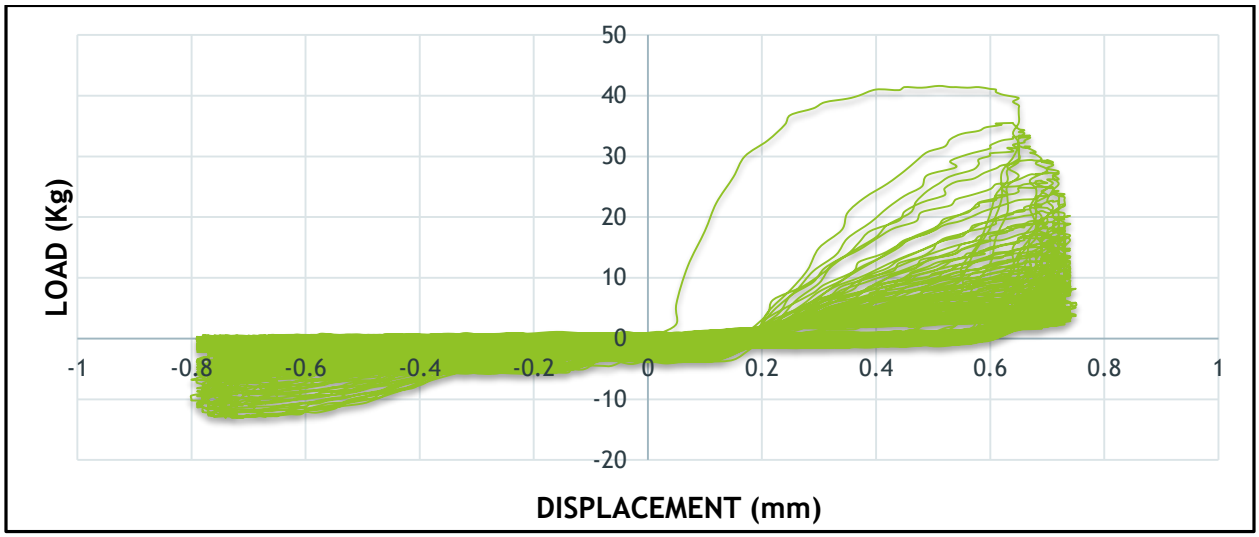

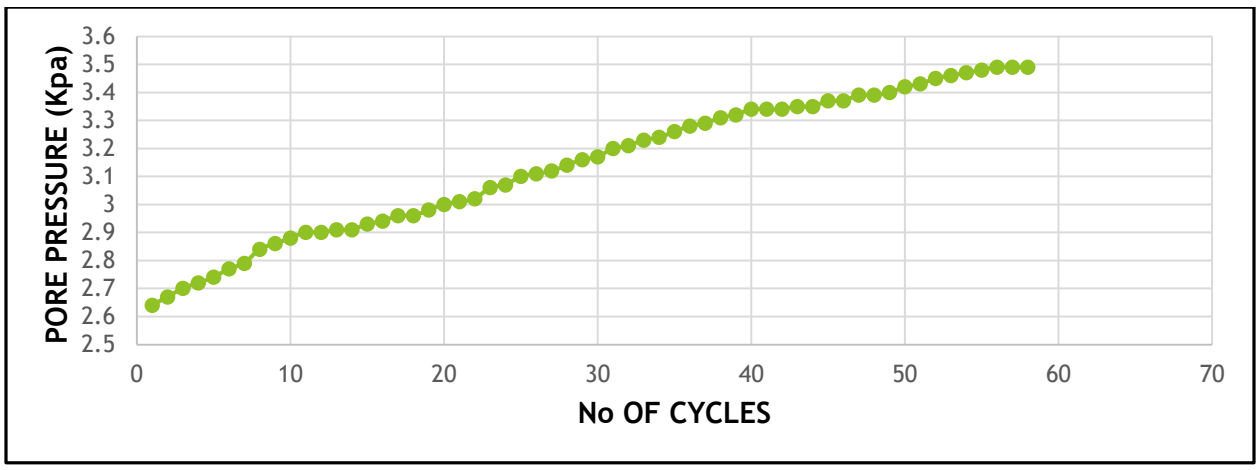

Fig 5.4 Relative Density 25% ; Effective confining pressure 100 KPa ; Amplitude 0.75mm

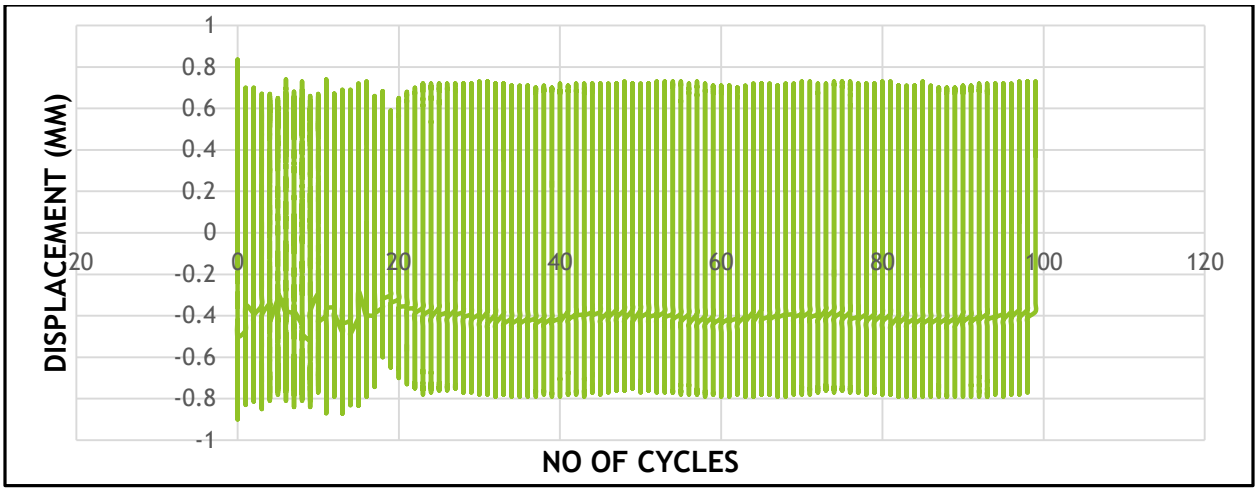

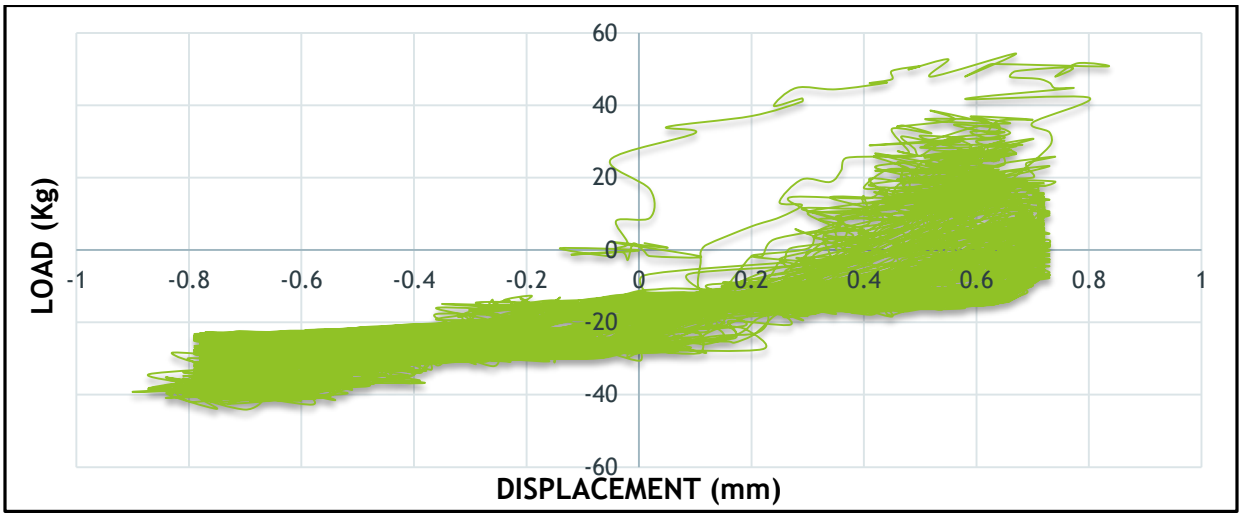

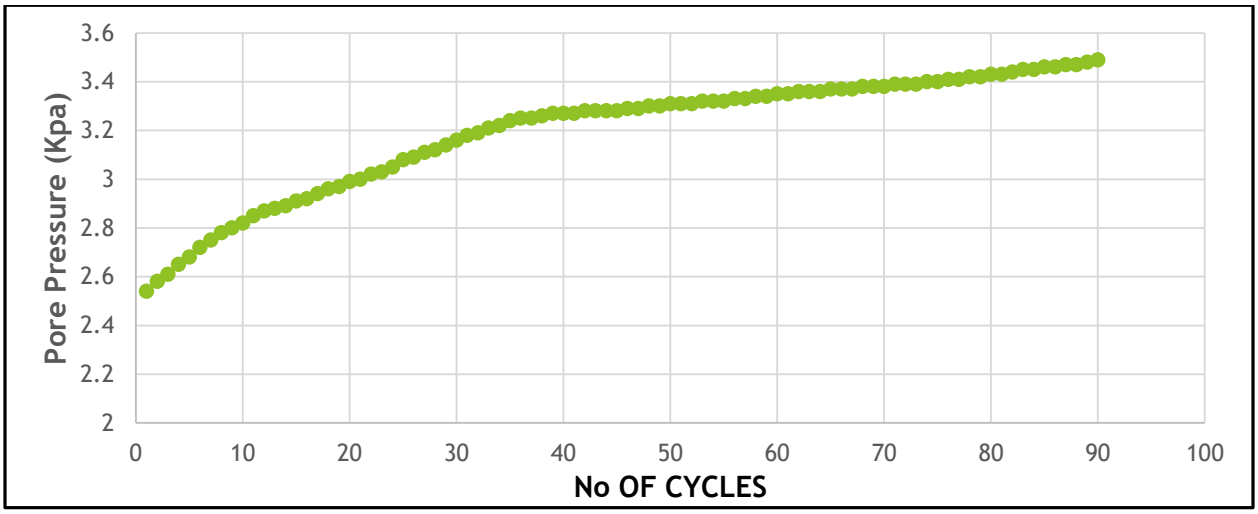

Fig 5.5 Relative Density 50% ; Effective confining pressure 100 KPa ; Amplitude 0.75mm

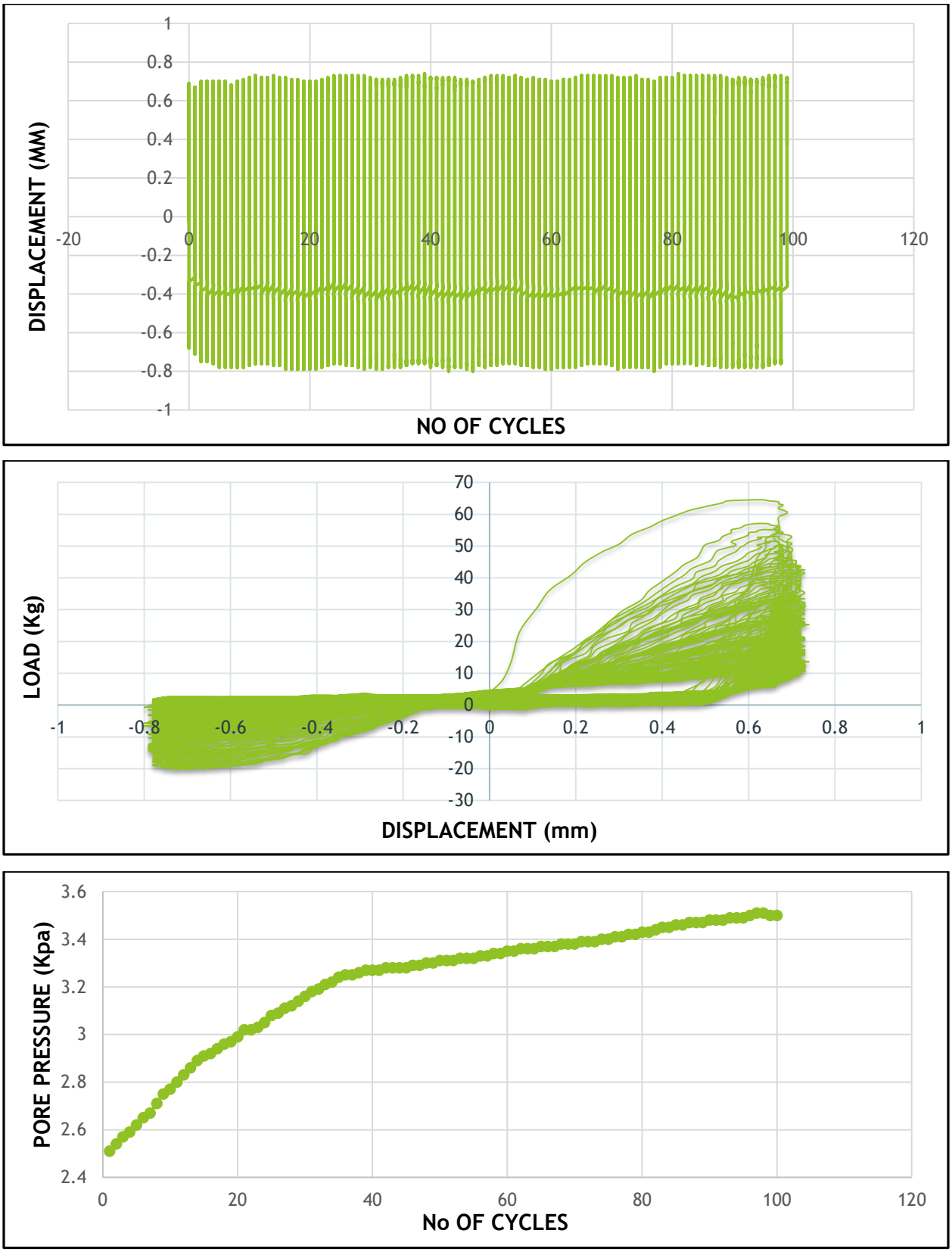

Fig 5.6 Relative Density 75% ; Effective confining pressure 100 KPa ; Amplitude 0.75mm

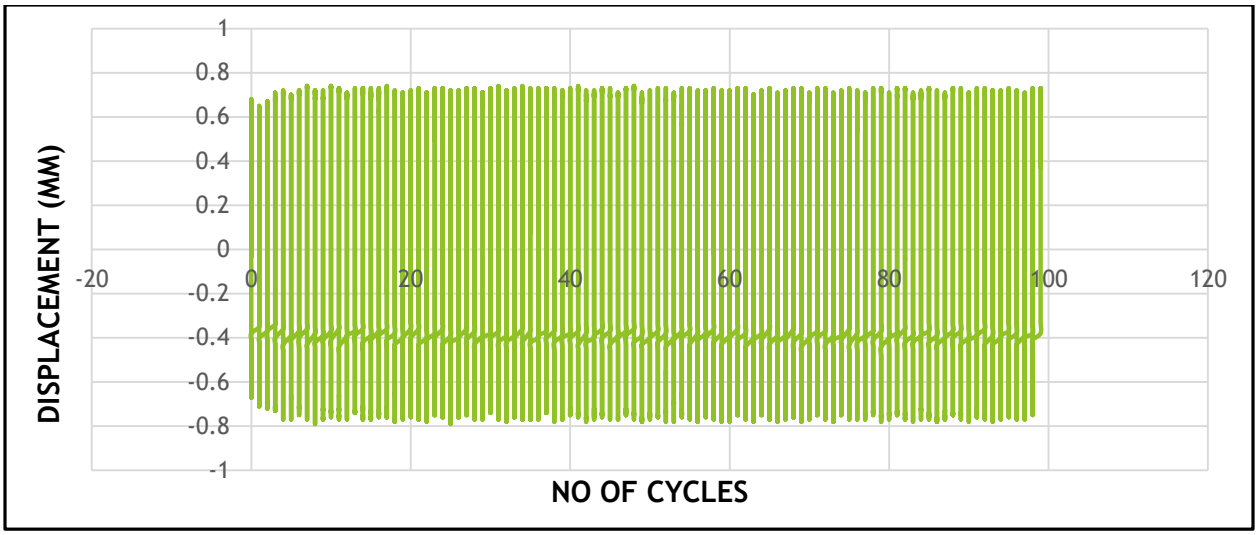

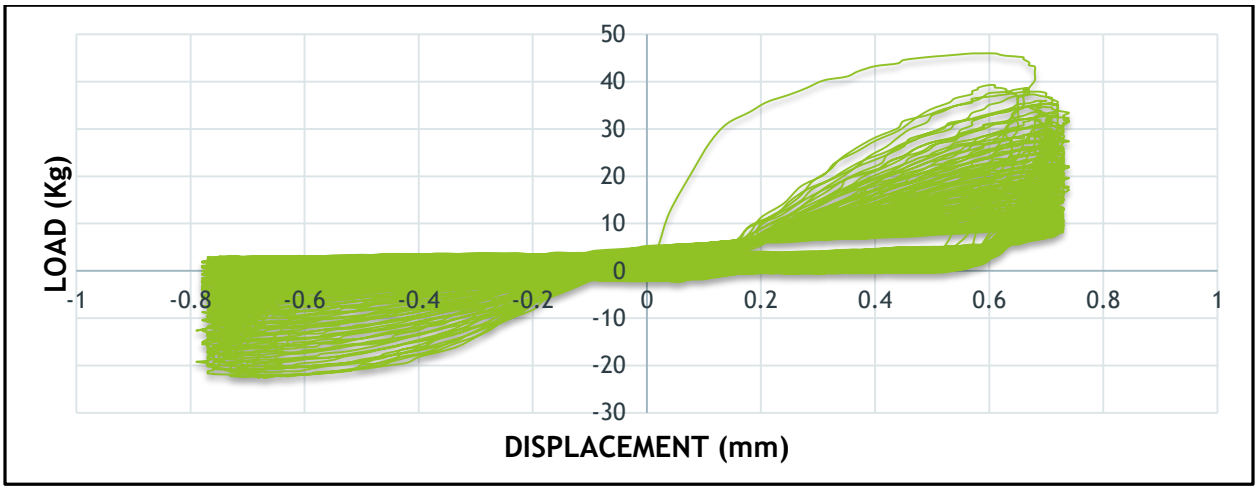

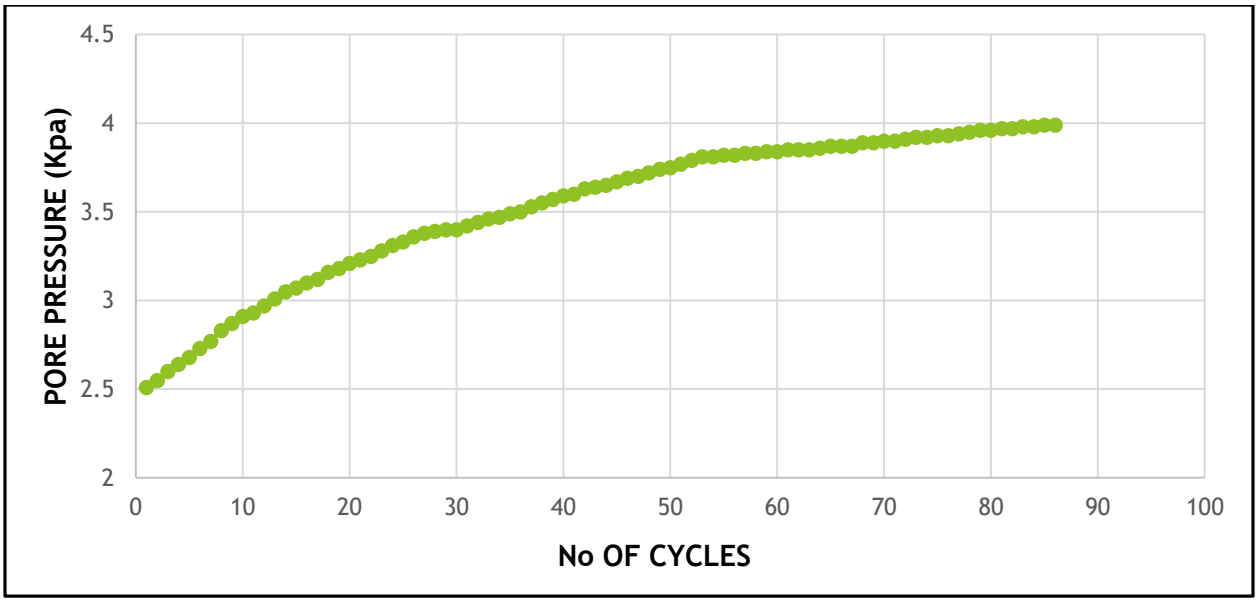

Fig 5.7 Relative Density 25% ; Effective confining pressure 150 KPa ; Amplitude 0.75mm

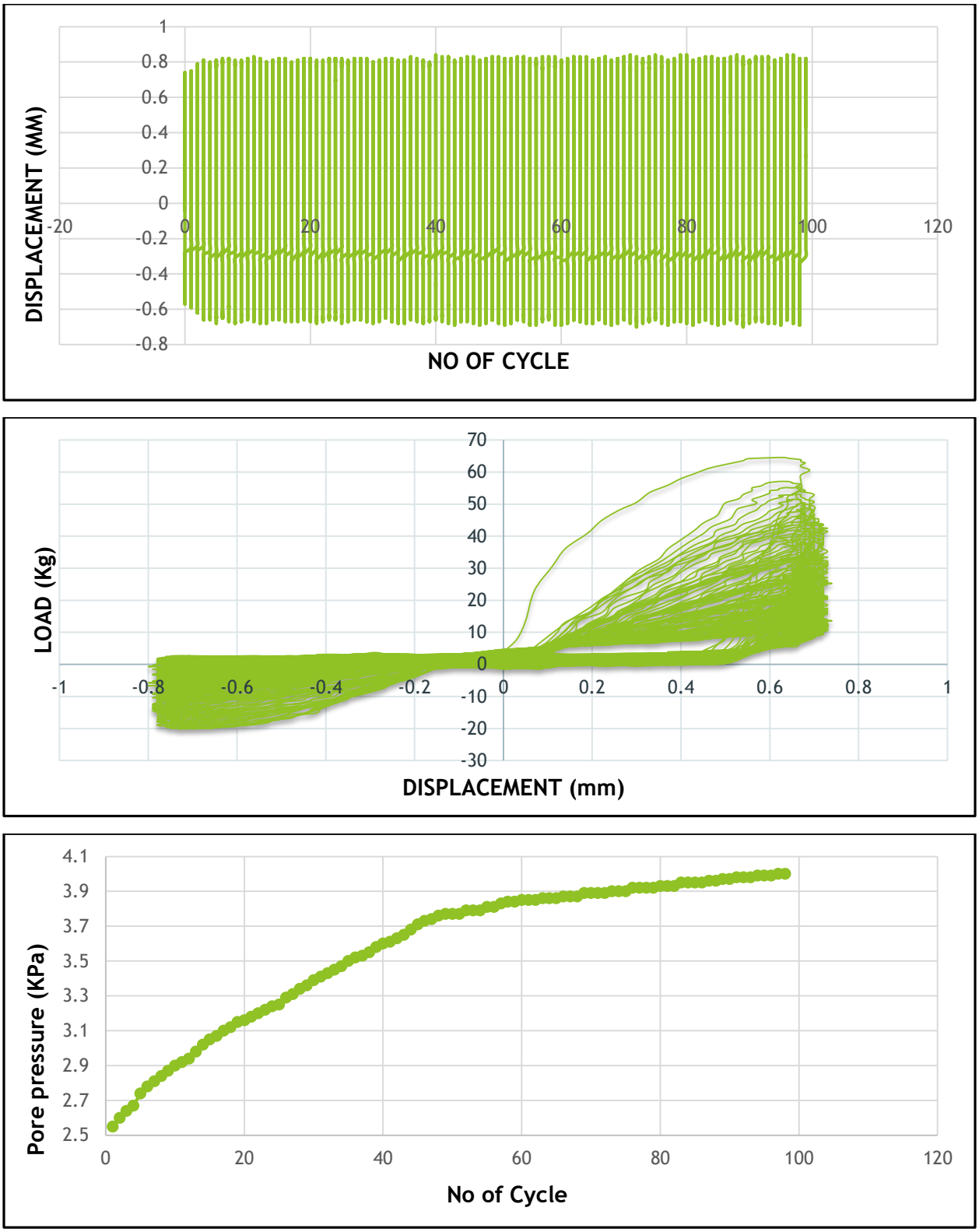

Fig 5.8 Relative Density 50% ; Effective confining pressure 150 KPa ; Amplitude 0.75mm

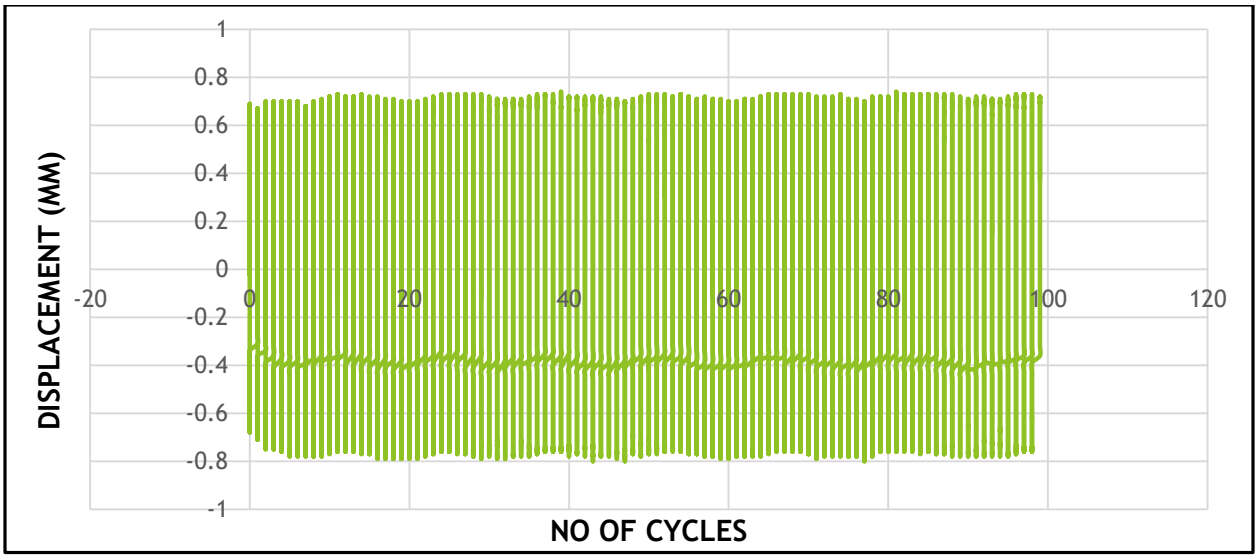

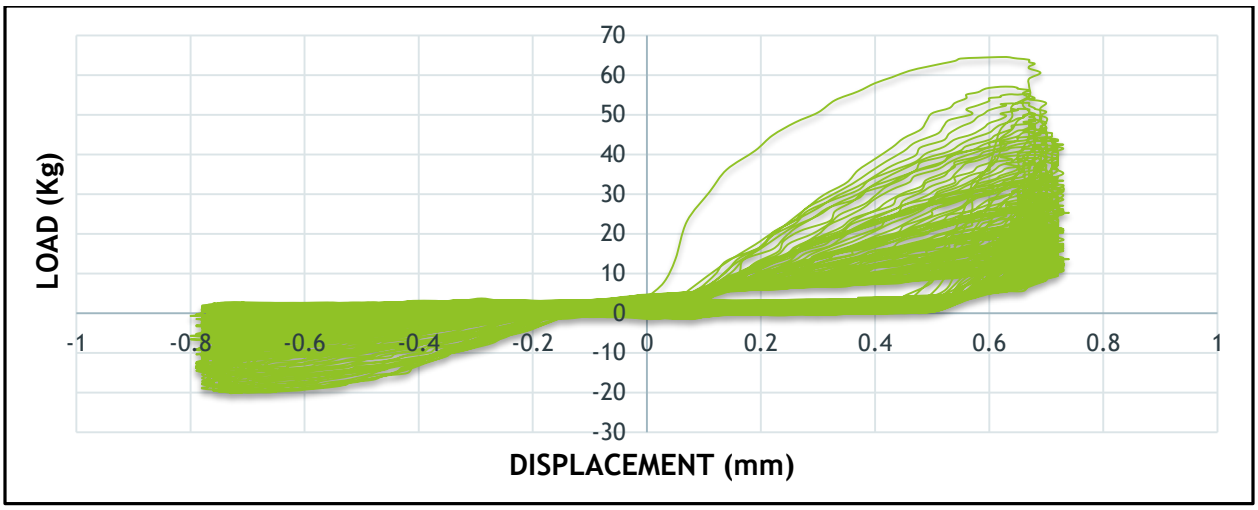

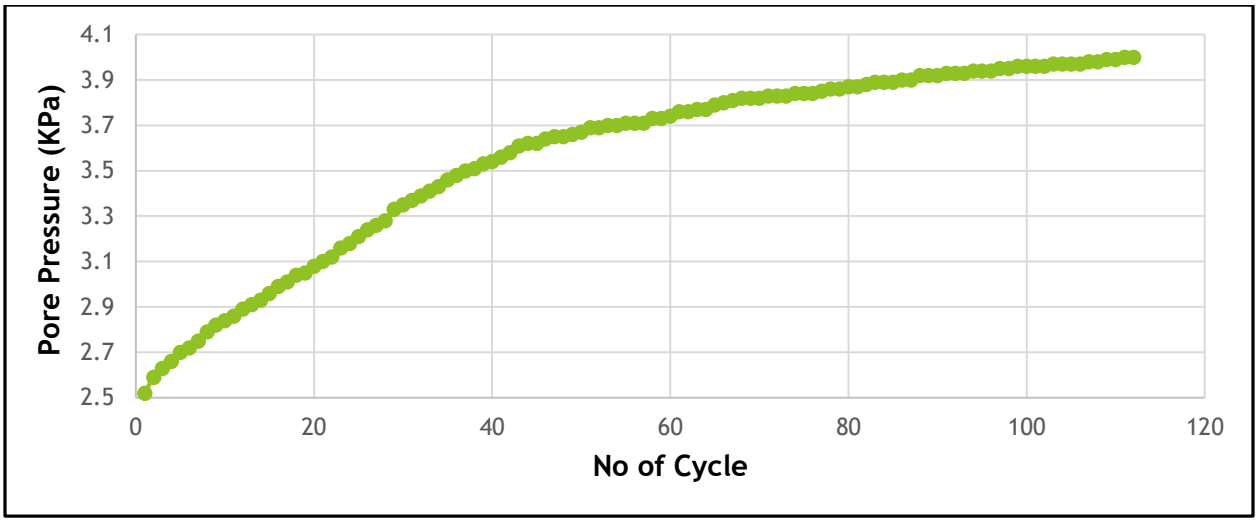

Fig 5.9 Relative Density 75% ; Effective confining pressure 150 KPa ; Amplitude 0.75mm

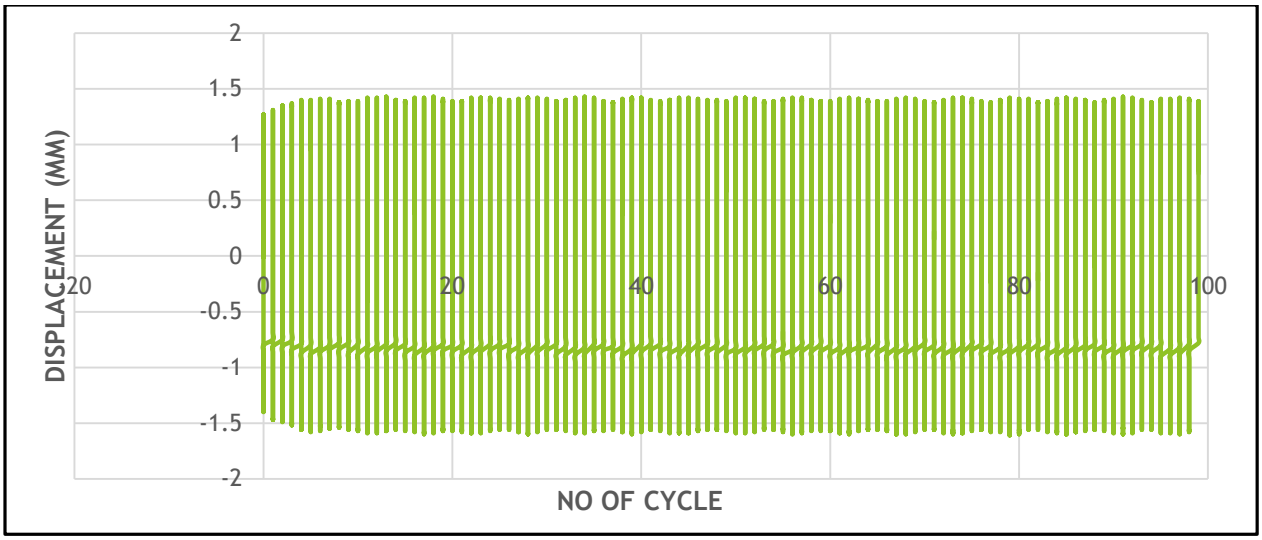

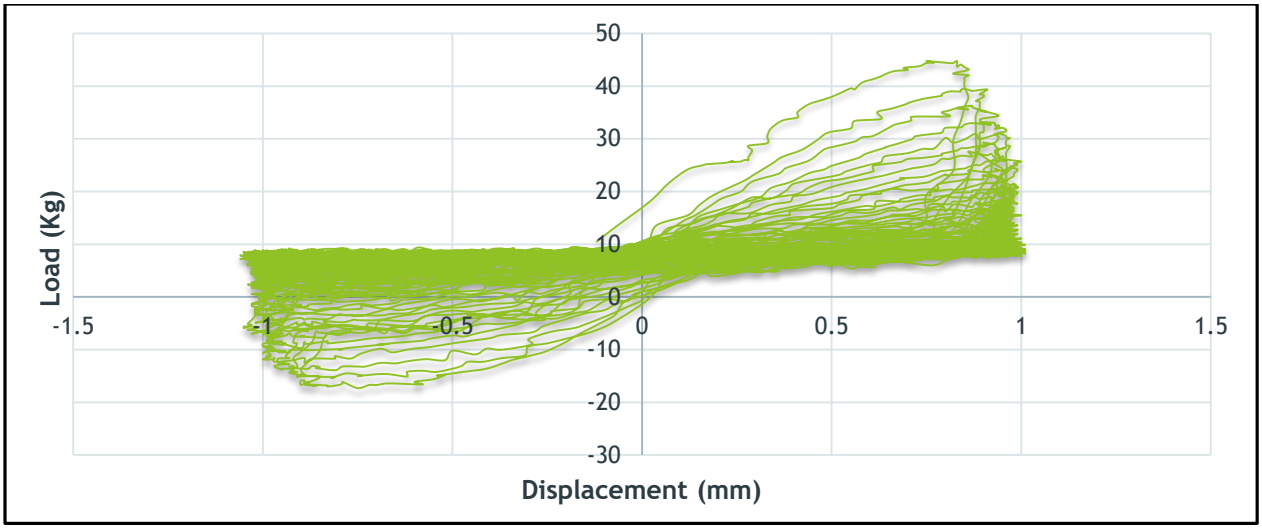

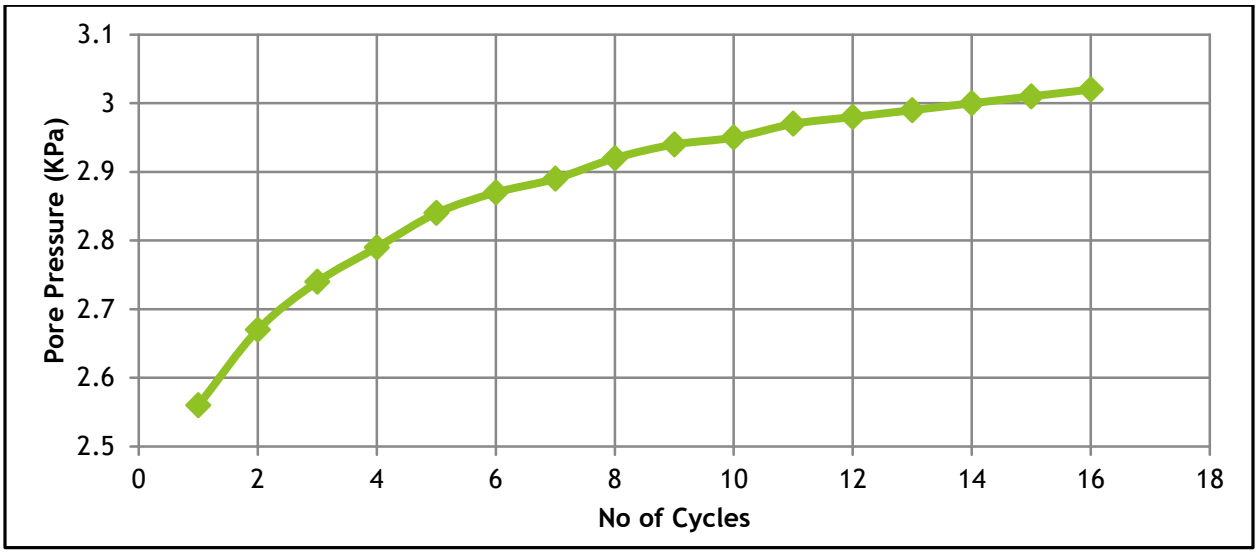

Fig 5.10 Relative Density 25% ; Effective confining pressure 50 KPa ; Amplitude 1.00mm

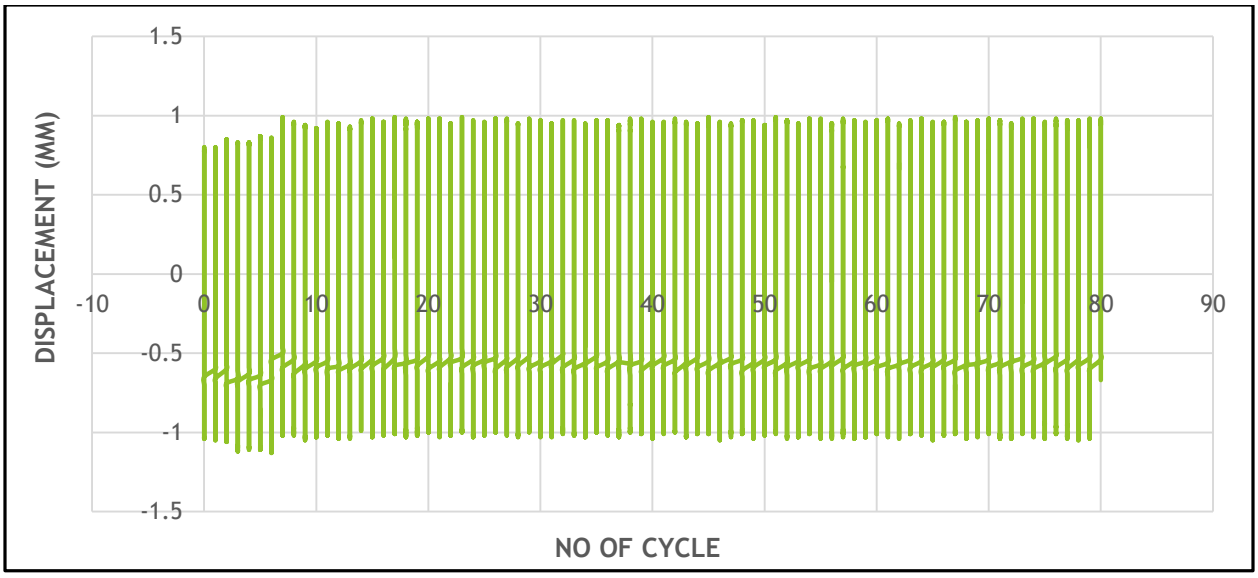

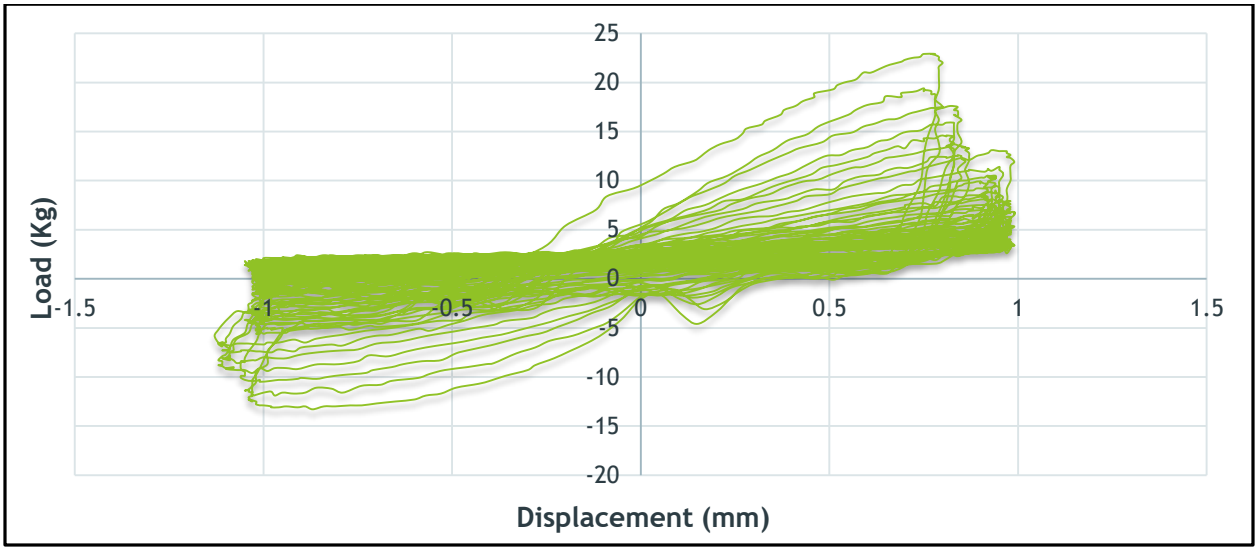

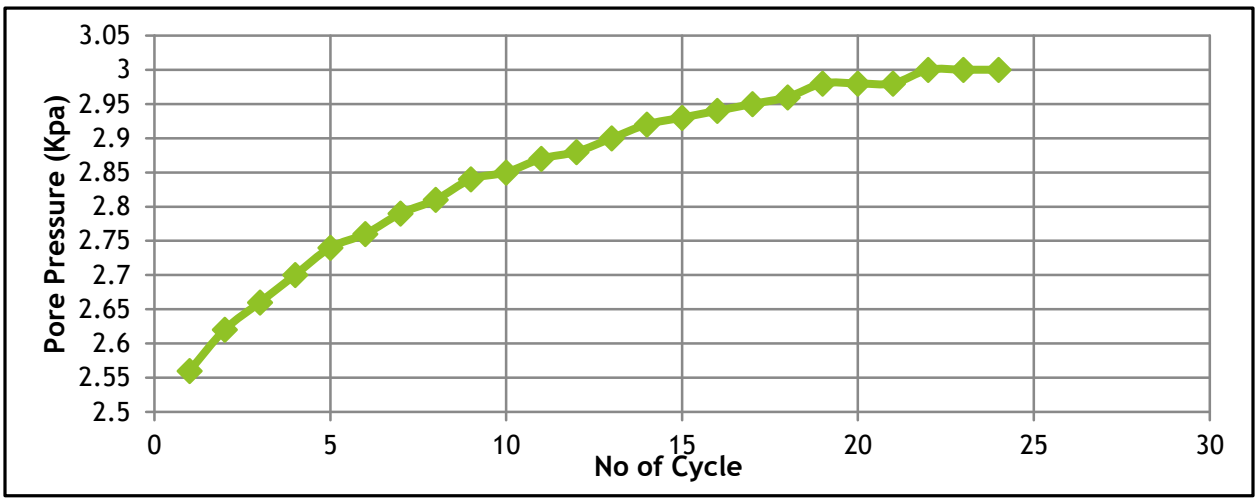

Fig 5.11 Relative Density 50% ; Effective confining pressure 50 KPa ; Amplitude 1.00mm

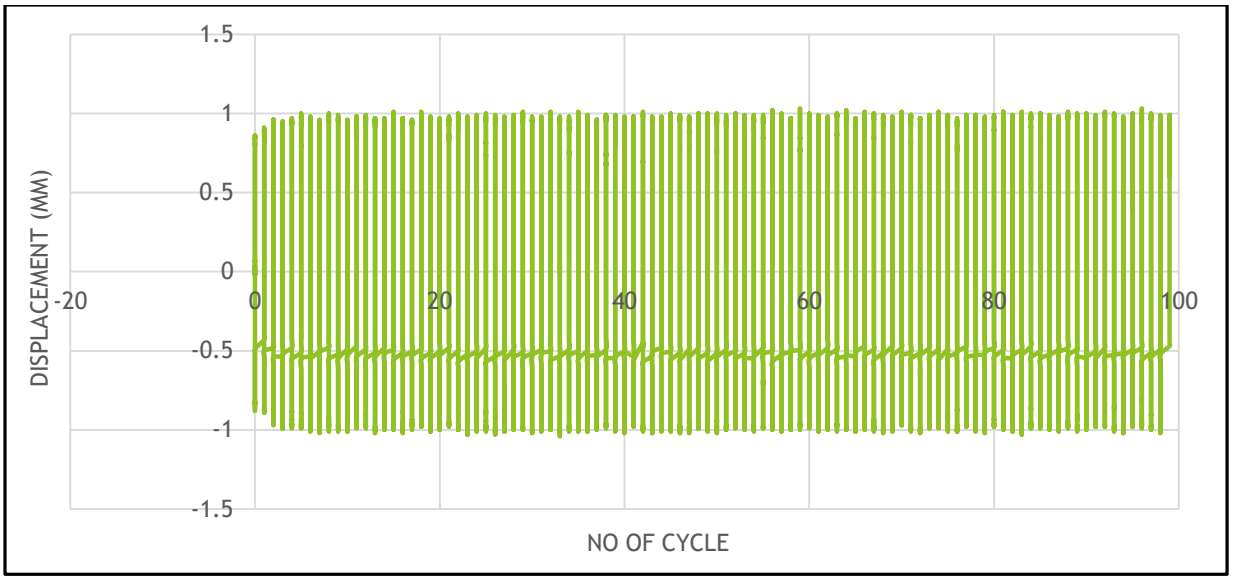

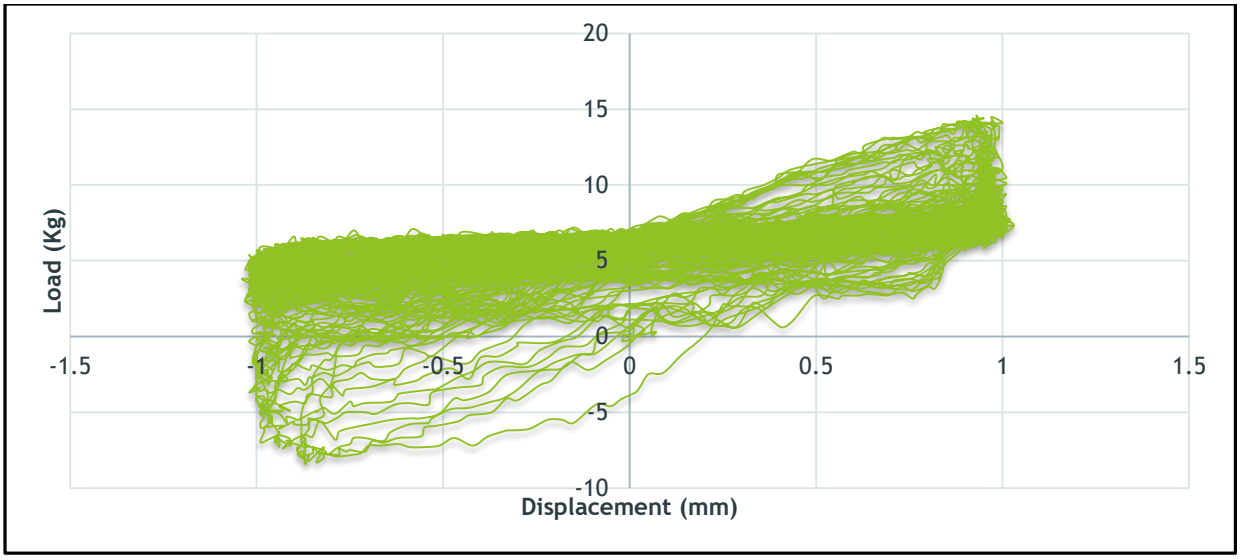

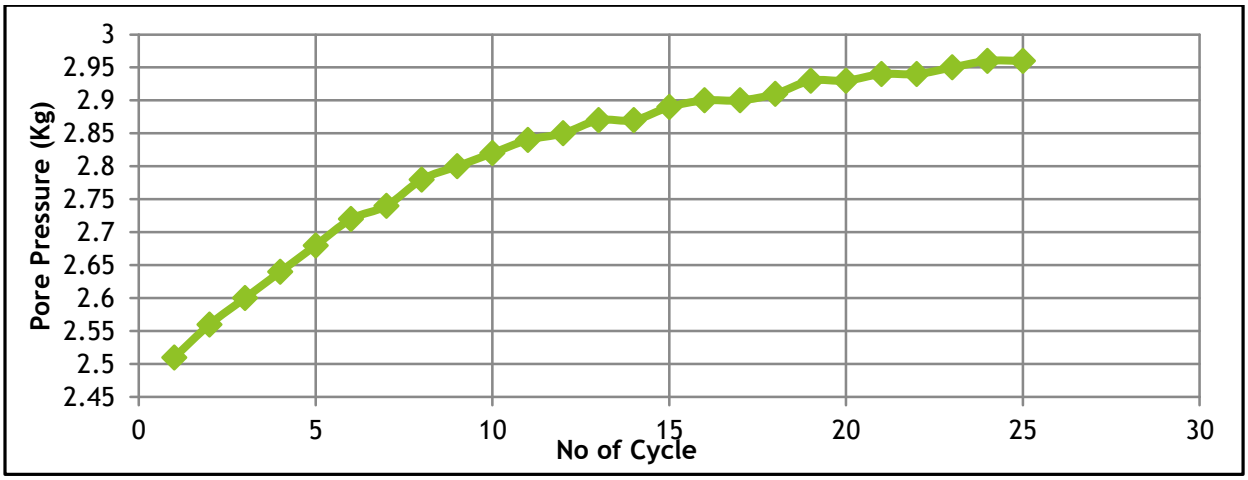

Fig 5.12 Relative Density 75% ; Effective confining pressure 50 KPa ; Amplitude 1.00mm

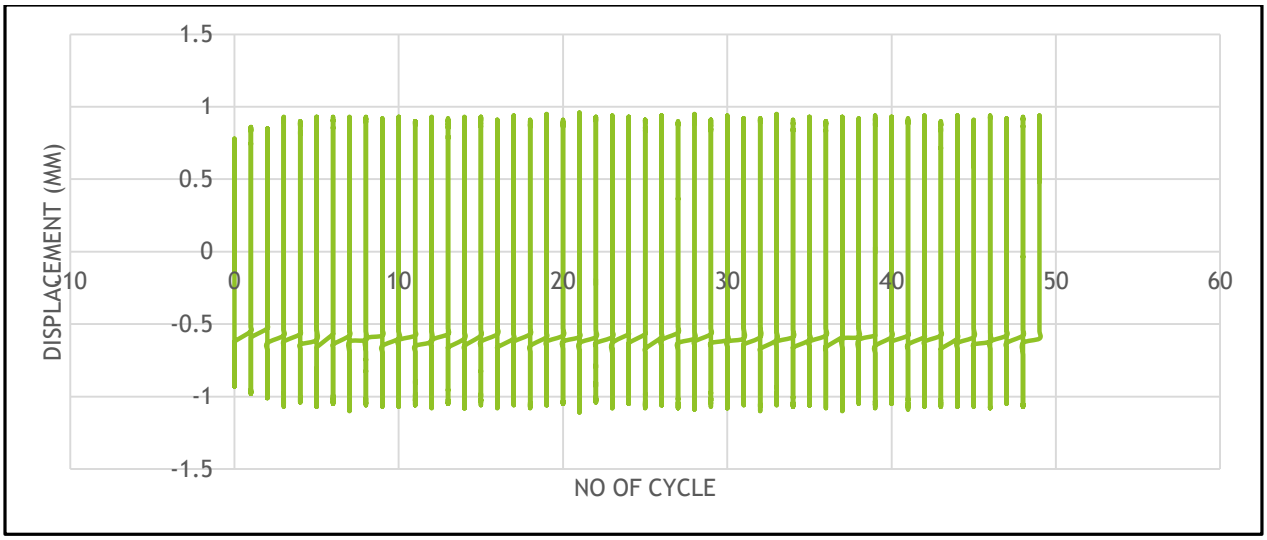

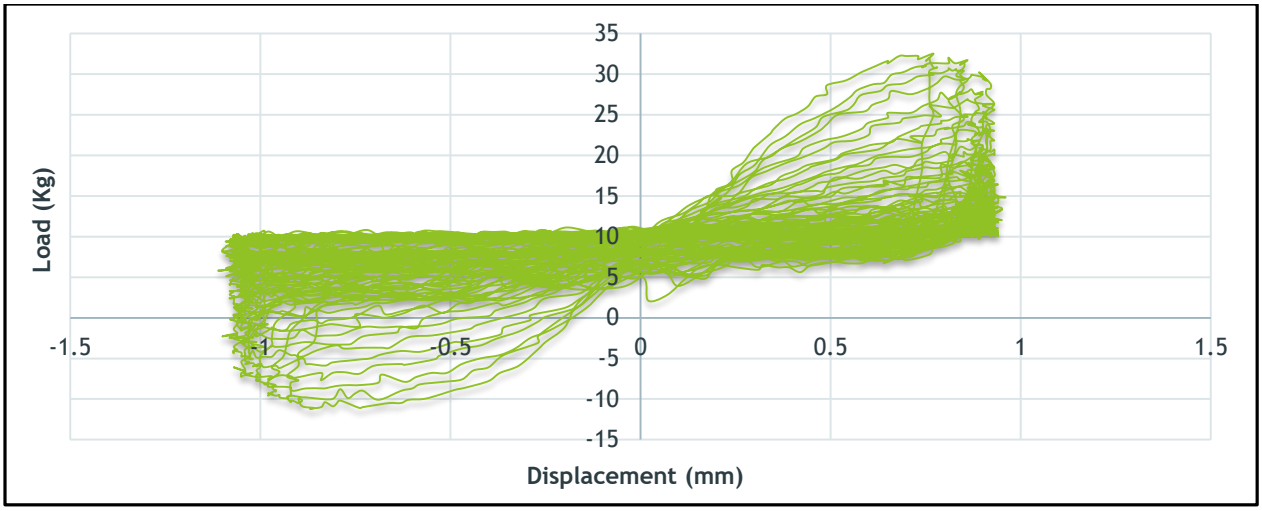

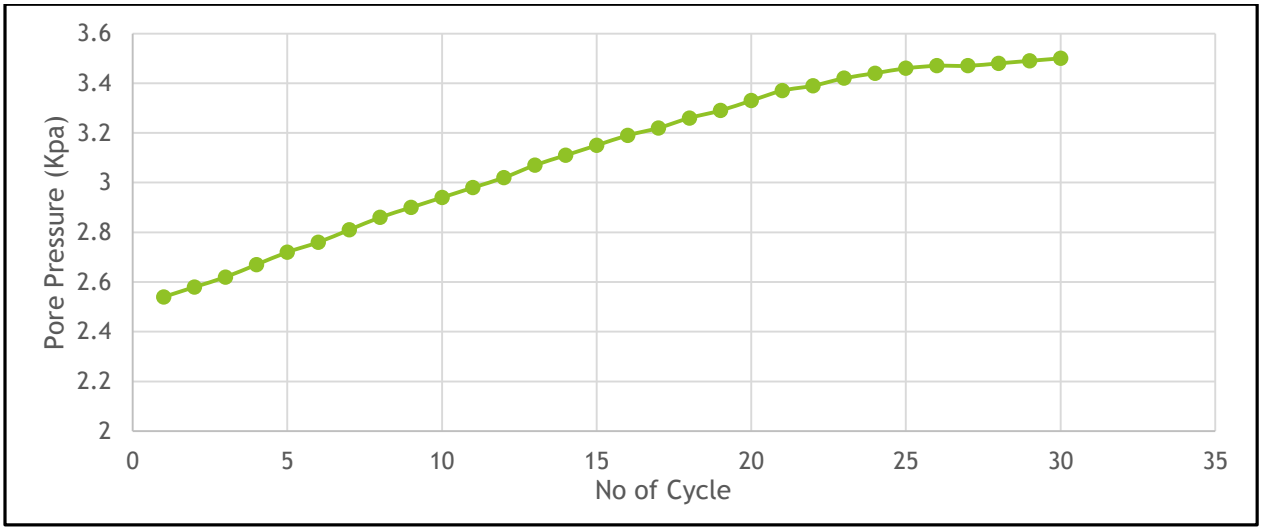

Fig 5.13 Relative Density 25% ; Effective confining pressure 100 KPa ; Amplitude 1.00mm

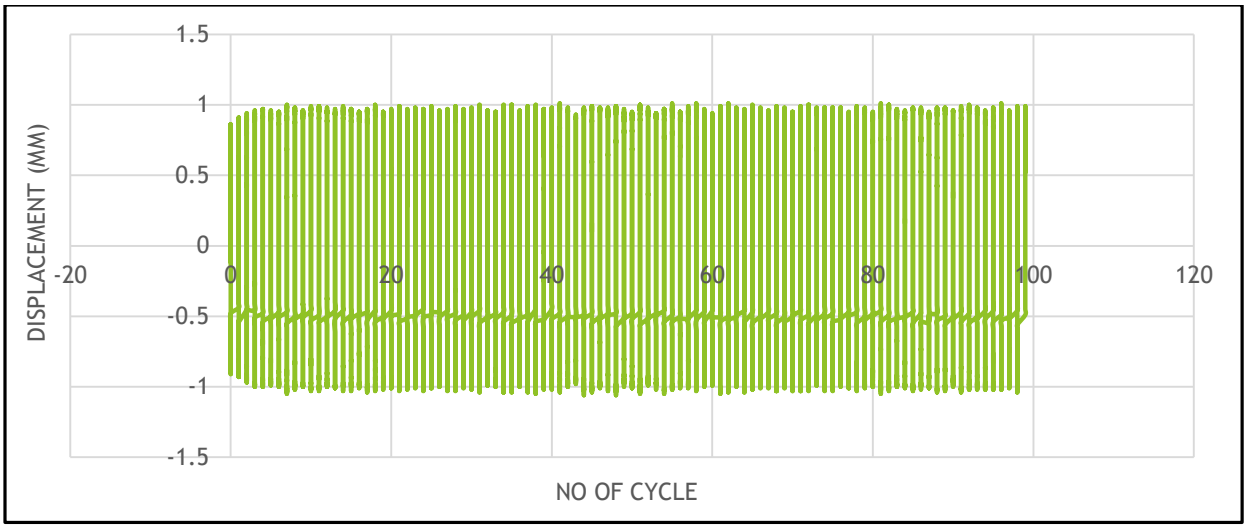

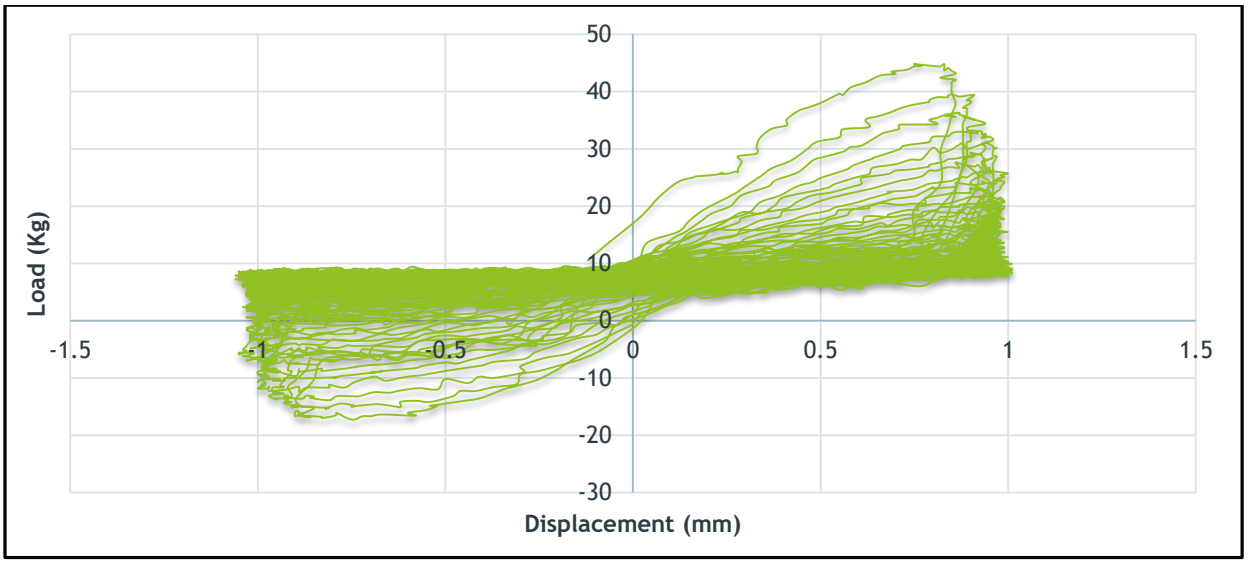

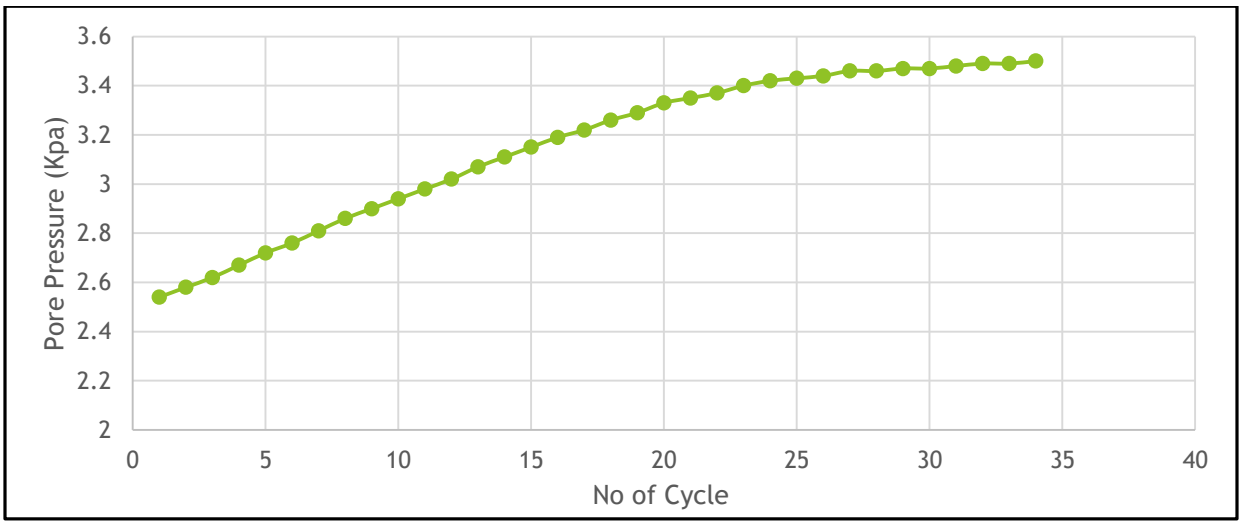

Fig 5.14 Relative Density 50% ; Effective confining pressure 100 KPa ; Amplitude 1.00mm

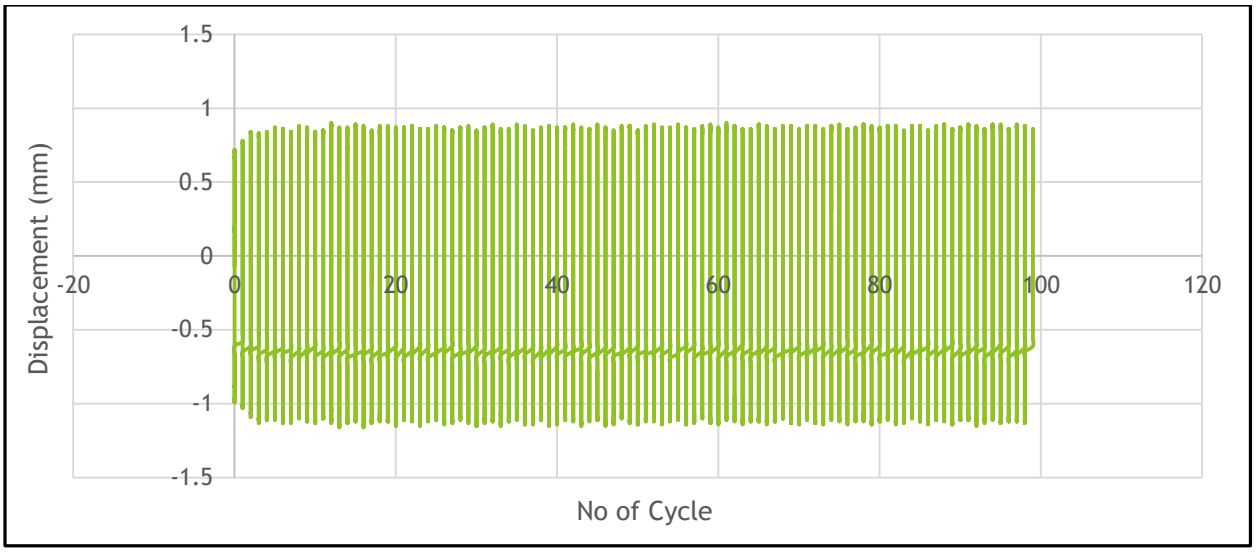

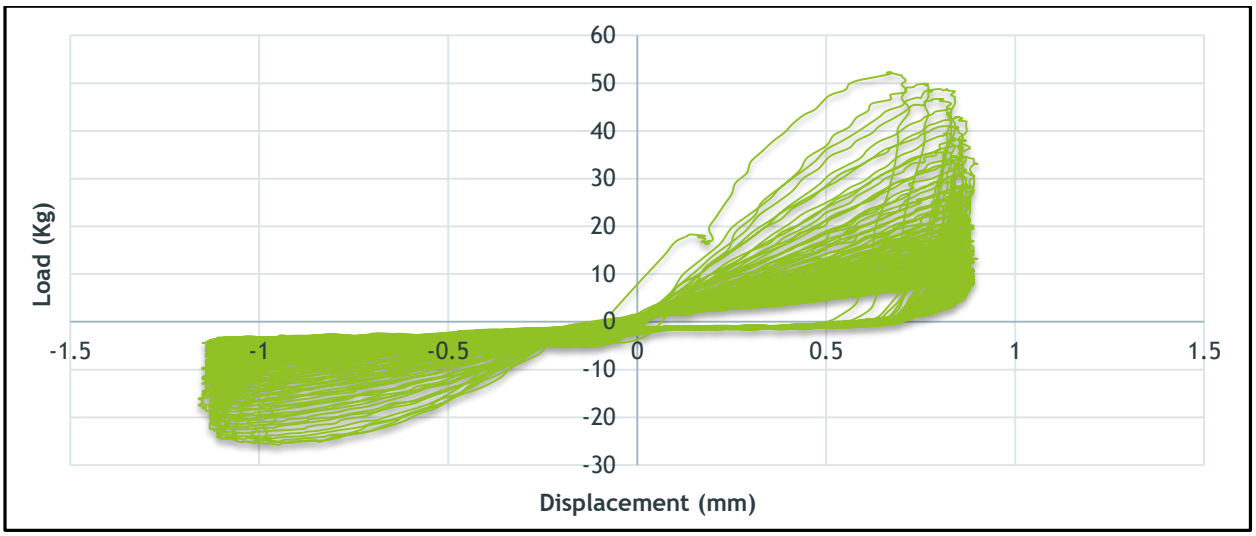

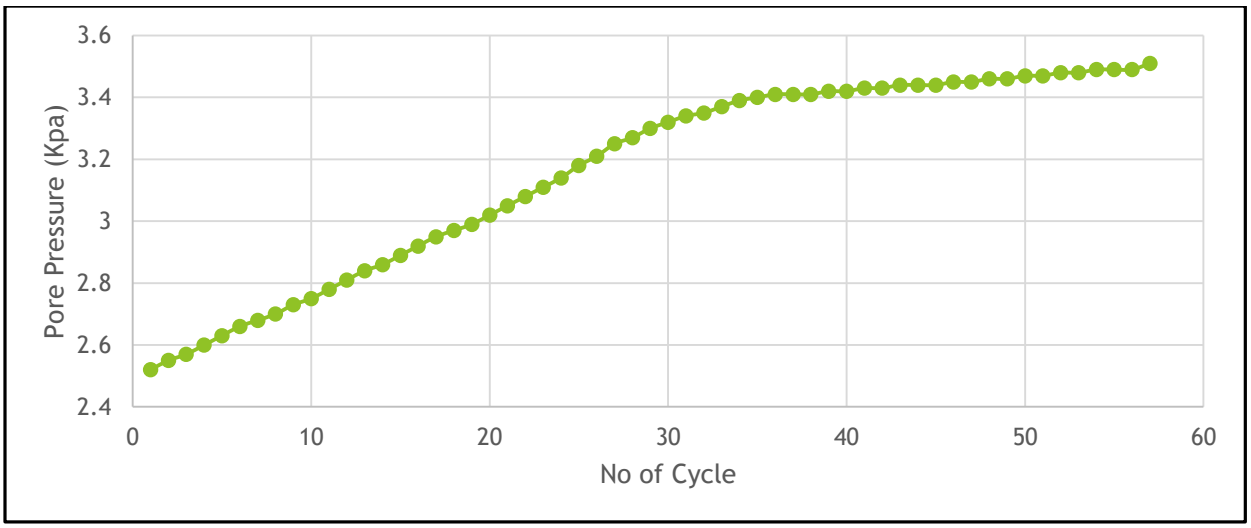

Fig 5.15 Relative Density 75% ; Effective confining pressure 100 KPa ; Amplitude 1.00mm

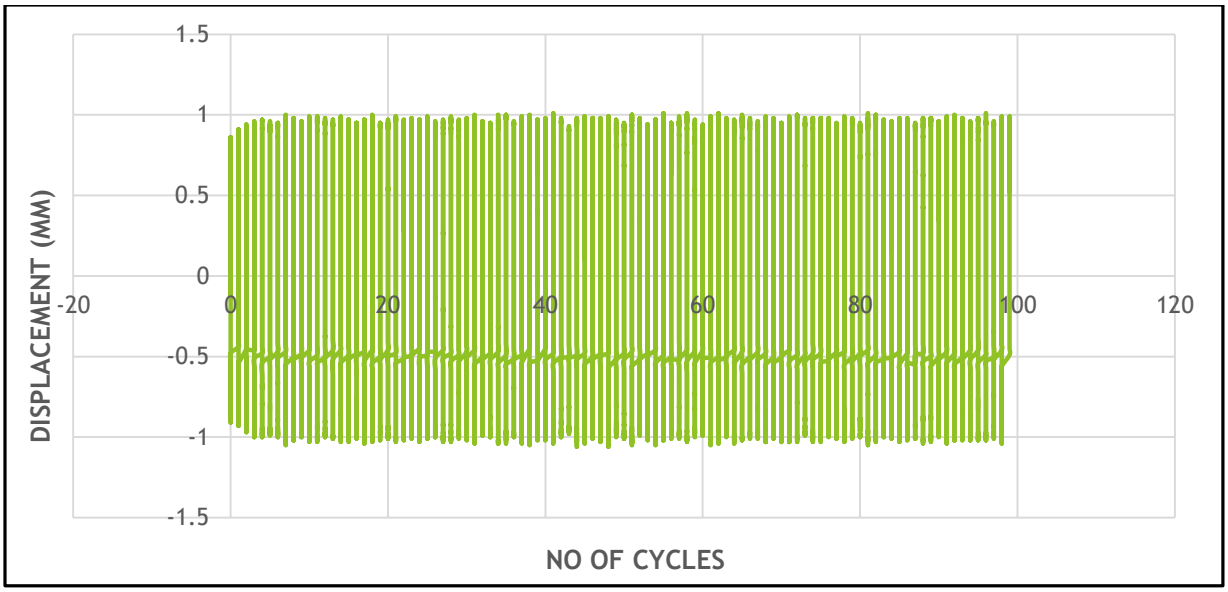

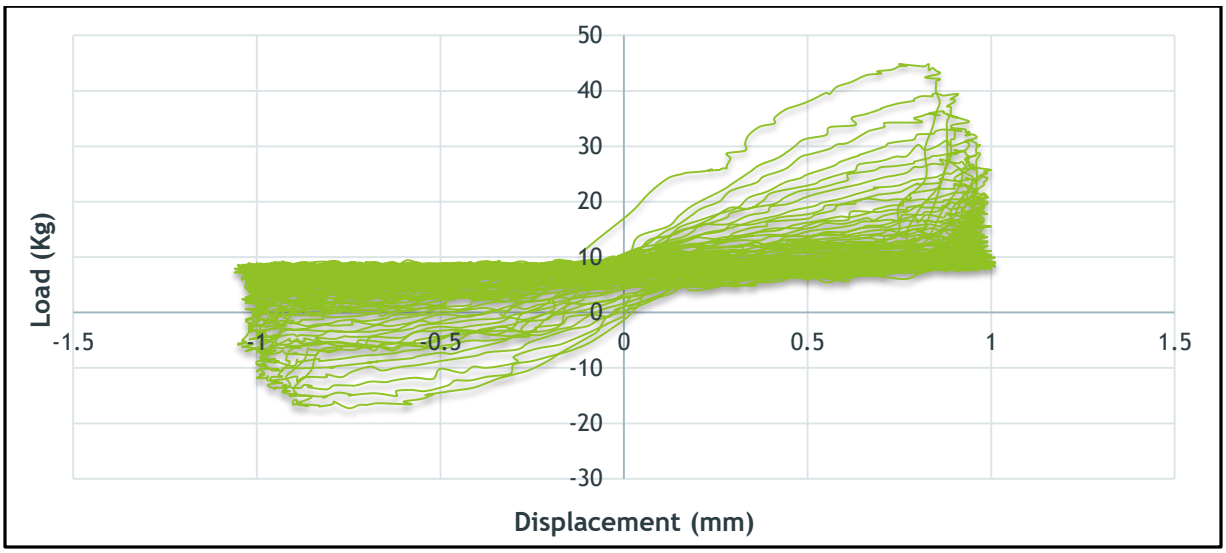

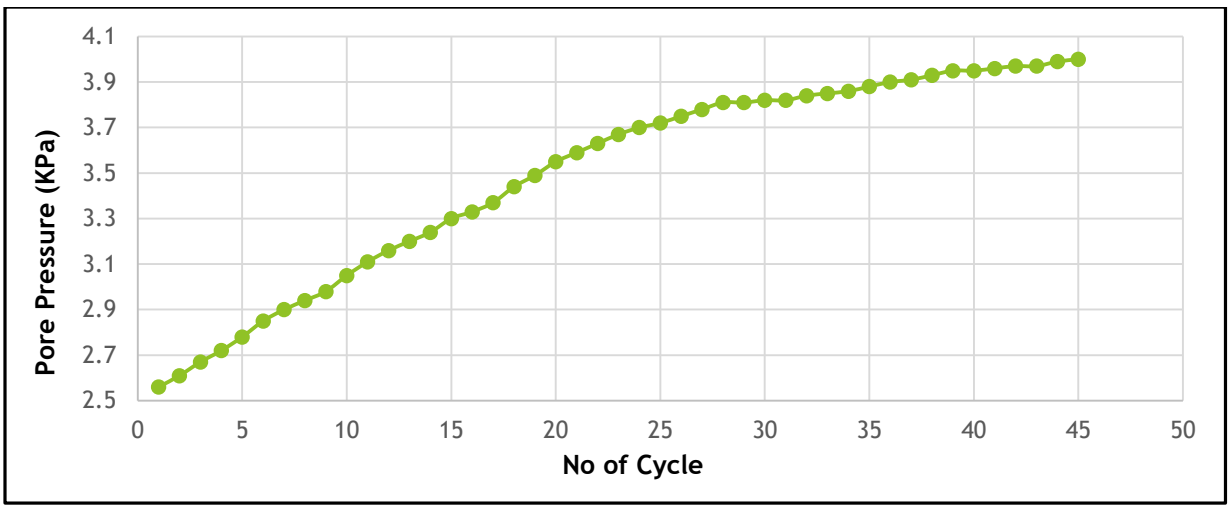

Fig 5.16 Relative Density 25% ; Effective confining pressure 150 KPa ; Amplitude 1.00mm

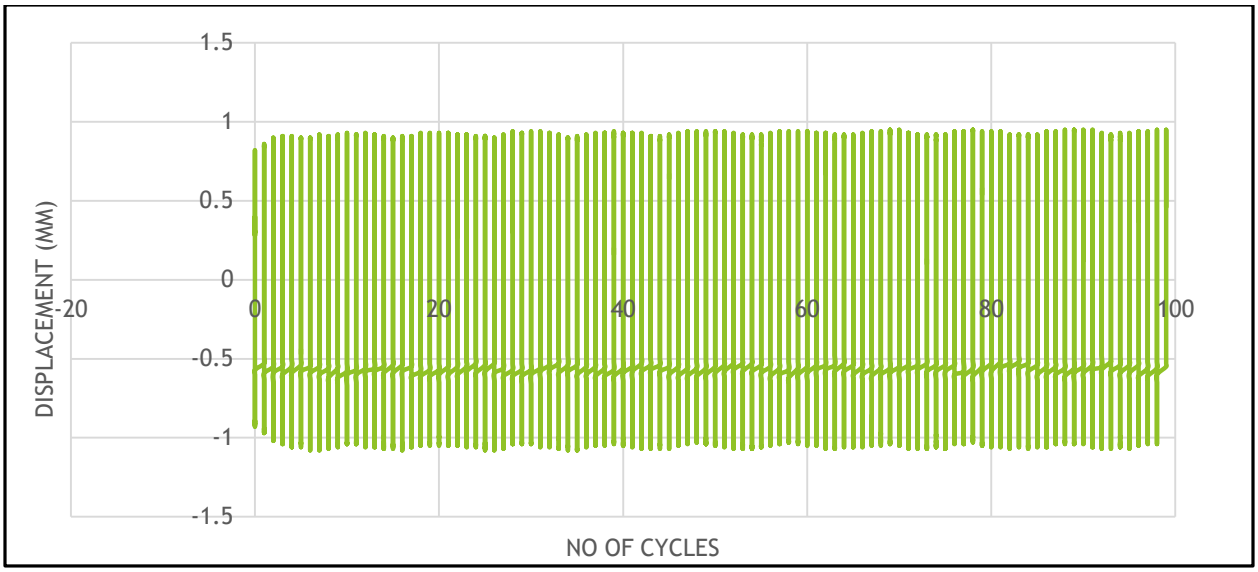

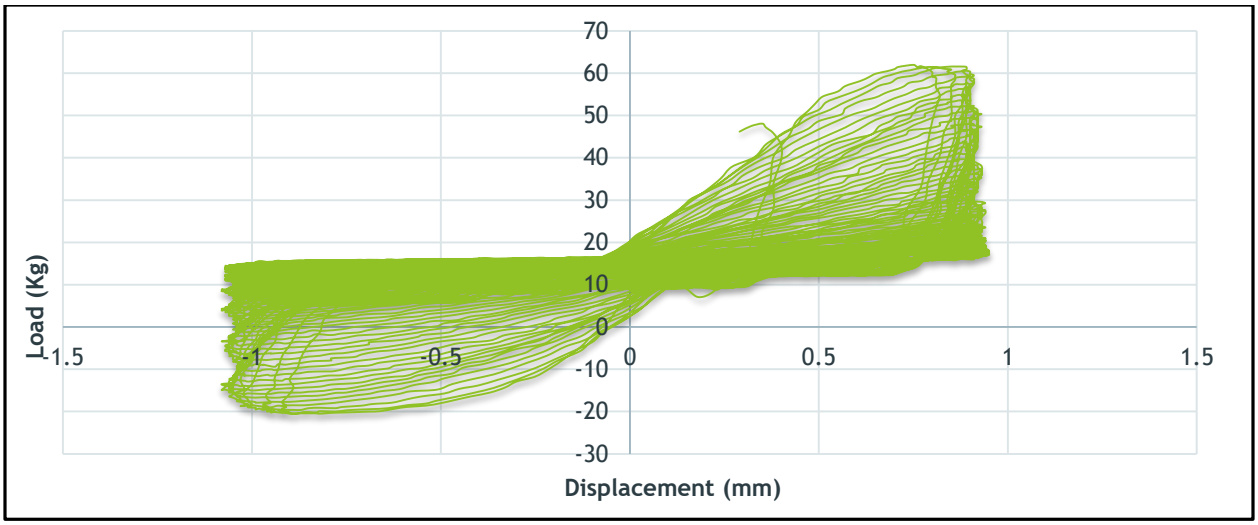

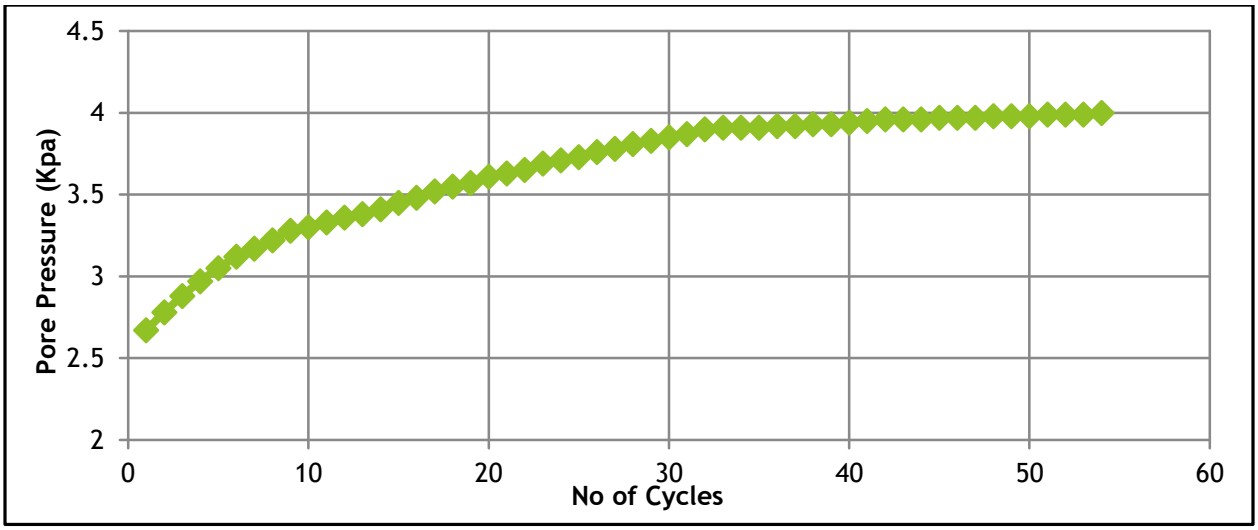

Fig 5.17 Relative Density 50% ; Effective confining pressure 150 KPa ; Amplitude 1.00mm

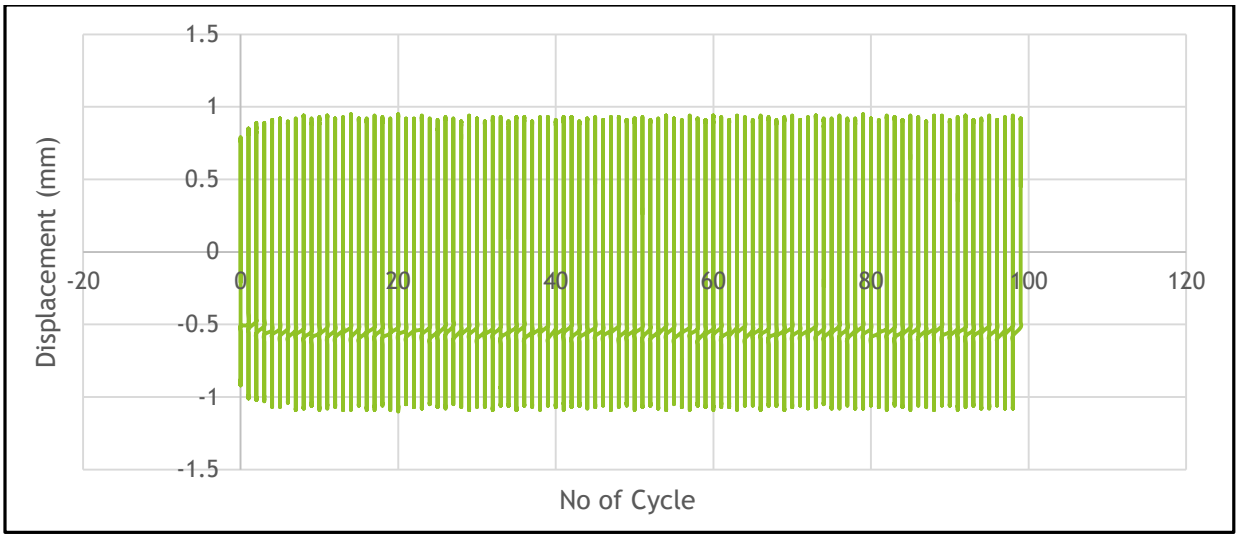

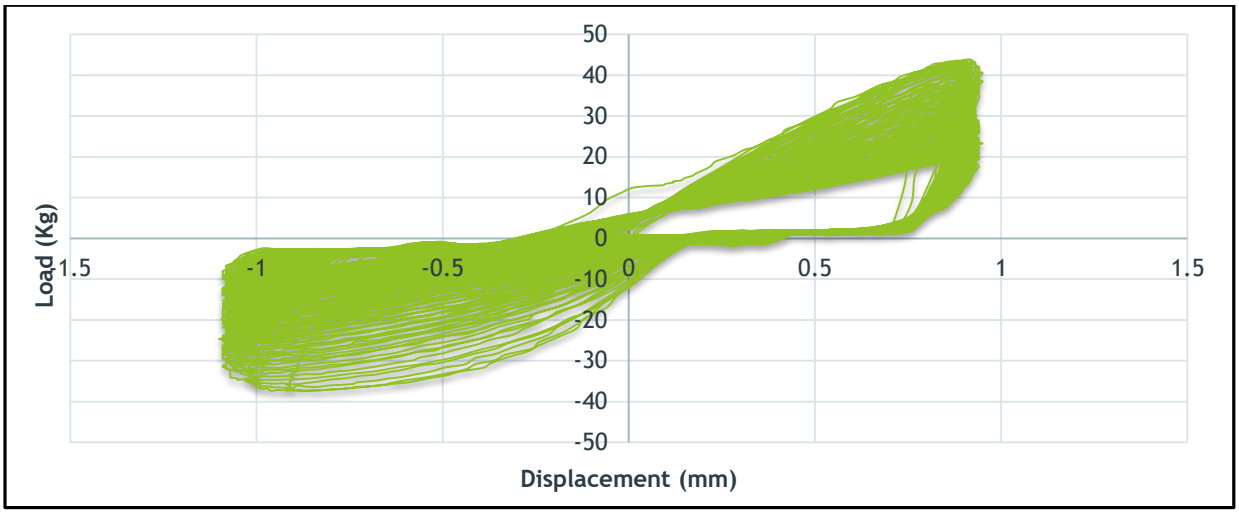

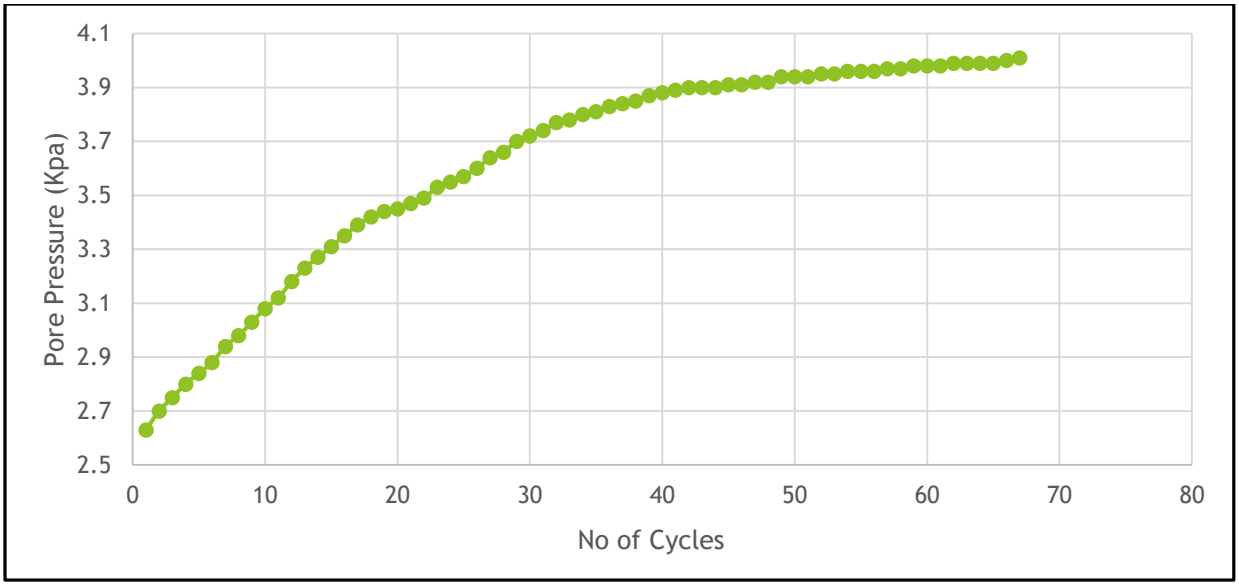

Fig 5.18 Relative Density 75% ; Effective confining pressure 150 KPa ; Amplitude 1.00mm

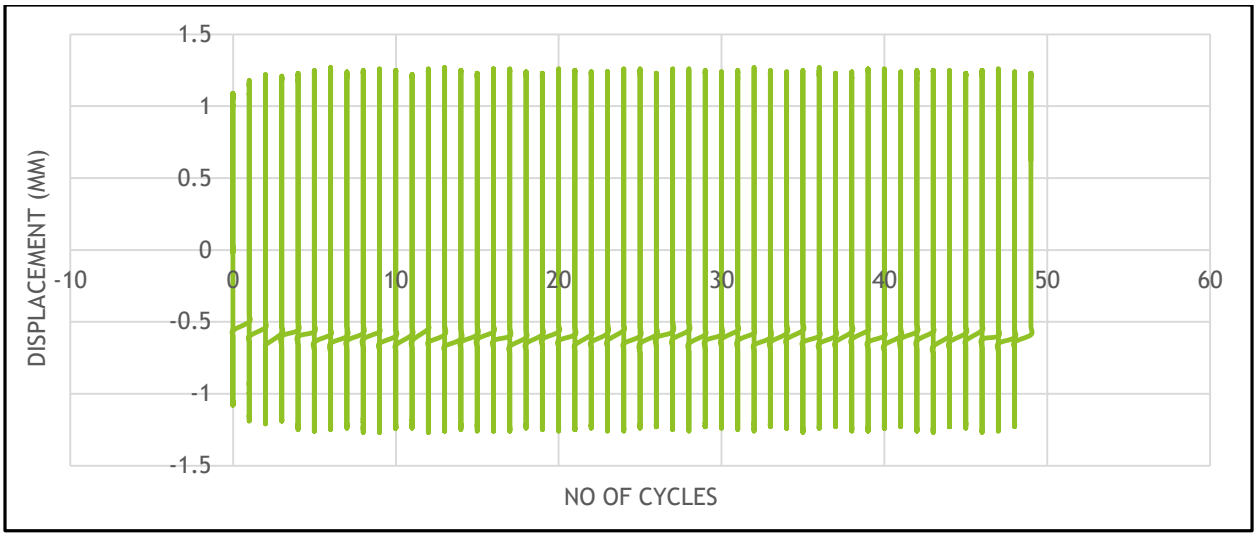

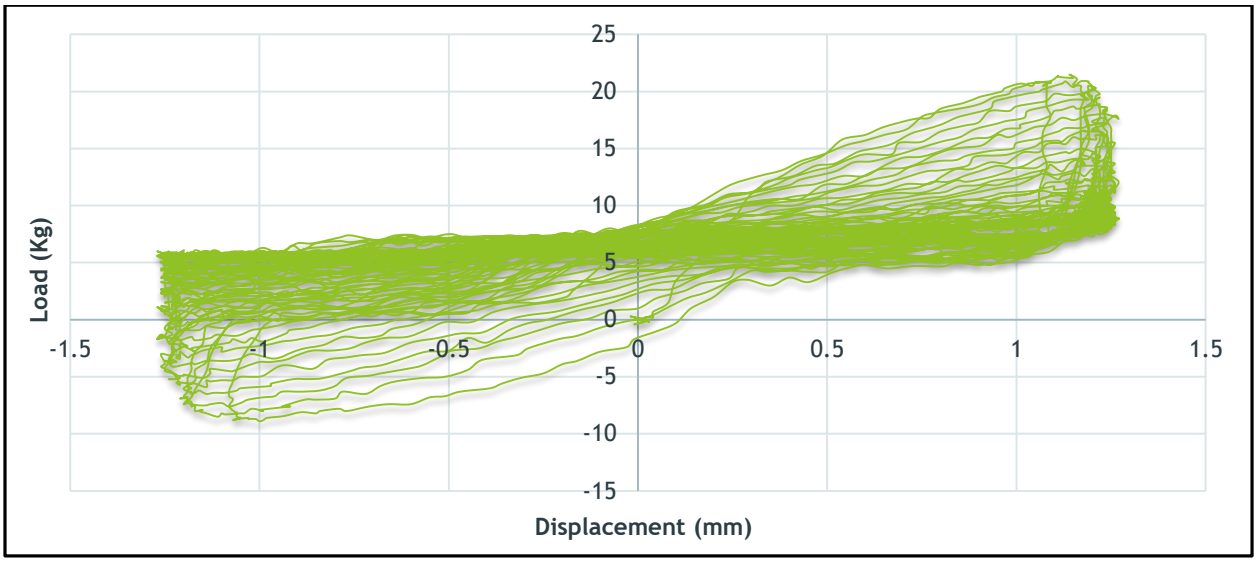

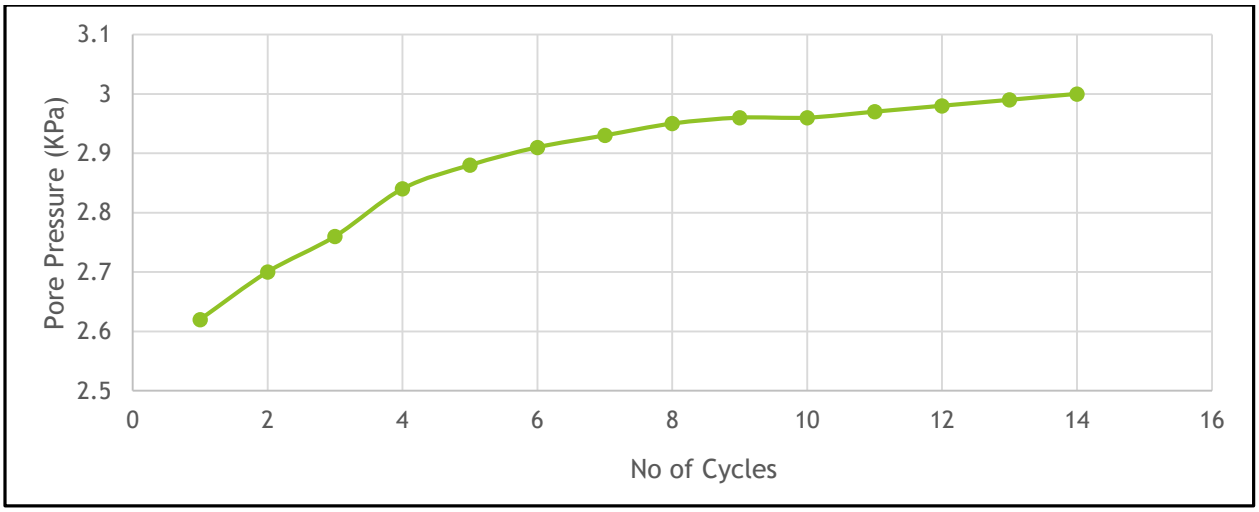

Fig 5.19 Relative Density 25% ; Effective confining pressure 50 KPa ; Amplitude 1.25mm

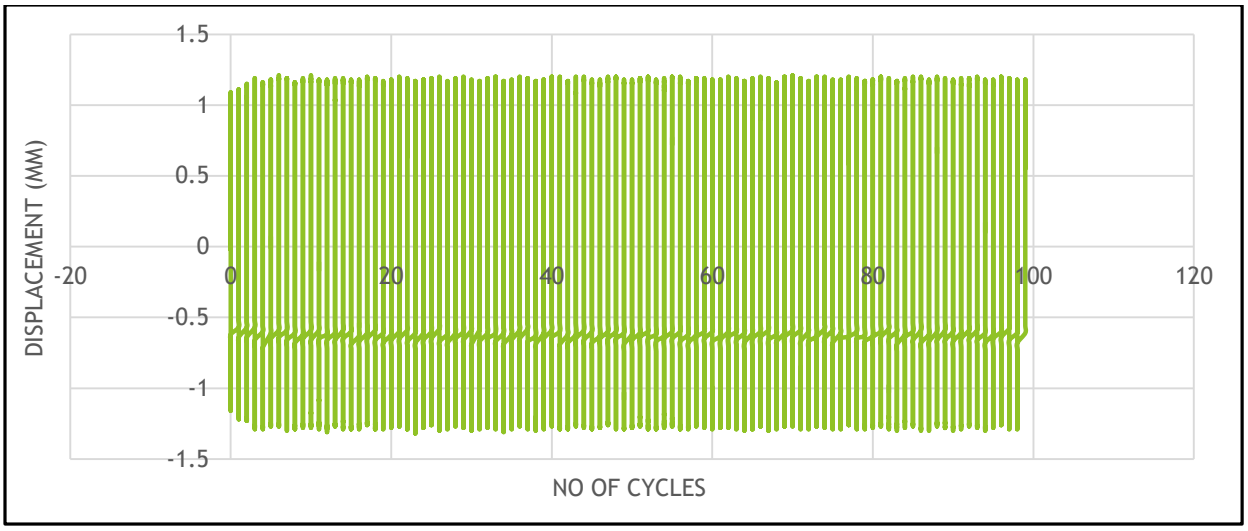

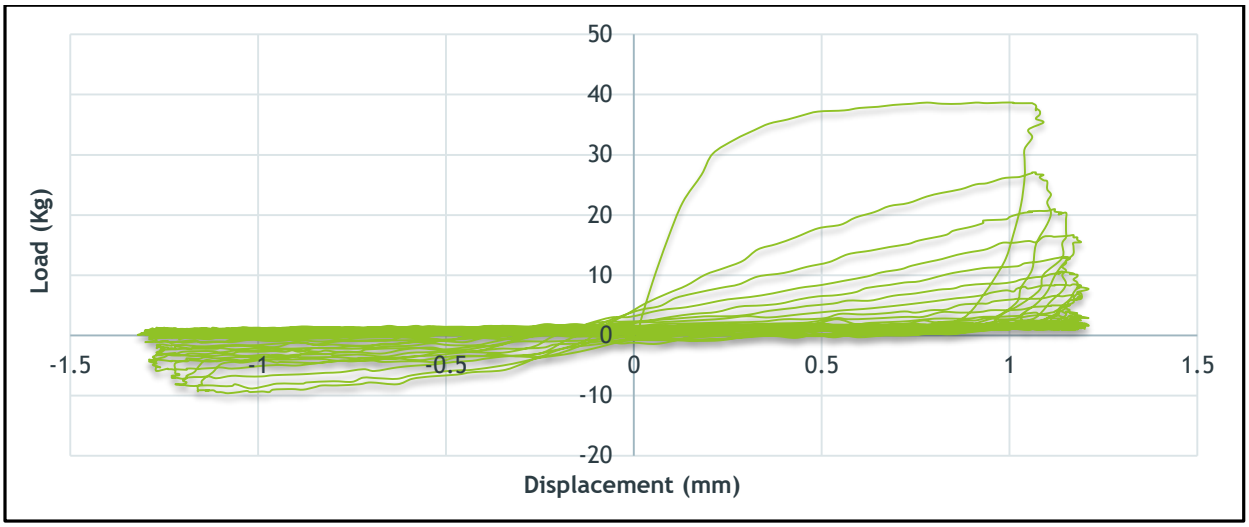

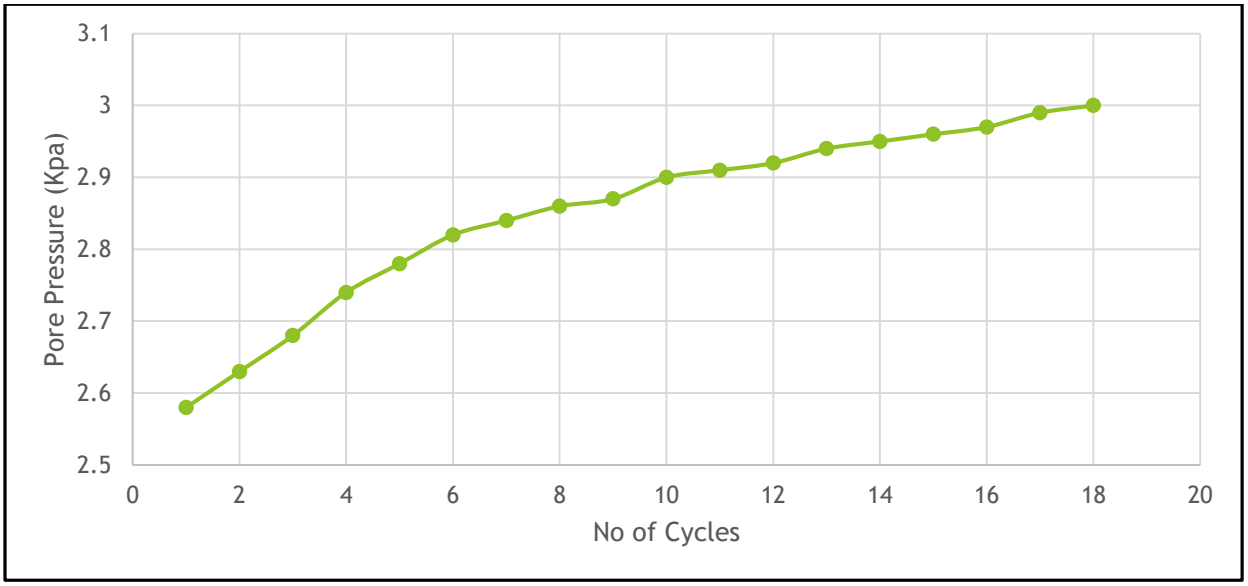

Fig 5.20 Relative Density 50% ; Effective confining pressure 50 KPa ; Amplitude 1.25mm

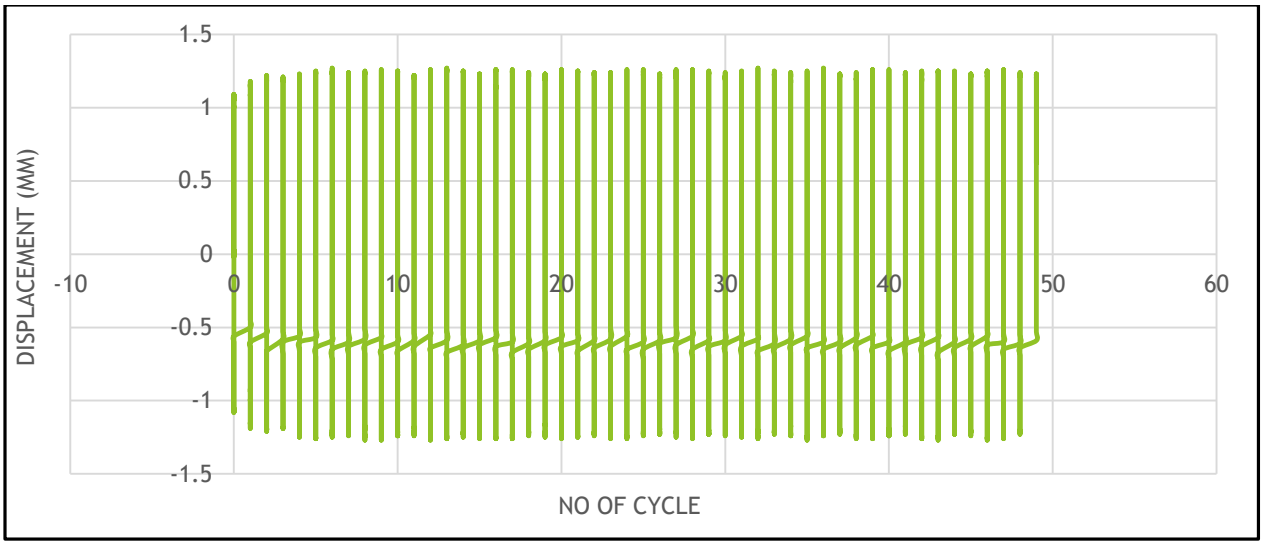

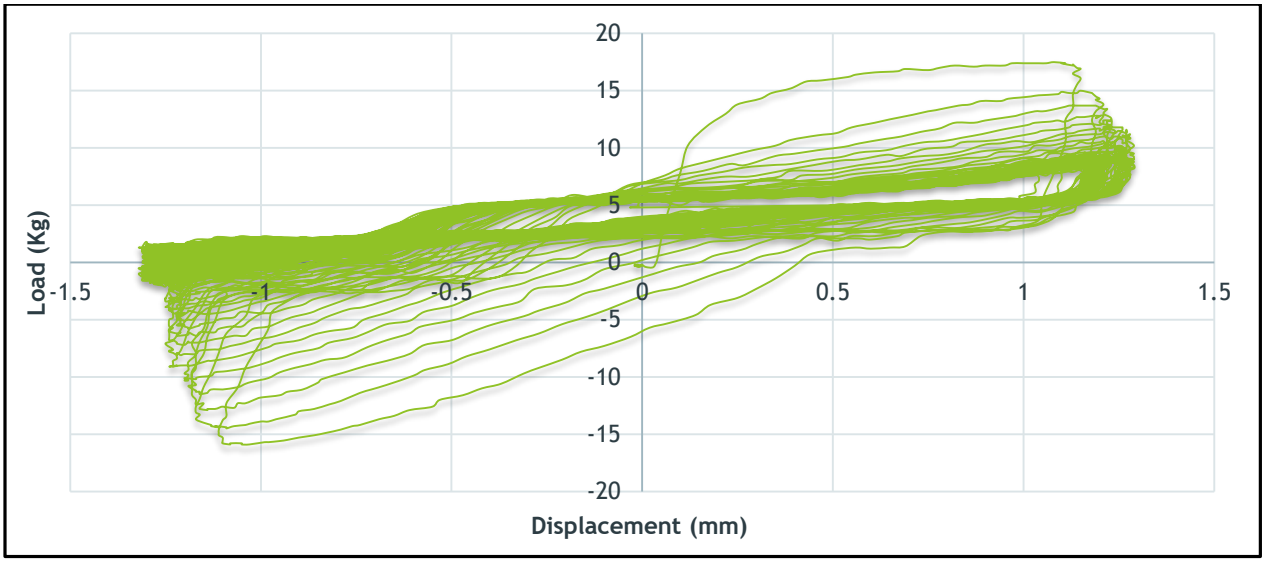

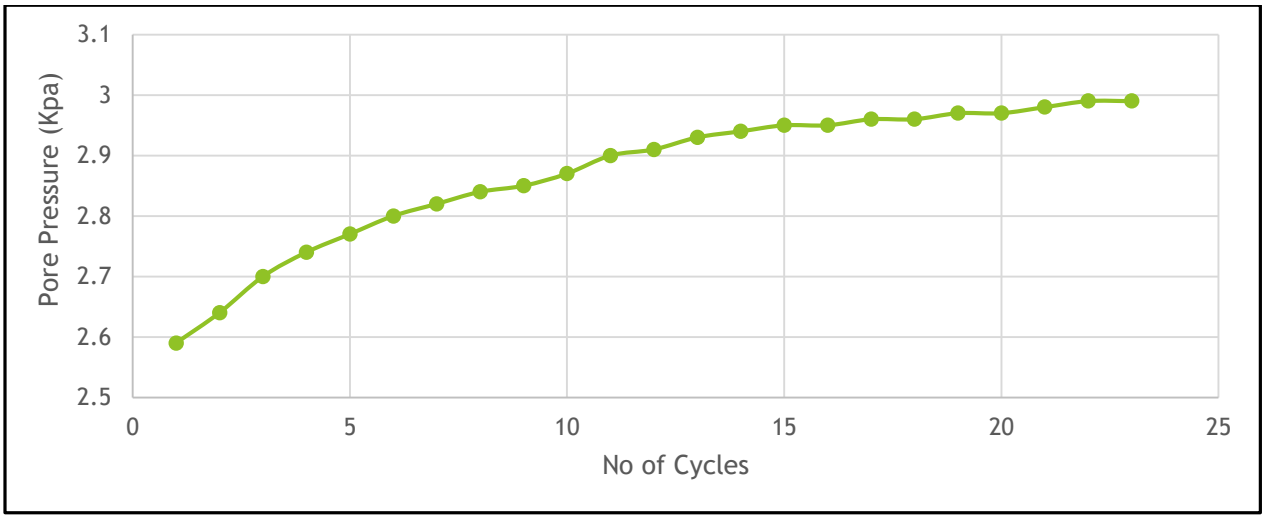

Fig 5.21 Relative Density 75% ; Effective confining pressure 50 KPa ; Amplitude 1.25mm

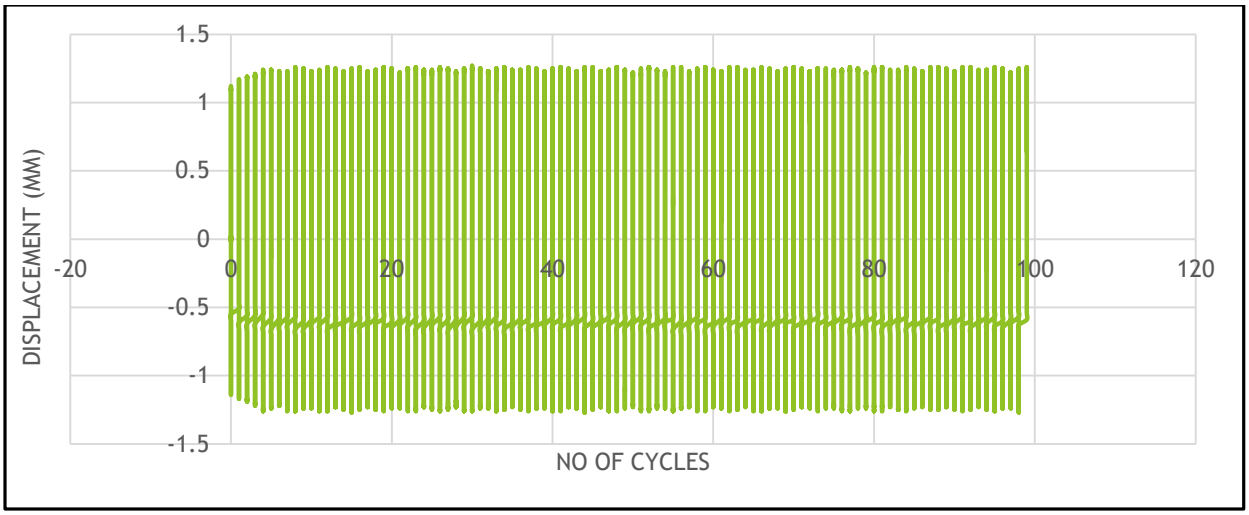

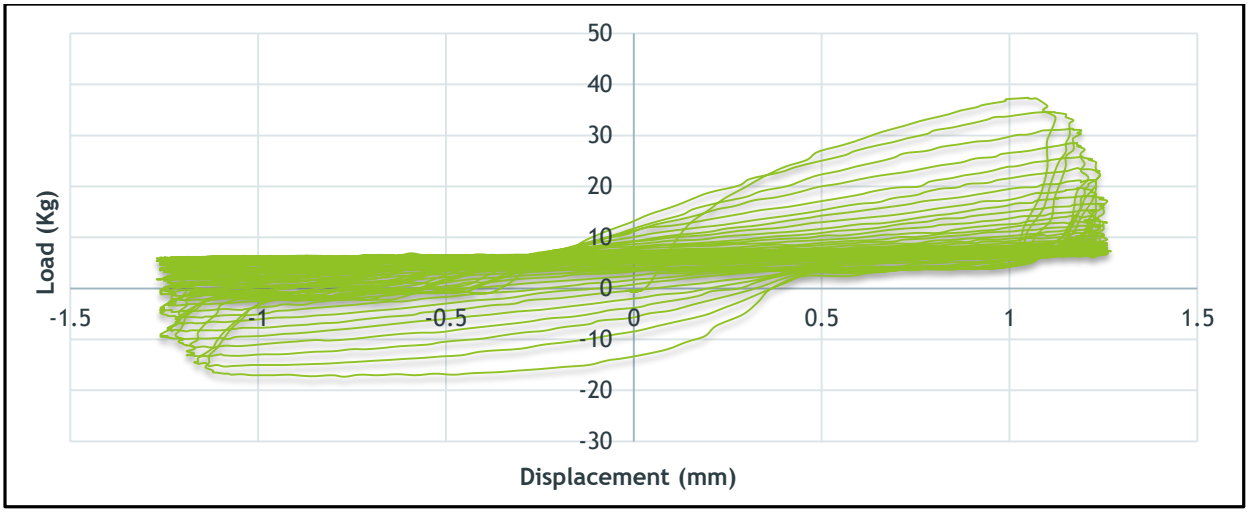

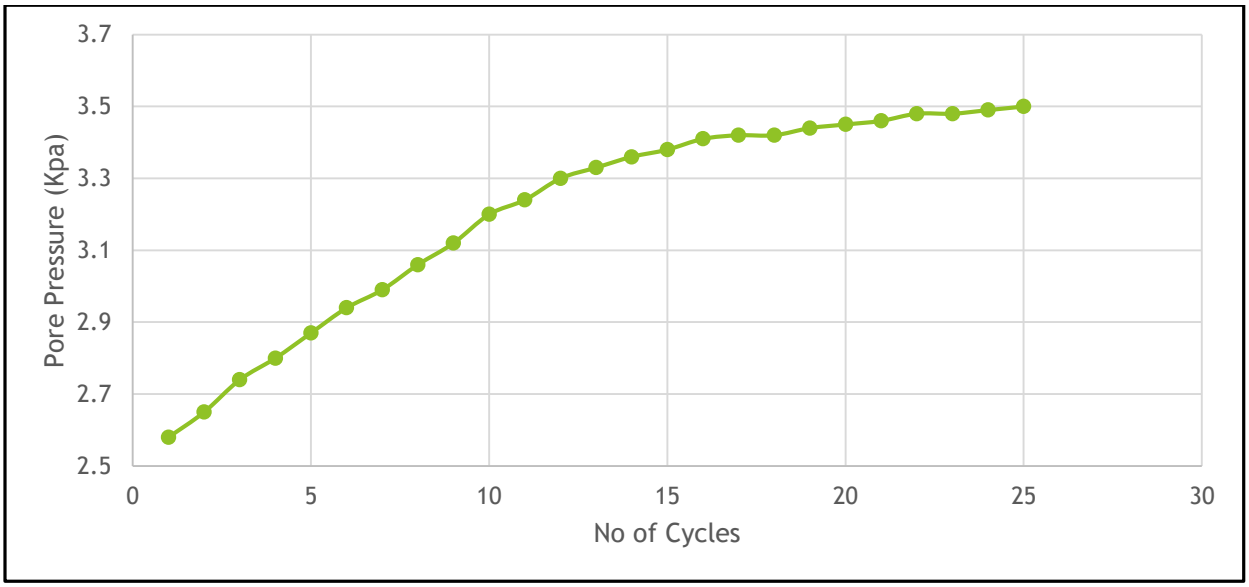

Fig 5.22 Relative Density 25% ; Effective confining pressure 100 KPa ; Amplitude 1.25mm

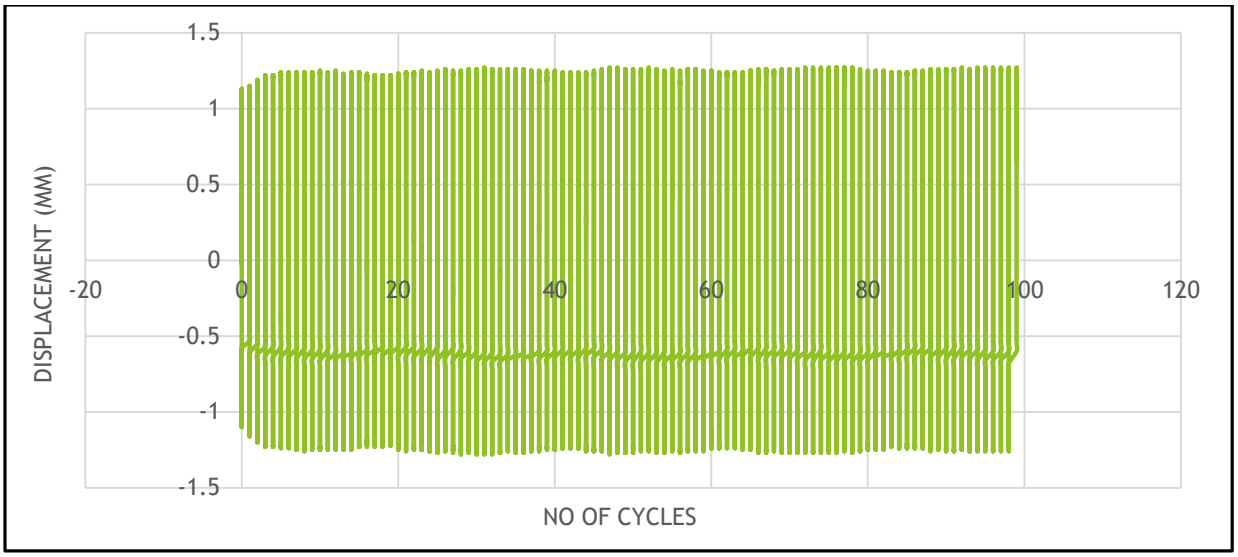

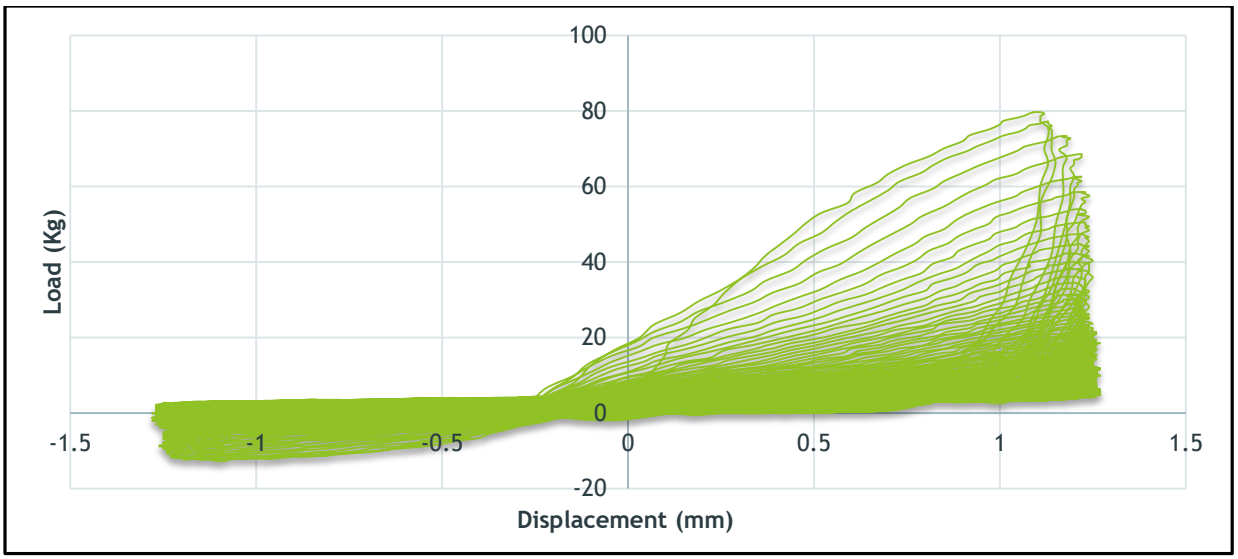

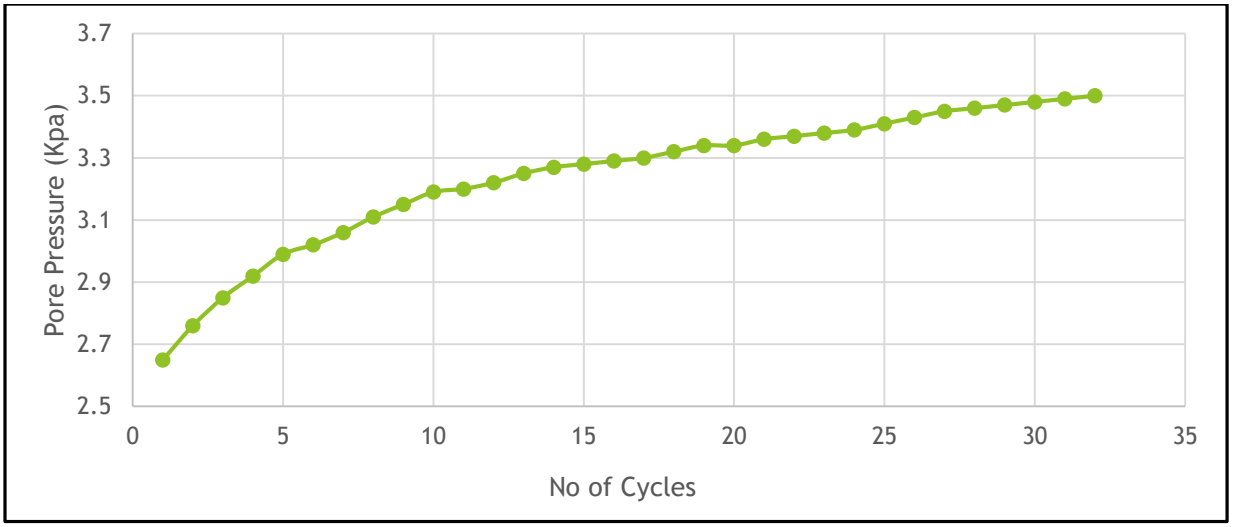

Fig 5.23 Relative Density 50% ; Effective confining pressure 100 KPa ; Amplitude 1.25mm

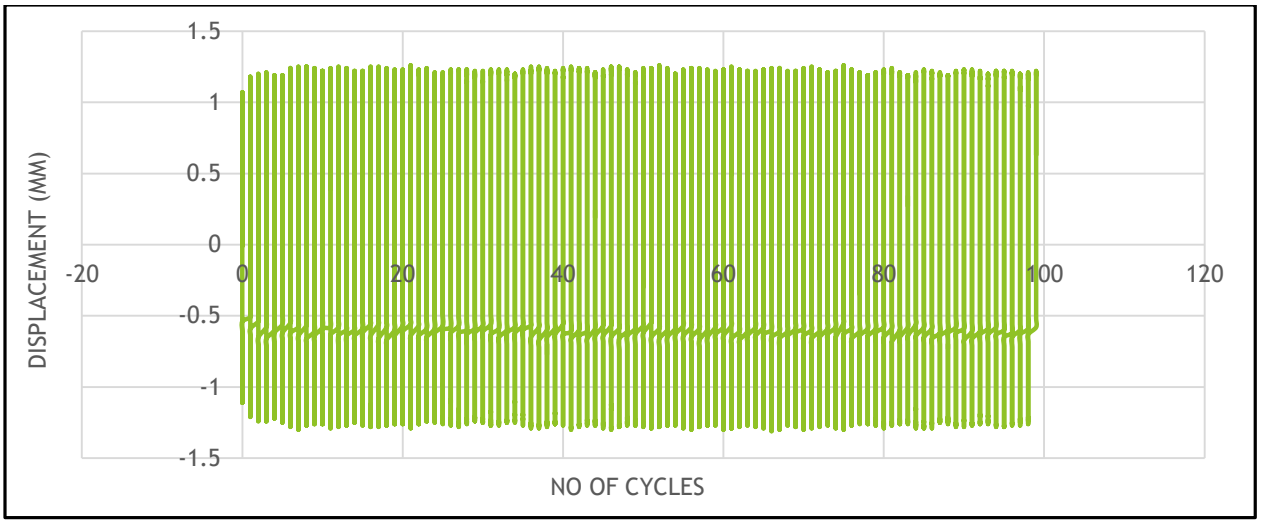

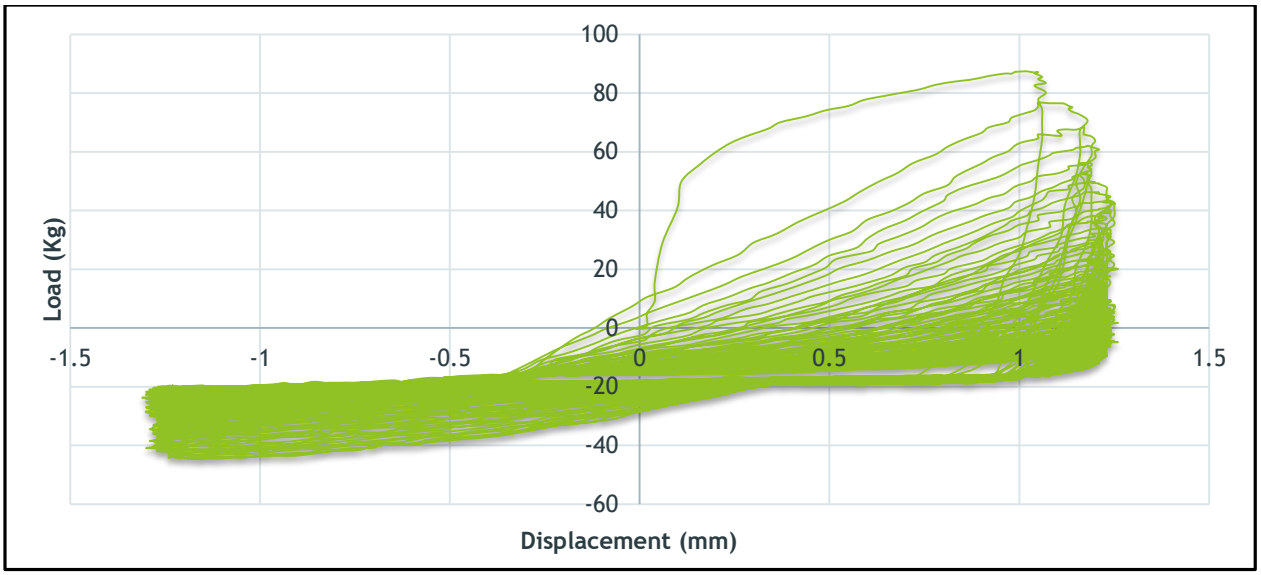

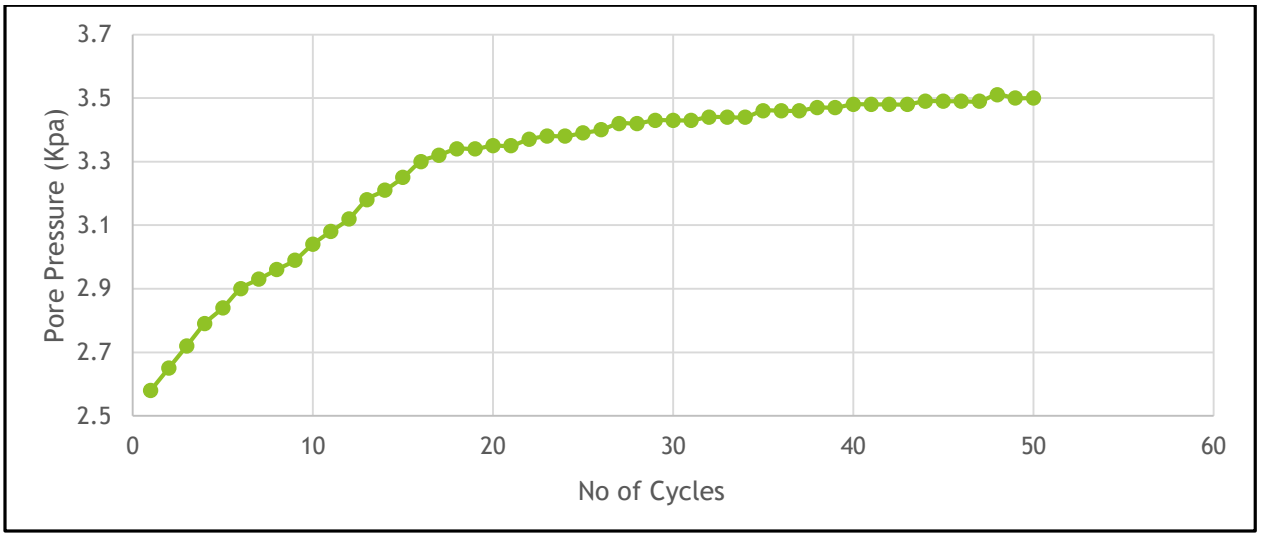

Fig 5.24 Relative Density 75% ; Effective confining pressure 100 KPa ; Amplitude 1.25mm

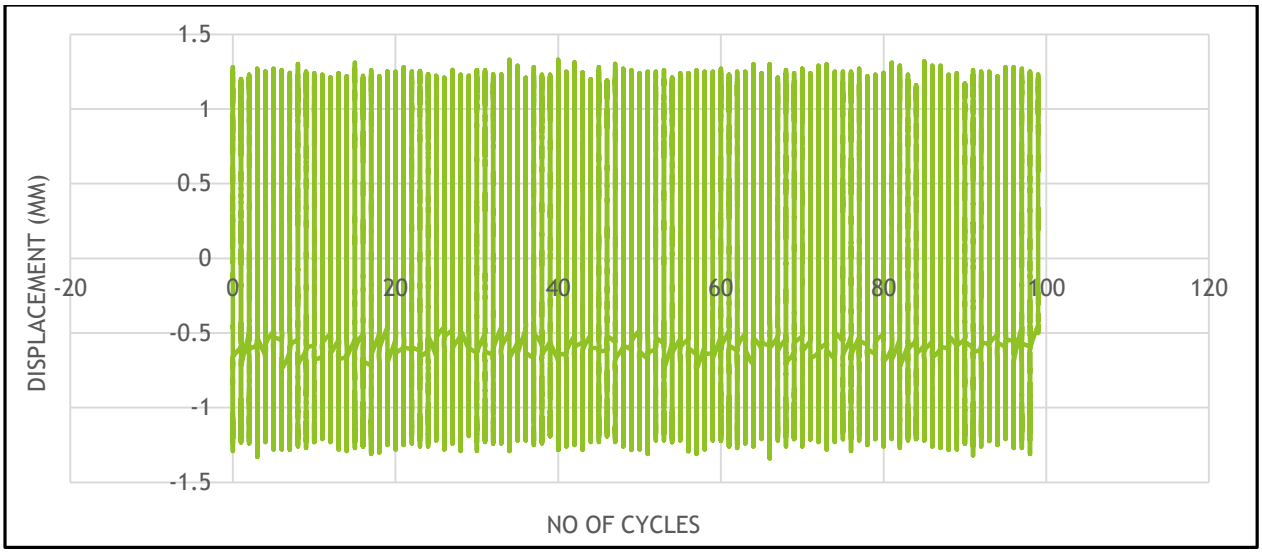

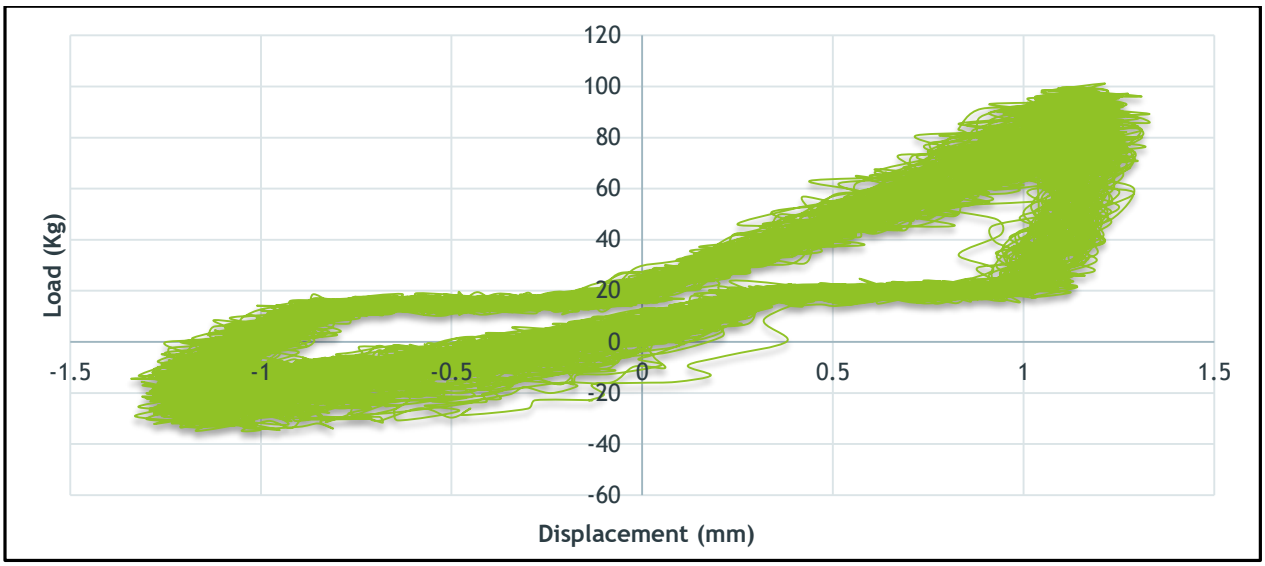

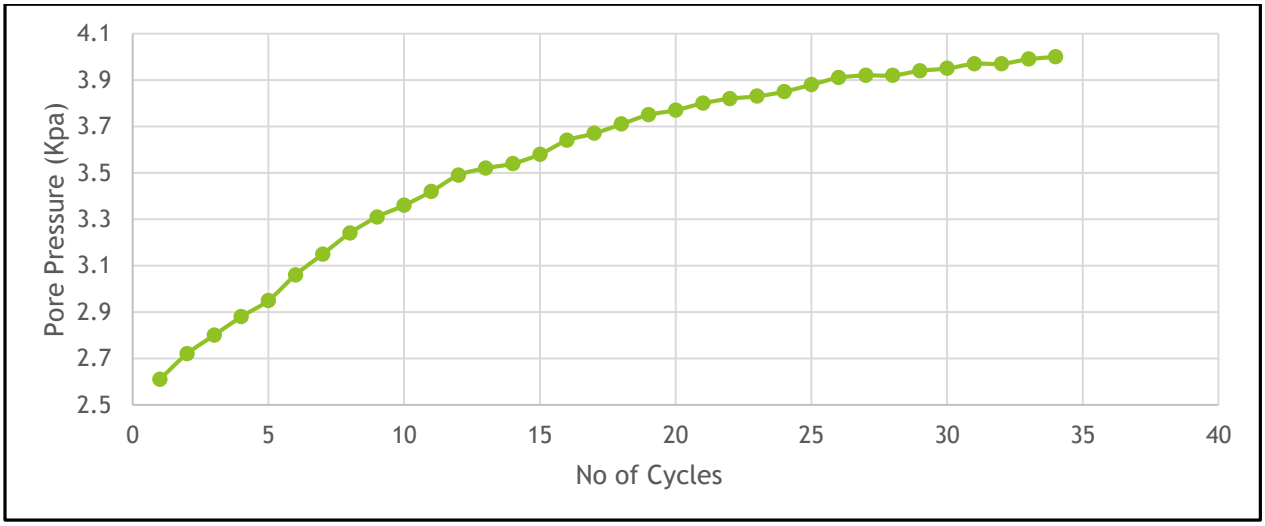

Fig 5.25 Relative Density 25% ; Effective confining pressure 150 KPa ; Amplitude 1.25mm

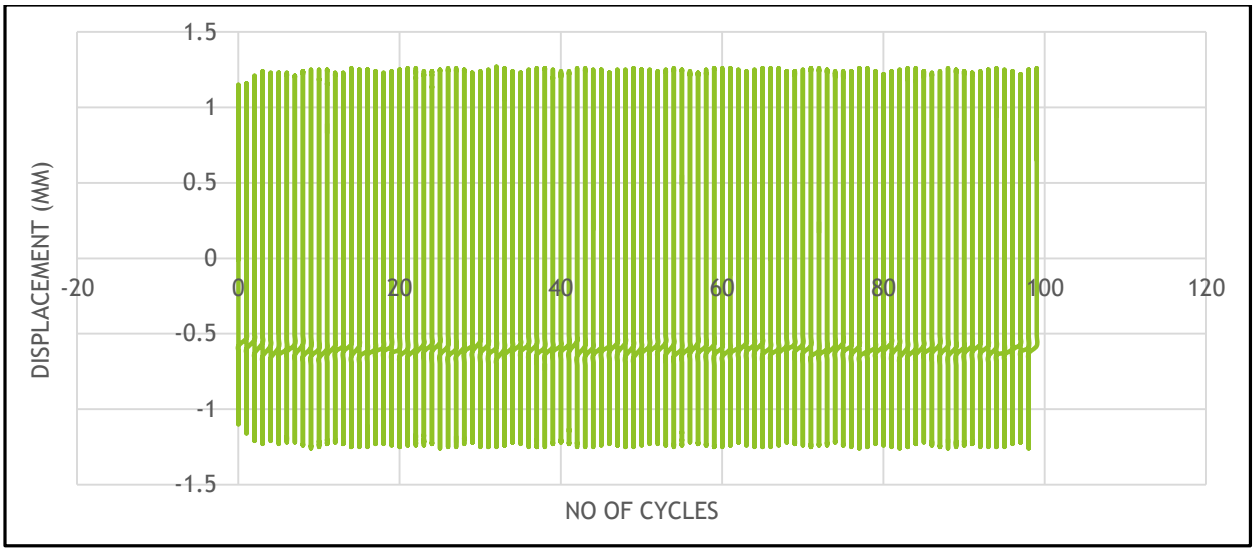

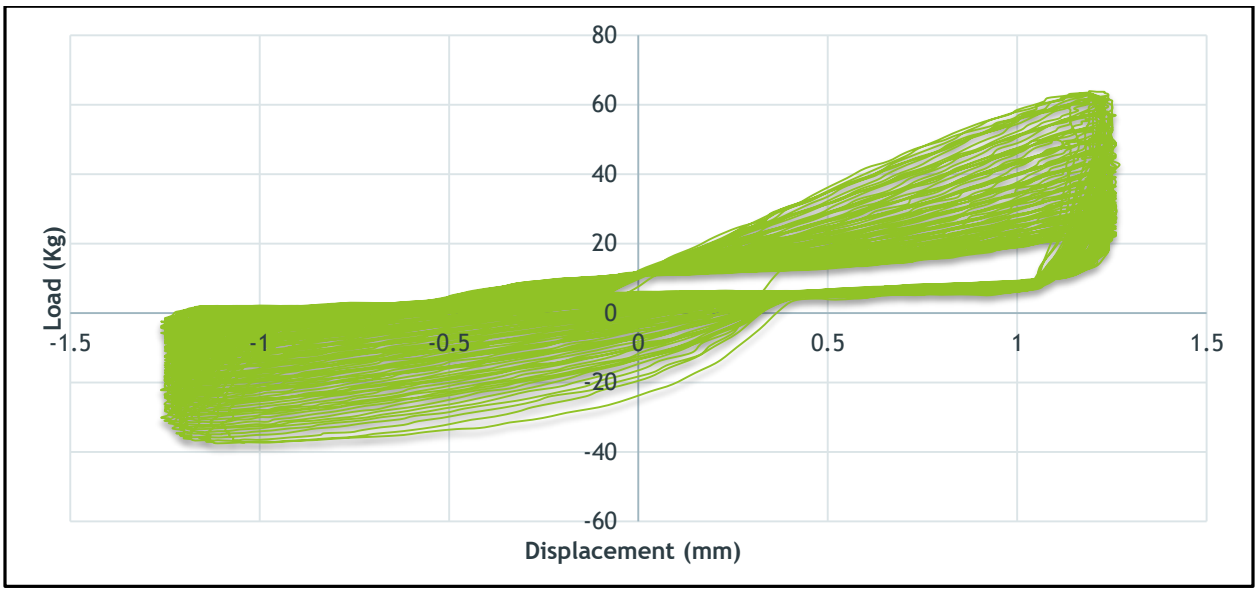

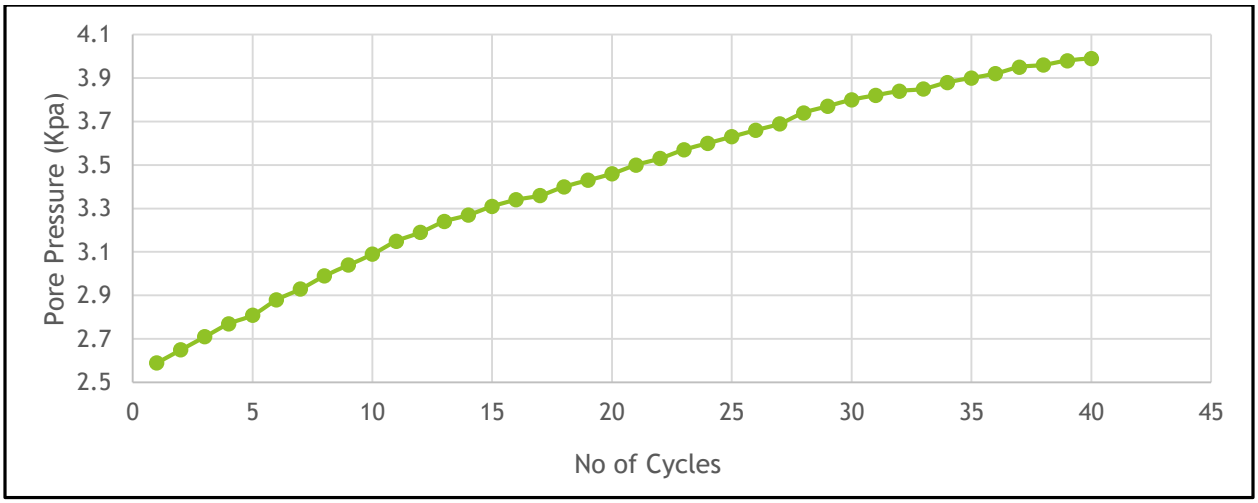

Fig 5.26 Relative Density 50% ; Effective confining pressure 150 KPa ; Amplitude 1.25mm

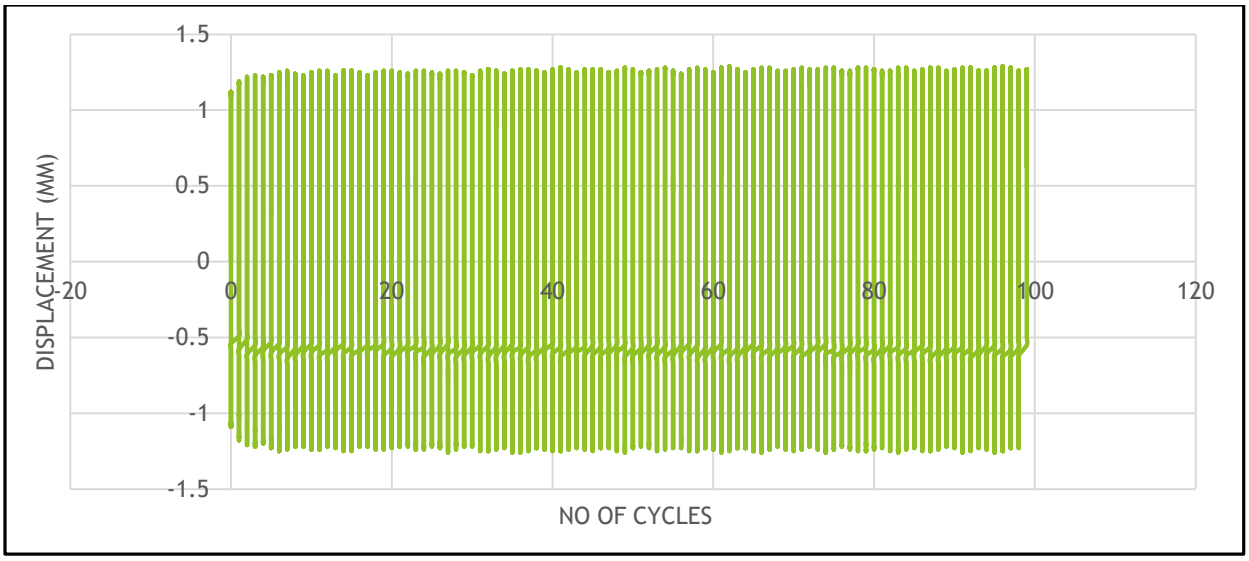

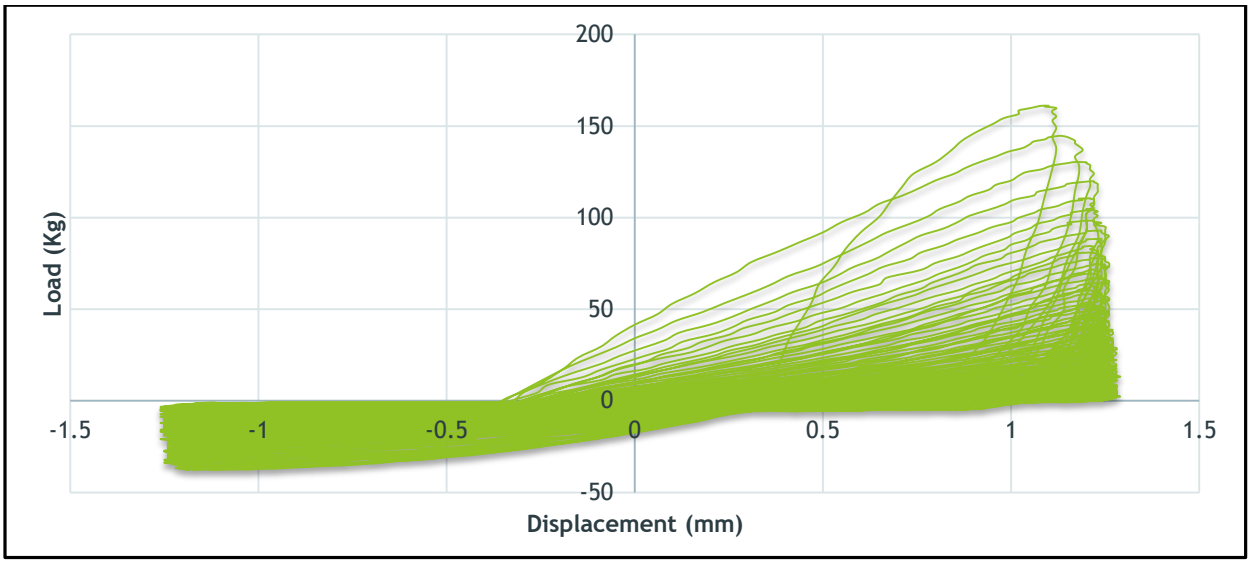

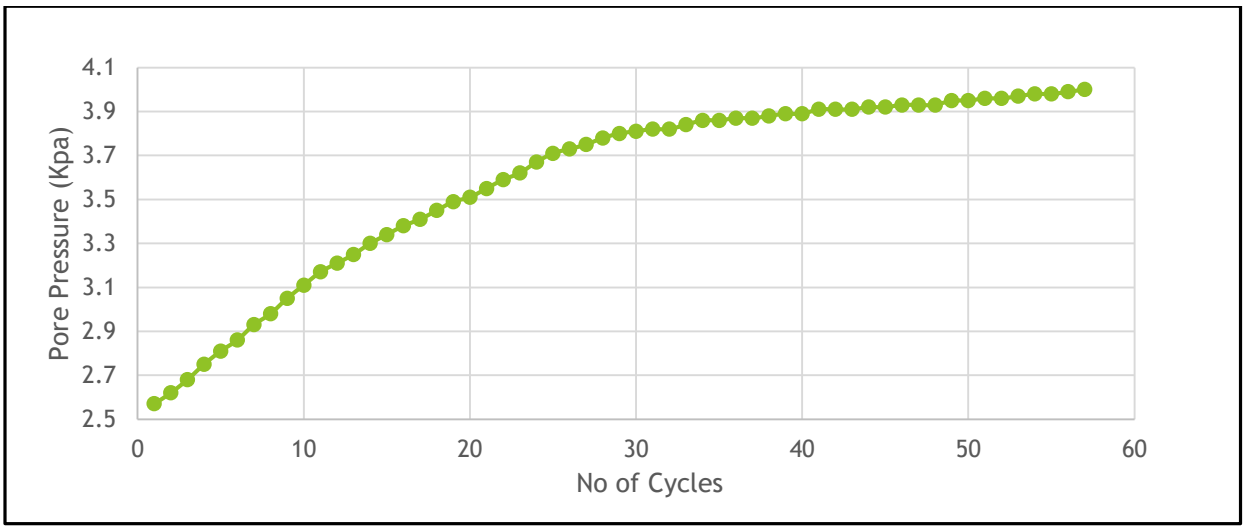

Fig 5.27 Relative Density 75% ; Effective confining pressure 150 KPa ; Amplitude 1.25mm

5.3 Characterization of Pore Pressure Generation

It has been observed that for every cyclic undrained strain controlled triaxial test just after application of the deviator stress the pore water pressure in the soil sample has been started to increase rapidly until the pore water pressure becomes equal to cell pressure. As the time passes, the rate of generation of pore pressure decreases rapidly. When the pore water pressure equals to confining pressure, the sample loses its strength which means liquefaction has been reached. After attaining liquefaction further application of deviator stress results no significant increase in pore water pressure.

5.4 Characterization of Load versus Displacement Graph during Liquefaction

During strain controlled cyclic triaxial test the load versus displacement graph has been obtained for each test. So, total twenty seven graphs have been obtained. The displacement (in mm) has been taken in X-axis (as the test is strain controlled) and corresponding value of load (in Kg) has been taken in Y-axis. It has been observed that load versus displacement curve was the steepest in the beginning, but became flattened when the soil became softer i.e. when the sample reached liquefaction.

CHAPTER 6

DISCUSSION ON TEST RESULTS

6.1 Cyclic Behavior in Terms of Number of Cycles at Failure

6.1.1 Effect of Relative Density

To assess the effect of relative density on liquefaction resistance of soil, cyclic triaxial tests have been conducted on saturated sand samples at three different relative densities. **Figure 6.1** illustrates variation of number of cycles at failure against relative density at three constant effective confining pressures and at three constant cyclic shear strains.

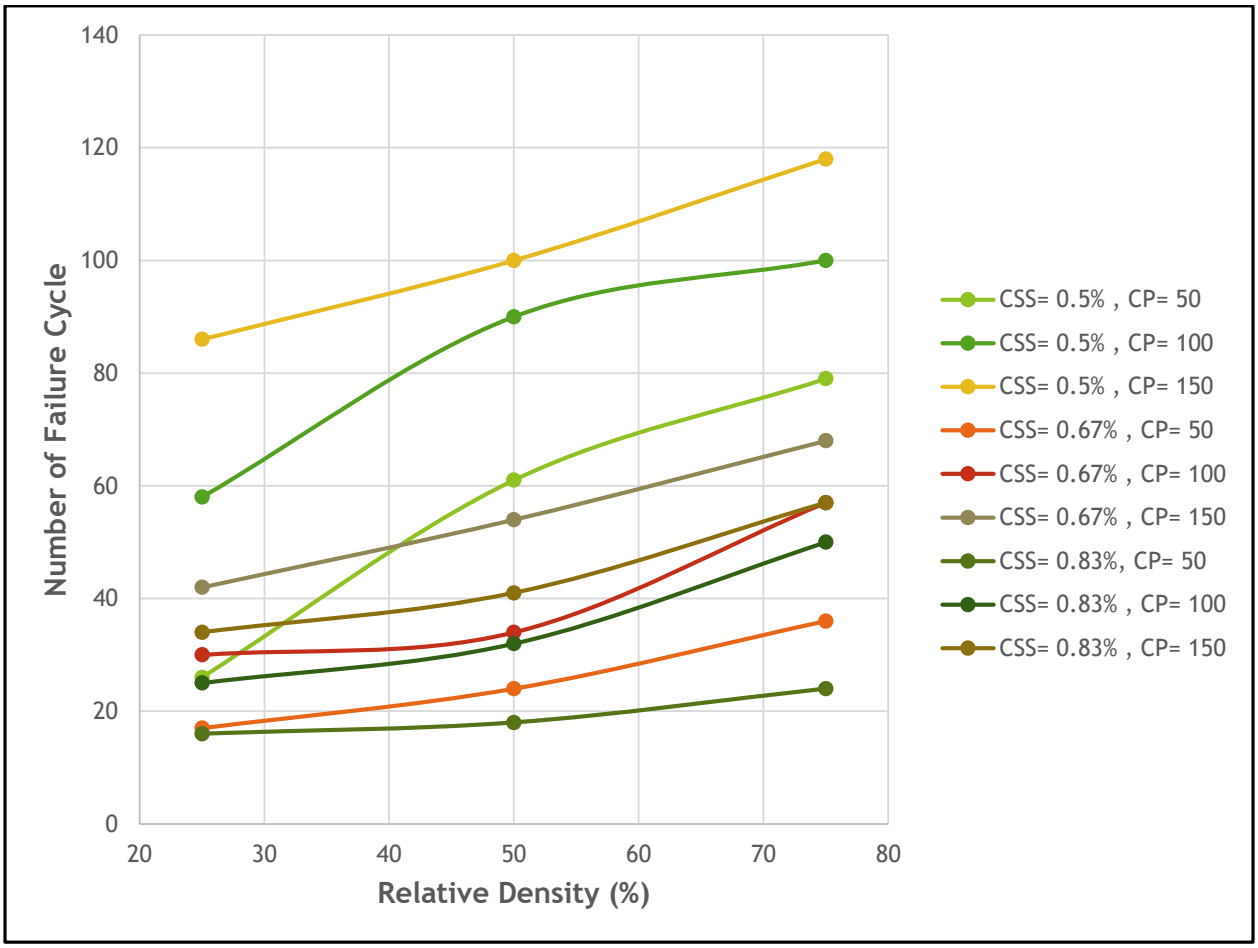

Fig 6.1: Number of failure cycle vs Relative Density

As we have seen from the graph, liquefaction occurred at 25% relative density requires very less number of cycles and it goes on increasing as the relative density increases to 75%. Due to increase in relative density the shear strength of the sand sample increases, so greater number of cycles are required to liquefy. It implies that chances of liquefaction reduces with increase in relative density.

6.1.2 Effect of Confining Pressure

To assess the effect of confining pressure on liquefaction resistance of soil, cyclic triaxial tests have been conducted on saturated sand samples at three different effective confining pressures. Figure 6.2 illustrates the test results obtained of number of cycles at failure against effective confining pressures at three constant relative densities and at three constant cyclic shear strains.

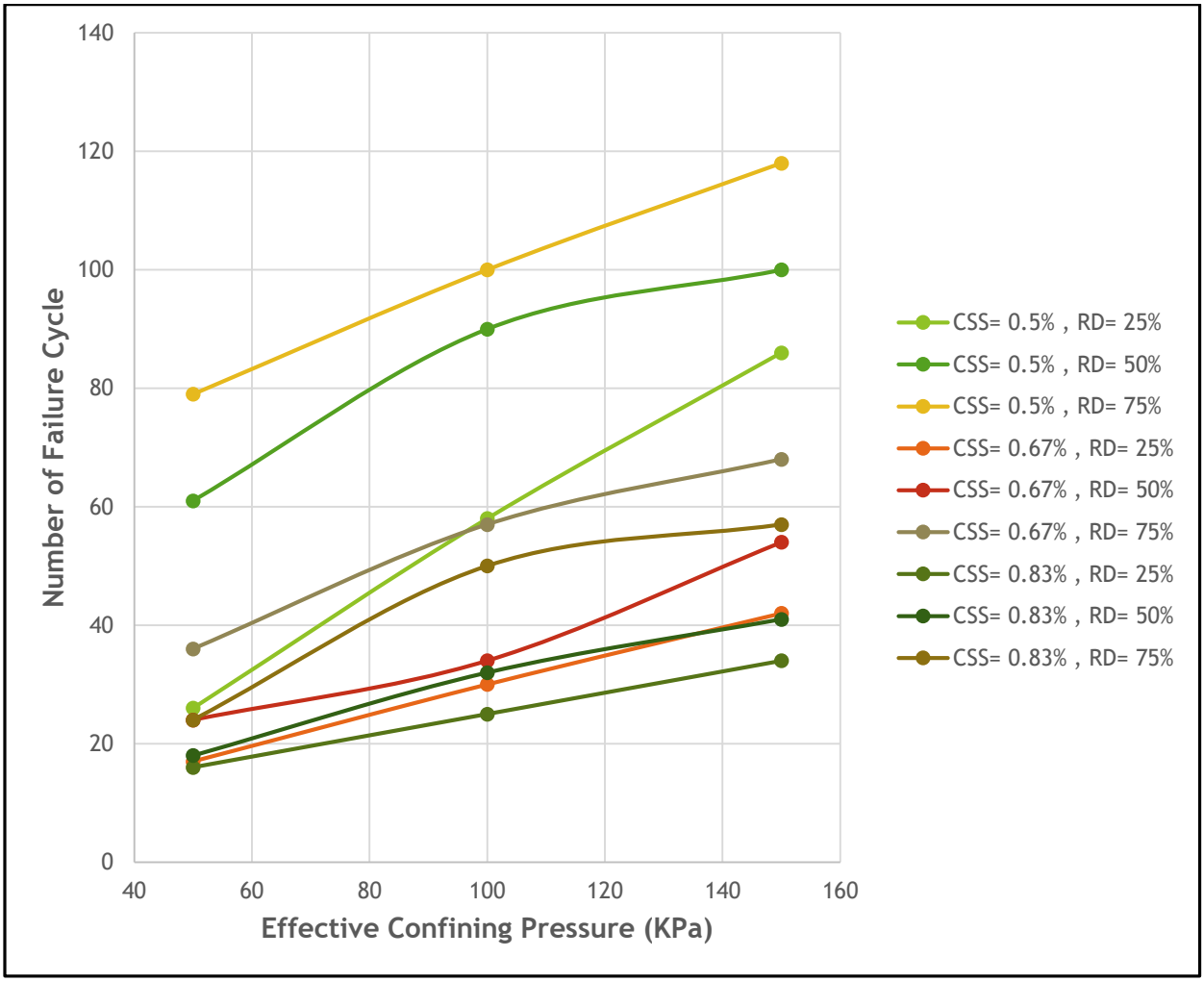

Fig 6.2 Number of Failure Cycles vs Effective Confining Pressure

At 50 kPa effective confining pressure, liquefaction occurred at lower number of cycles and, liquefaction occurred at higher number of cycles when effective confining pressure was increased to 150 kPa. The result shows that liquefaction resistance of the sand increases with increase in confining pressure as shear strength of the sand sample increases with increase in confining pressure. So pore water pressure builds up slowly and there is triggering of liquefaction at higher number of cycles.

6.1.3 Effect of Cyclic Shear Strain

To assess the effect of cyclic shear strain on liquefaction resistance of soil, cyclic triaxial tests have been conducted on saturated sand samples at three constant cyclic shear strains. Figure 6.3 illustrates the test results obtained from number of cycles at failure against cyclic shear strains at three constant relative densities and at three constant effective confining pressures.

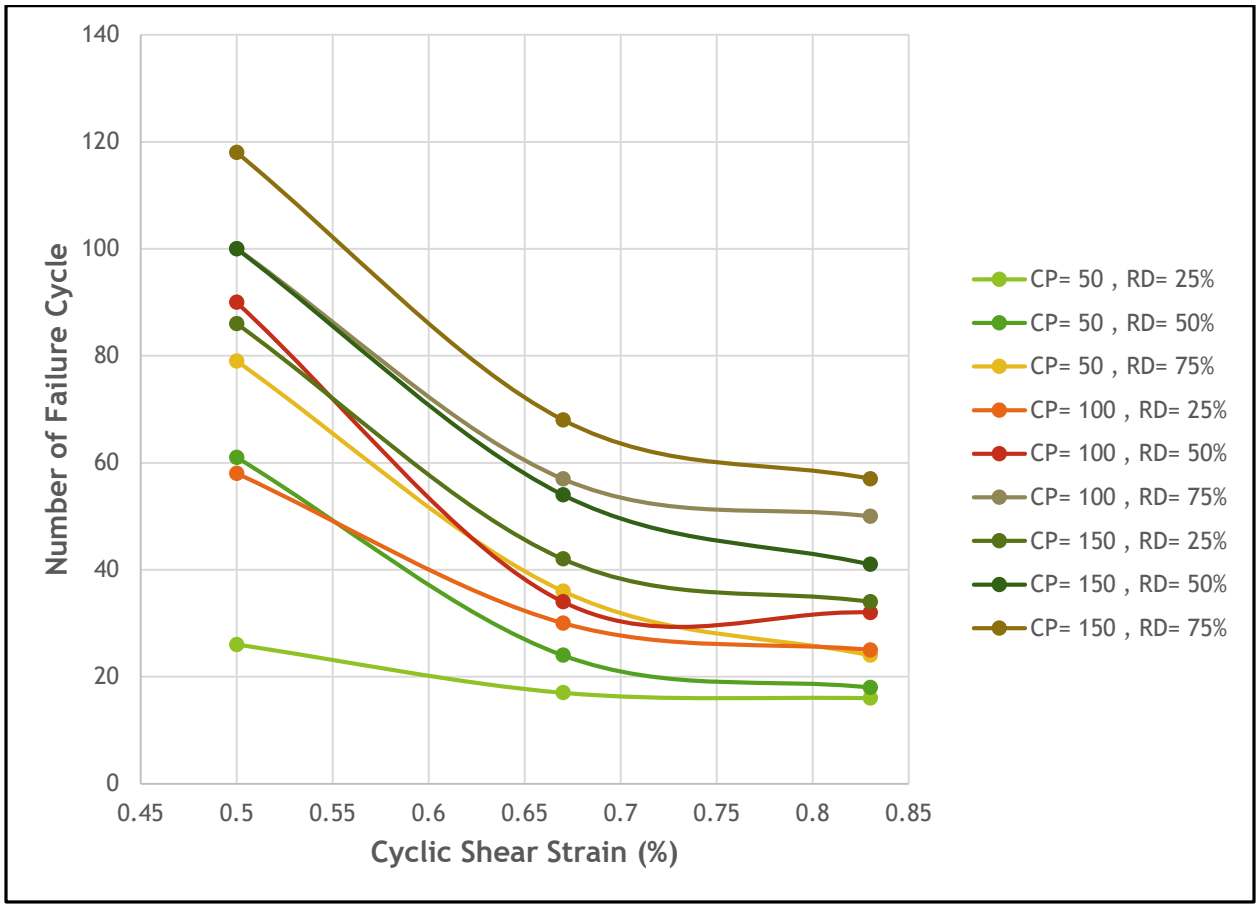

Fig 6.3 Number of Failure Cycle vs Cyclic Shear Strain

At lower cyclic shear strain, liquefaction occurred at higher number of cycles and liquefaction occurred at lower number of cycles when cyclic shear strain of the sample was higher. It implies that with increase in cyclic shear strain, the soil sample loses its strength rapidly and reaches to liquefaction at lower number of cycles.

6.2 Pore Pressure Generation Characteristics

6.2.1 Preview of Kondner (1963) Model

Kondner (1963) proposed a hyperbolic model for stress-strain relationship. If we plot stress along Y axis and strain along X axis, we shall get a hyperbolic relationship. Based on standard triaxial test, the model approximates the stress-strain by the following hyperbolic relation:

$\sigma_d = \sigma_1 - \sigma_3 = \frac{\varepsilon_1}{a+b\varepsilon_1}$

where, σ_1 , σ_3 are major and minor principal stresses and ε_1 is the major principal strain.

If we plot (ε_1/σ_d) along Y axis and ε_1 along X axis, then we shall get a straight line from which we can easily calculate the two parameters 'a' and 'b'

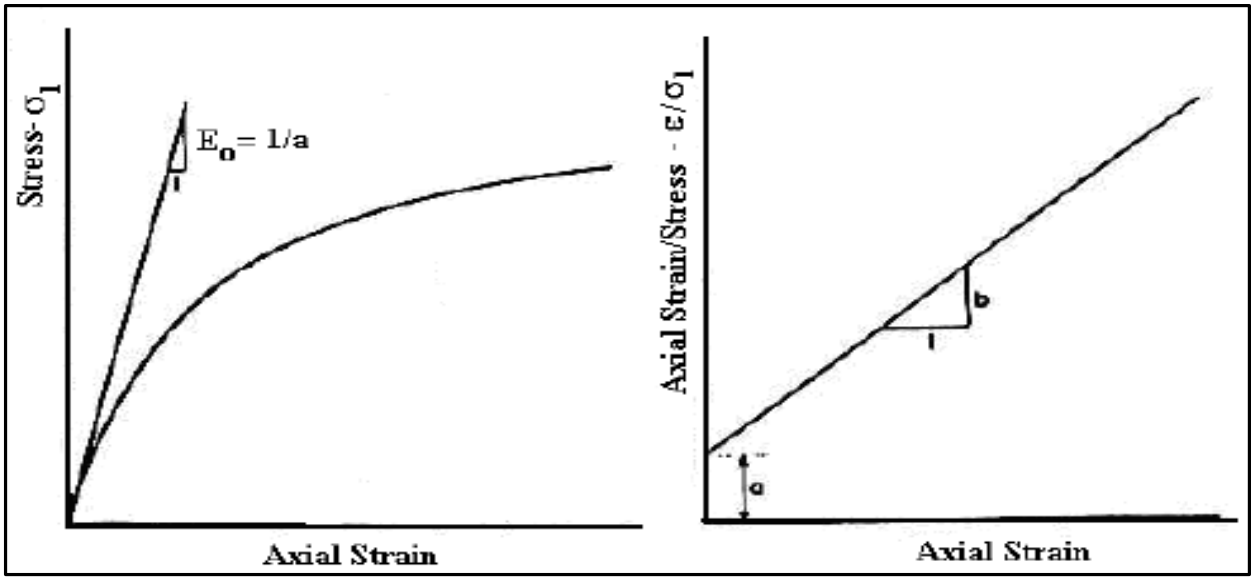

Fig 6.4 Hyperbolic Model proposed by Kondner (1963)

Here, 'a' is the inverse of the Initial Tangent modulus and 'b' is the inverse of the asymptotic value of the hyperbolic curve and is related to soil strength.

6.2.2 Hyperbolic Model of our Experiment

In order to develop a pore pressure generation model, the variation of ($\Delta u/\sigma_c'$) with respect to (N/N_f) has been studied and the curve shows an asymptotic nature. The graph for amplitude 1.25 mm and R_d= 50% has been given below for reference.

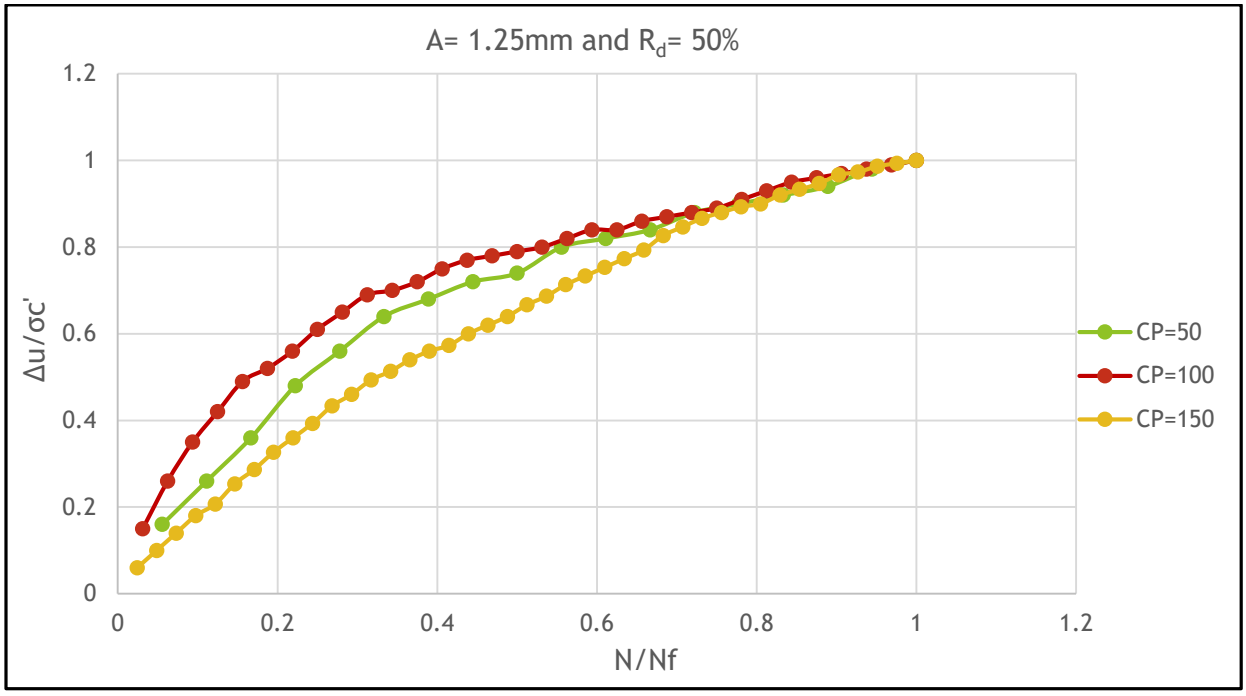

Fig 6.5 ($\Delta u/\sigma_c$) vs (N/N_f) plot for amplitude = 1.25 mm and R_d= 50%

The nature of the graph shows that it is clearly asymptotic in nature and the basic equation for this graph will be:

$$(\Delta u/\sigma'_c) = \frac{N/N_f}{a+b(N/N_f)}$$

Where, Δu= Change in pore pressure

σ_c'= Effective confining pressure

N= N^{th} number of cycle

N_f= Number of cycles to failure

Our aim is to find the unknown parameters 'a' and 'b'.

Hence, we have plotted [$(N/N_f)/(\Delta u/\sigma_c)$] along Y axis and ($N/N_f$) along X axis to get a straight line plot and hence to find the parameters 'a' and 'b'.

The straight line fits are given below:

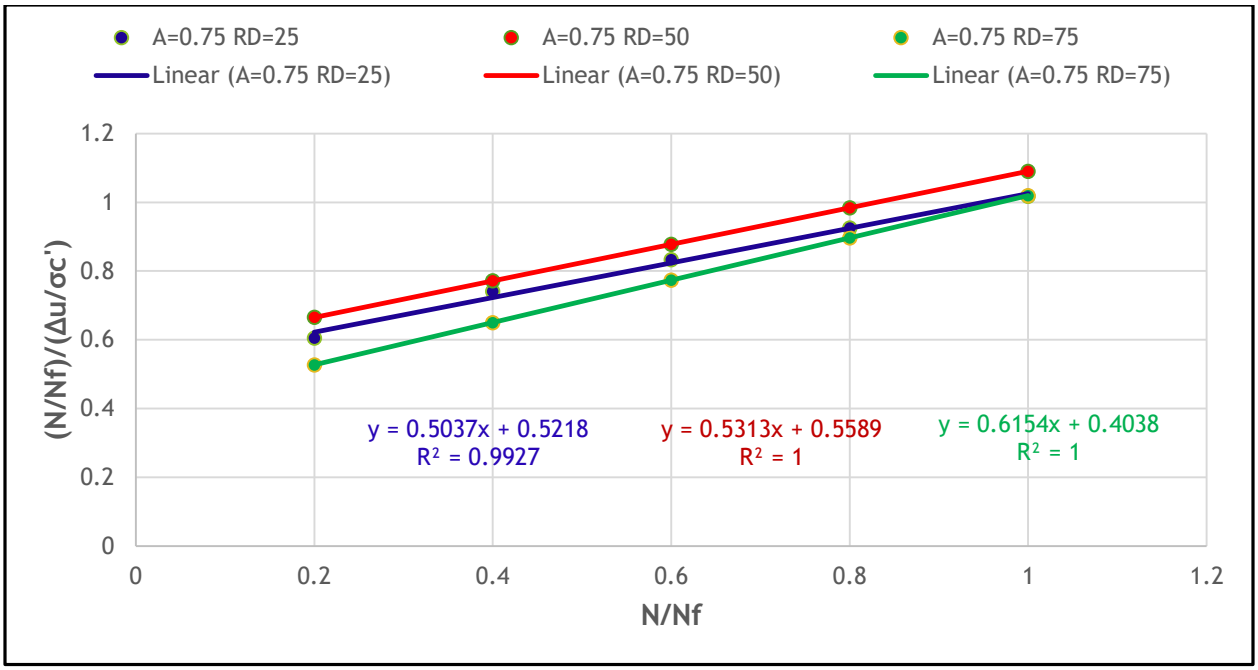

Fig 6.6 Hyperbolic Model for Amplitude = 0.75 mm

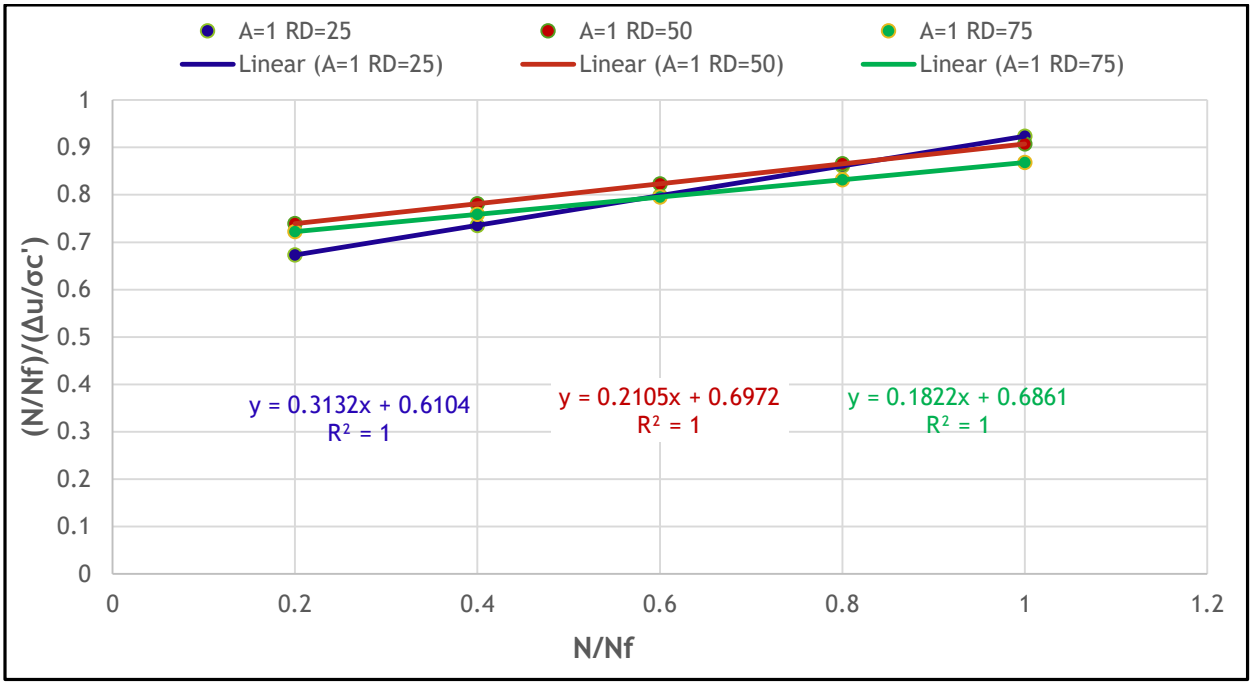

Fig 6.7 Hyperbolic Model for Amplitude = 1.00 mm

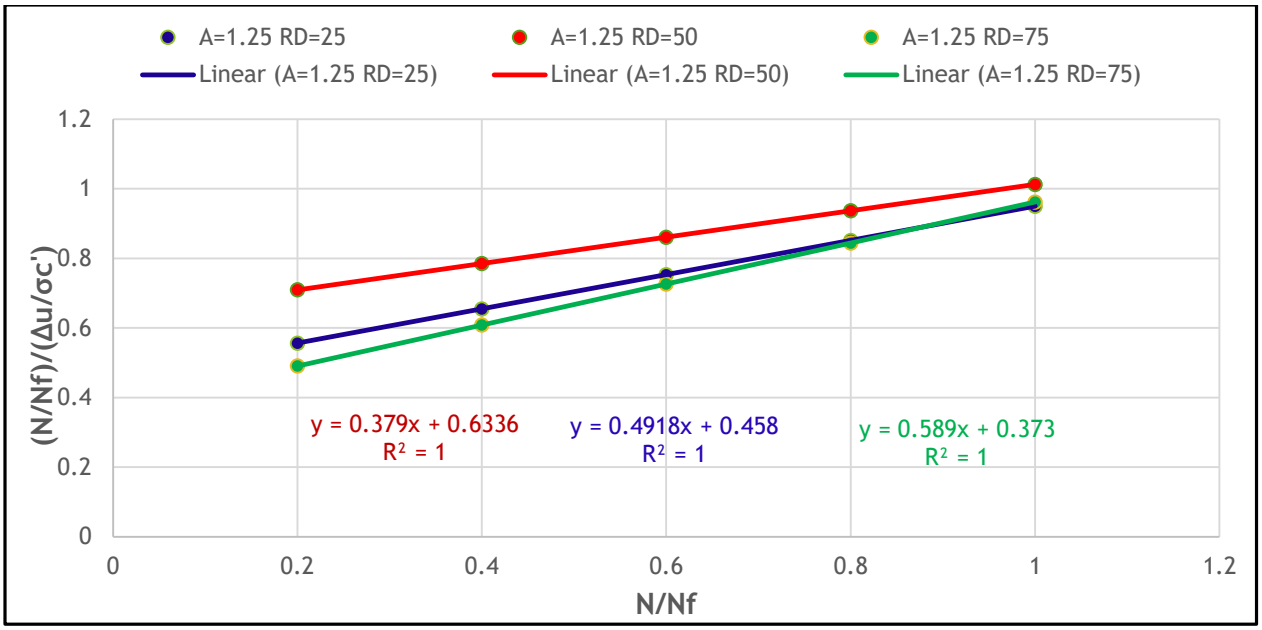

Fig 6.8 Hyperbolic Model for Amplitude = 1.25 mm

From these 3 graphs, we can easily find the 'a' and 'b' parameters of the hyperbolic model and the values are listed below:

Table 6.1 Parameters of Hyperbolic Model

Amplitude (mm)	Relative Density (%)	a-value	b-value	Average of a	Average of b
0.75	25	0.5218	0.5037	0.4948	0.5501
0.75	50	0.5589	0.5313		
0.75	75	0.4038	0.6154		
1.00	25	0.6104	0.3132	0.6645	0.2353
1.00	50	0.6972	0.2105		
1.00	75	0.6861	0.1822		
1.25	25	0.4580	0.4918	0.4882	0.4886
1.25	50	0.6336	0.3790		
1.25	75	0.3730	0.5890		
			Average values for	0.5492	0.4240

From the above table, we have seen that, the parameters are more or less independent of relative density but depends upon the cyclic shear strain. With the increase of cyclic shear strain, the 'a' value increases first and then decreases and on the contrary, 'b' value decreases first and then increases.

Hence, we can say that as we increase the rate of strain, the rate of generation of pore pressure decreases upto a certain threshold value of cyclic strain and then increases and the maximum pore pressure increases upto that certain threshold value of shear strain and then decreases. As in our case, we can say that the threshold value lies somewhere in between 1.00 and 1.25 mm i.e. in between cyclic shear strain values of 0.67% and 0.83%

If we can have an average value of these parameters, we can say that it is approximately a= 0.55 and b= 0.42

Hence our pore pressure generation equation after elapse of N number of cycles in hyperbolic model comes out as:

$$\frac{\Delta u}{\sigma_c'} = \frac{N/N_f}{0.55+0.42\,N/N_f}$$

Where, Δu = Change in pore pressure

σ_c' = Effective confining pressure

N_f = Number of cycles to failure

CHAPTER 7

SUMMARY AND CONCLUSION

7.1 Summary

This thesis paper is about the study of liquefaction characteristics of the river channel deposit in Kolkata. The sample was collected from the deposits of Adi Ganga Channel, a distributary of river Ganga. This sample is a mixture of sand and silt.

Twenty seven numbers of isotropically consolidated undrained triaxial tests have been performed under three different relative densities, three confining pressures and three cyclic shear strain. Each sample have been saturated applying a cell pressure of 280 KPa and back pressure of 250 KPa for about 2.5 hours for R_d= 75%, 2 hours for R_d= 50% and 1.5 hours for R_d= 25%.

Form the test output, we have made three curves, viz,

(i) Number of Cycles vs Displacement

(ii) Displacement vs Load

(iii) Number of Cycles to Pore Pressure

From these graphs, we have found a tri-linear relationship between Number of Cycles to failure and Relative Density, Cyclic Shear Strain and Effective Confining Pressure when any two of the factor remain constant.

After that we have tried to develop a pore pressure generation characteristics with the number of cycle elapsed. In doing so we have noticed that this relation can be best fitted by a hyperbolic model. Hence, we have proposed a generalized hyperbolic relation for this type of soil only.

7.2 Conclusion

The observation from the test results have been summarized as below:

(i) Cyclic Shear Strain is an important parameter for liquefaction of this type of soil. The liquefaction potential increases with increase in cyclic shear strain and lesser number of cycles are required for failure.

(ii) Another important factor to liquefaction is the Relative Density. As the relative density increases, liquefaction potential decreases and more number of cycles are required to failure.

(iii) Effective Confining Pressure is also controlling the liquefaction potential. When the confining pressure increases, the shear strength of soil increases, thereby more number of cycles are required to failure.

(iv) In the pore pressure generation curve, it has been seen that the rate of generation of excess pore water pressure is very rapid at the start of the test and it decreases severely as the failure point is approached.

(v) In the pore pressure generation model, we have seen that it is greatly influenced by the cyclic shear strain and not too much affected by relative density.

(vi) As we increase the rate of strain, the rate of generation of pore pressure decreases upto a certain threshold value of cyclic strain and then increases and the maximum pore pressure increases upto that certain threshold value of shear strain and then decreases.

(vii) For this type of soil, this threshold value may lie in between 0.67% and 0.83% of cyclic shear strain.

(viii) Finally we can express the relation between generation of excess pore pressure and number of cycles as:

$$\frac{\Delta u}{\sigma_c'} = \frac{N/N_f}{0.55+0.42\,N/N_f}$$

7.3 Future scope of Work

This thesis work may be considered as a basic work as far as the pore pressure generation characteristic is concerned. The findings of this thesis may serve as the basis of various future investigations.

The future scope of works may be as under:

(1) As we have collected the sample from only one location, there is a requirement of collecting samples from other locations also so that we can get a distinct result depending upon the soil conditions.

(2) In our sample we have got about 17% silt. Hence the silt content may be varied by mixing different amount of silt to get the liquefaction susceptibility pattern depending upon the quantity of silt in soil.

References

BIBLIOGRAPHY

1) Andrews, D.C.A & Martin G.R (2000)— "Criteria for Liquefaction of silty soil."

2) Arab A. and Belkhatir M. (2002) "Fines Content and Cyclic Preloading Effect on Liquefaction Potential of Silty Sand: A Laboratory Study", *Acta Polytechnica Hungarica, Vol. 9, No. 4.*

3) Chakraborty P., Pandey A.D., Mukerjee S. and Bharghava A. (2004) "Liquefaction Assessment For Microzonation Of Kolkata City", *13th World Conference on Earthquake Engineering Vancouver, B.C., Canada, Paper No. 82, August 1-6, 2004.*

4) Chen Y.C. & Liao T.S. (1992) "Studies of the state parameter and liquefaction resistance of sand"

5) Chien L.K, Oh Y.N, Chang C.H. (2000) "Evaluation of Liquefaction Resistance & Liquefaction induced settlement for Reclaimed soil"

6) Ishihara K. (1974) "Liquefaction of Subsurface Soils during Earthquakes".

7) Kramer S.L. Textbook on "Geotechnical Earthquake Engineering", *Prentice Hall, Inc. Upper Saddle River, New Jersey.*

8) Kumar Shiv Shankar, Krishna Murali A, Dey Arindam, "Dynamic Soil Properties of Brahmaputra sand using Cyclic Triaxial Test", *NES Geocongress on Advances in Geotechnical Engineering, 2014*

9) Paul Sanjay & Dey Ashim Kanti "Cyclic Triaxial Testing on Fully & Partially Saturated Soil at Silchar", *4th International Conference on Earthquake Geotechnical Engineering, June, 2007*

10) Ravishankar B.V & Sitharam T.G. "Dynamic Properties of Ahmedabad Sand at Large Strains", *Indian Geotechnical Congress, Ahmedabad, 17-19th December, 2005*

11) Swami Saran Textbook on "Soil Dynamics & Machine Foundations", *Galgotia Publications Pvt. Ltd., New Delhi.*

12) Xenaki V.C & Athanasopoulos G.A. "Liquefaction resistance of sand-silt mixtures: an experimental investigation of effect of fines*", December, 2002*

13) Youd T.L. & Idriss I.M. (2001) "Liquefaction Resistance of Soils: Summary Report From The 1996 NCEER AND 1998 NCEER/NSF Workshops On Evaluation Of Liquefaction Resistance Of Soils".